METHANOL STEAM REFORMING OVER SILICA AEROGEL SUPPORTED CATALYST FOR HYDROGEN PRODUCTION

A THESIS SUBMITTED TO
THE GRADUATE SCHOOL OF NATURAL AND APPLIED SCIENCES
OF
MIDDLE EAST TECHNICAL UNIVERSITY

BY

PINAR DEĞİRMENCİOĞLU

IN PARTIAL FULFILLMENT OF THE REQUIREMENTS
FOR
THE DEGREE OF MASTER OF SCIENCE
IN
CHEMICAL ENGINEERING

JUNE 2018

Approval of the thesis:

METHANOL STEAM REFORMING OVER SILICA AEROGEL SUPPORTED CATALYST FOR HYDROGEN PRODUCTION

submitted by **PINAR DEĞİRMENCİOĞLU** in partial fulfillment of the requirements for the degree of **Master of Science in Chemical Engineering Department, Middle East Technical University** by,

Prof. Dr. Halil Kalıpçılar
Dean, Graduate School of **Natural and Applied Sciences** _____

Prof. Dr. Pınar Çalık
Head of Department, **Chemical Engineering** _____

Prof. Dr. Naime Aslı Sezgi
Supervisor, **Chemical Engineering Dept., METU** _____

Prof. Dr. Timur Doğu
Co-Supervisor, **Chemical Engineering Dept., METU** _____

Examining Committee Members:

Prof. Dr. Halil Kalıpçılar
Chemical Engineering Dept., METU _____

Prof. Dr. Naime Aslı Sezgi
Chemical Engineering Dept., METU _____

Prof. Dr. Timur Doğu
Chemical Engineering Dept., METU _____

Assoc. Prof. Dr. Dilek Varışlı
Chemical Engineering Dept., Gazi University _____

Asst. Prof. Dr. Bahar İpek
Chemical Engineering Dept., METU _____

Date: 25.06.2018

I hereby declare that all information in this document has been obtained and presented in accordance with academic rules and ethical conduct. I also declare that, as required by these rules and conduct, I have fully cited and referenced all material and results that are not original to this work.

Name, Last name : Pınar DEĞİRMENCİOĞLU

Signature :

ABSTRACT

METHANOL STEAM REFORMING OVER SILICA AEROGEL SUPPORTED CATALYST FOR HYDROGEN PRODUCTION

Değirmencioğlu, Pınar
M.S., Department of Chemical Engineering
Supervisor: Prof. Dr. Naime Aslı Sezgi
Co-Supervisor: Prof. Dr. Timur Doğu

June 2018, 104 pages

Our energy demand shows an increasing trend parallel to the increase in population. An important issue while we are meeting our energy need is that the source of energy should not pollute the environment. It is seen that hydrogen becomes a suitable choice as energy source when the fact that depletion of fossil fuels is considered.

Hydrogen, which is not found in pure form in nature, is to be produced by some methods. In this study, hydrogen was produced from methanol steam reforming reaction. By doing so, maximum 3 moles of hydrogen can be produced per mole of alcohol. Type of the catalyst support is an important parameter that affects the performance of the catalyst during alcohol reforming reactions. A mesoporous catalyst support, silica aerogel, is synthesized by following sol-gel technique and after that convenient type of metal (Cu, Zn, etc.) was loaded into this support via wet impregnation method.

Metal loaded catalysts are first calcined, then reduced and finally placed in reaction environment in order to obtain a long term stable catalyst which will provide obtaining hydrogen gas with very low side product content. It was seen that methanol conversion increased with an increase in calcination temperature, and the highest methanol converison (86.1%) is reached with the catalyst calcined up to 700°C, namely 10Cu-SA Air/Ar 700. The best result in methanol steam reforming

at 280°C is obtained from 15Cu-SA Air/Ar 700 catalyst which provided 2.75 average hydrogen yield, 92.1% methanol conversion and 3.6% coke formation. Adsorbents such as huntite and hydrotalcite were used to capture the side product CO_2, in methanol steam reforming reactions and the best result was obtained with hydrotalcite which captured CO_2 for 55 minutes when mixed with 15Cu-SA Air/Ar 700 at 200°C in 1/15 weight base. It was seen that 15Cu-SA Air/Ar 700 was a stable and regenerable catalyst.

Keywords: Methanol Steam Reforming, Hydrogen Production, Mesoporous Material, Silica Aerogel, Copper, Zinc

ÖZ

SİLİKA AEROJEL DESTEKLİ KATALİZÖR İLE BUHARLI METANOL REFORMLAMA REAKSİYONUNDAN HİDROJEN ÜRETİMİ

Değirmencioğlu, Pınar
Yüksek Lisans, Kimya Mühendisliği Bölümü
Tez Yöneticisi: Prof. Dr. Naime Aslı Sezgi
Ortak Tez Yöneticisi: Prof. Dr. Timur Doğu

Haziran 2018, 104 sayfa

Giderek artan nüfusa paralel olarak enerji ihtiyaçlarımız da artma eğilimi göstermektedir. Enerji ihtiyaçlarımızı karşılarken önemli bir nokta kullanılan enerji kaynağının çevreyi kirletmemesidir. Fosil yakıtların giderek tükenmekte olduğu gerçeği düşünüldüğünde hidrojenin uygun bir enerji kaynağı olduğu görülmektedir. Doğada saf halde bulunmayan hidrojen çeşitli yöntemlerle üretilmektedir. Bu çalışmada hidrojenin, buharlı metanol reformlama reaksiyonu ile üretilmesi amaçlanmaktadır. Böylelikle 1 mol alkol başına en çok 3 mol hidrojen elde edilebilecektir. Alkol reformlama reaksiyonlarında kullanılan katalizör desteğinin türü, katalizörün performansını etkileyen önemli bir parametredir. Mezo gözenekli bir malzeme olan silika aerojel sol-jel tekniği ile sentezlendikten sonra bu katalizör desteğine ıslak emdirme yöntemiyle uygun metal (Cu, Zn, vb.) yüklenmiştir.

Metal yüklenmiş katalizörlerden uzun süre kararlılığını koruyan ve çıkış gazında çok az yan ürün içeren hidrojen eldesi için katalizörler öncelikle ısıl işlem görmekte, sonrasında indirgenmekte ve son olarak reaksiyon ortamına sokulmaktadır. Artan ısıl işlem sıcaklığı ile metanol dönüşümünün arttığı ve en yüksek metanol dönüşümüne (%86,1) 700°C'ye kadar ısıl işlem gören 10Cu-SA hava/Ar 700 katalizörüyle ulaşıldığı görülmüştür. Buharlı metanol reformlama reaksiyonunda en iyi sonuç 280°C'de 2,75 ortalama hidrojen verimi, %92,1

metanol dönüşümü ve %3,6 kok oluşumu sağlayan 15Cu-SA hava/Ar 700 katalizöründen elde edilmiştir.

Yan ürün olarak oluşan karbon dioksiti tutmak için buharlı metanol reformlama reaksiyonunda huntit ve hidrotalsit gibi adsorbanlar kullanılmış ve en iyi sonuç 55 dakika boyunca karbon dioksit tutma kapasitesiyle 15Cu-SA hava/Ar 700 katalizörüyle ağırlıkça 1/15 oranında karıştırıldıktan sonra 200°C'de reaksiyona giren hidrotalsitten elde edilmiştir. 15Cu-SA hava/Ar 700 katalizörünün kararlı ve rejenere edilebilen bir katalizör olduğu görülmüştür.

Anahtar Kelimeler: Buharlı Metanol Reformlama, Hidrojen Üretimi, Mezo gözenekli Malzeme, Silika Aerojel, Bakır, Çinko

To my beloved family…

ACKNOWLEDGMENTS

To start with, I would like to express my sincere thanks to my supervisor Prof. Dr. Naime Aslı Sezgi for her endless contributions, patience and compassion at hard times. Without her belief in me, I could not be able to complete this thesis. I would like to present my greatest gratitude to my co-supervisor Prof. Dr. Timur Doğu for the valuable things he taught me and for his strong support on me.

I would like to thank to my dear lab friend Arzu Arslan Bozdağ for her patience, kindness and helping me anytime I was in need. I also would like to thank to my lab partner Merve Sarıyer for her accompany for almost three years in the lab. Without her favor and helpfulness, the experiments could have been harder to complete. I would also like to thank to İlker Şener for his critical thoughts, kindness and patience. I wish to thank to my lab mates Seda Sivri, Sohrab Nikazad, Abdul Rehman Habib and Saeed Khan for their friendship and support.

I would also like to thank to Mihrican Açıkgöz and Doğan Akkuş for their helpfulness with my characterization results. Thanks to the staff at METU Central Lab and Department of Chemical Engineering.

Most importantly, I would like to express my gratitude to my beloved family. Their endless belief in me, and the way they supportod me throughout my entire life made me who I am. I would be glad to thank to my dear mother Filiz Değirmencioğlu for the sacrifices she has done for me and her limitless love she gaved to me. I also would like to thank to my dear father Levent Değirmencioğlu for being there whenever I needed him. They taught me valuable things related to life.

Lastly, Turkish Scientific and Technological Research Council (TUBITAK) grant (115M425), is gratefully acknowledged.

TABLE OF CONTENTS

LIST OF TABLES

TABLES

LIST OF FIGURES

FIGURES

NOMENCLATURE

A_i **:** Area of component i read from GC

B : Full width at half maximum, radian

c : Crystal shape factor

$C_{gas\ total}$ **:** Total concentration of the gas at 20°C and 1 atm, mol/ml

F_i **:** Molar flow rate of species i, mol/s

F_{CH3OH_0} **:** Molar flow rate of liquid methanol in the feed, mol/s

MW_{CH3OH} **:** Molecular weight of methanol, g/mol

n_i **:** Number of moles of species i

P : Pressure, Pa

P_0 **:** Pressure at reference state, Pa

Q_{Ar} **:** Volumetric flow rate of argon, ml/s

$Q_{Ar\ free\ gas}$ **:** Volumetric flow rate of gases without argon, ml/s

$Q_{gas\ total}$ **:** Total volumetric flow rate of gaseous species, ml/s

Q_{liq} **:** Total volumetric flow rate of the liquid, ml/s

R : Ideal gas constant, J/mol.K

S_{H2} Selectivity of hydrogen

T : Room temperature, °C

$t_{crystallite}$ **:** Crystallite size, nm

X_{CH3OH} **:** Conversion of methanol

y_i **:** Mole fraction of species i

Y_{H2} **:** Yield of hydrogen

Greek Letters

βi : Beta factor of component i

ρ_{CH3OH} **:** Density of methanol at 20°C, g/ml

λ **:** Wavelength of radiation, nm

θ : Bragg angle, °

Abbreviations

APD : Ambient Pressure Drying

BET : Brunauer Emmett Teller

BJH : Barrett Joyner Halenda

DMFC : Direct Methanol Fuel Cell

EDX : Energy Dispersive X-Ray Spectroscopy

GC : Gas Chromatograph

HTl : Hydrotalcite

IEA : International Energy Agency

ICP-MS : Inductive Couple Plasma Mass Spectroscopy

IUPAC : International Union of Pure and Applied Chemistry

K-HTl : Potassium carbonate promoted hydrotalcite

MCM-41 : Mobile Composition Matter No. 41

MD : Methanol Decomposition

MFC : Mass Flow Controller

MSR : Methanol Steam Reforming

PEMFC : Polymer Exchange Membrane Fuel Cell

SBA-15 : Santa Barbara Amorphous-15

SEM : Scanning Electron Microscopy

SESRM: Sorption Enhaced Steam Reforming of Methanol

SRM : Steam Reforming of Methanol

TCD : Thermal Conductivity Detector

TEOS : Tetraethyl orthosilicate

TMCS : Trimethylchlorosilane

TGA : Thermogravimetric Analysis

TPD : Temperature Programmed Desorption

WGS : Water Gas Shift

XRD : X-Ray Diffraction

CHAPTER 1

INTRODUCTION

1.1 The Search for Clean Energy

In recent years, fast depletion of primary energy sources (such as natural gas, coal, petroleum, etc) has initiated significant research to develop alternative clean energy carriers. As it was reported by International Energy Agency (IAE) global energy demand would increase 1.37 times between 2012 and 2040 (World Energy Outlook, 2014). Thus, finding a clean source of energy has become a vital issue to meet the growing energy need.

Fossil fuels, which have been used for decades to meet the global energy needs, give more harm to environment than the benefit they provide to humans. They are not to be named as sustainable energy sources due to their short consumption lives and the damage they cause to environment when they are burned. Fossil fuels are being used as primary source of energy, but they are limited and cause significant environmental issues. Considering the increasing population and its energy needs, renewable sources of energy are to be searched and used more commonly to decrease the dependency on fossil fuels and to tackle the negative effects of these energy sources such as global warming. The most widely known renewable sources of energy are wind, sun and biomass. But the fact that the energy generated from these sources can not be stored limits their sustainable usage. At this point, hydrogen is considered as an alternative energy carrier. Hydrogen has carbon-free nature and clean combustion properties. When compared to other types of fuels, such as natural gas or petroleum, hydrogen has the highest energy per unit mass. In addition to this, systems in which hydrogen is used release water or water vapor to the environment. Moreover, fuel cells, which convert chemical energy into electrical energy, need hydrogen feed to accomplish this. All these benefits make hydrogen a good candidate to reduce the dependency on fossil fuels and lead to a

greener world. However, hydrogen is not available in molecular form, in nature. Hence, it should be produced from hydrogen containing compounds, like natural gas, alcohols etc.

1.2 Hydrogen Energy & Fuel Cells

The first element of periodic table, hydrogen, comes from the Greek words *hydro* and *genes* and stands for "water generator". It is the simplest and the most abundant element in the world (Erdener, 2013). It forms compounds with other elements and is not readily available in nature. Hydrogen has no C-C bonds, which means it does not contribute to any greenhouse gas formation when combusted. It can be produced mainly by thermal, chemical and biological methods (Figure 1)

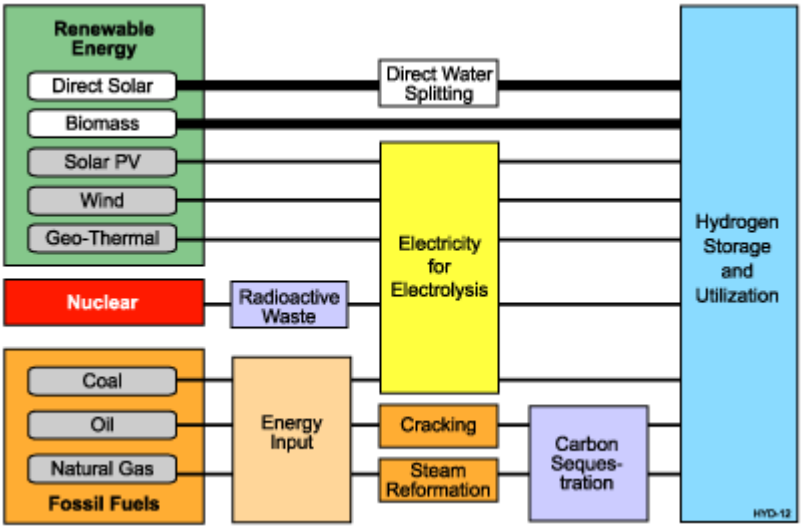

Figure 1: Hydrogen Production Paths (Florida Solar Energy Center, 2004)

With the help of thermal energy, hydrogen is produced from non-renewable sources (coal, oil, natural gas) via coal gasification, natural gas reforming, biomass gasification and water splitting at high temperatures. Hydrogen is also produced from water by means of splitting it into elements via electrical energy. To obtain hydrogen biologically, microorganisms and bacteria can be used.

Hydrogen has plenty of usage areas such as hydrogenation of unsaturated hydrocarbons and oils, methanol synthesis, ammonia synthesis, coal and oil refining, fuel in aerospace industry, and most importantly, energy carrier.

Hydrogen has several advantages; it releases no greenhouse gas when combusted so it is environmentally benign. It can be fed to fuel cells to generate electricity or can be directly used in fuel cell vehicles. It can be produced both from renewable and non-renewable sources. Among all fuels, it has the highest energy content per unit mass. One kilogram of hydrogen contains the same amount of energy as 2.8 kg of petroleum or 2.1 kg of natural gas has (Erdener, 2013).

Even though hydrogen is a considered as a potential energy carrier of the 21st century, important issues to be solved are the storage and security problems related to its transportation. Hydrogen starts to burn if ignited when it reaches more than 4 volume percent in the air. In order to handle this gas safely, some precautions should be taken such as installing fans or vents inside the facilities (Toshiba, 2015). Hydrogen can be stored in tanks in gas or liquid form as well as it can physically be stored in carbon nanotubes or chemically as hydride (Table 1) (Republic of Turkey, Ministry of Energy and Natural Resources, 2012).

Table 1: Hydrogen Storage Methods (adapted from Nikolaidis, 2017)

Storage Method	**Temperature (°C)**	**Pressure (MPa)**
High pressure gaseous H_2	Ambient	77
Cryogenic liquid	-252.87	atmospheric
Adsorbed on carbon nanotubes	-196.15	6
Adsorbed to form hydrides	Ambient	atmospheric
Adsorbed to form complex hydrides	>100	atmospheric

On-board production of hydrogen in fuel-cell derived motor vehicles may be considered as a solution to transportation and storage problems of hydrogen. Fuel cells are devices that generate electrical energy by using the chemical energy of the fuel. There are several types of fuel cells depending on the fuel and the membrane used. Some of which are polymer electrolyte membrane fuel cells (PEMFC), direct methanol fuel cells (DMFC), alkaline fuel cells, phosphoric acid fuel cells, solid oxide fuel cells, etc. Storage and transportation problem of hydrogen could be overcome by using an on board fuell cell.

By feeding hydrogen to a fuel cell, electrical energy can be generated. If hydrogen is produced from renewable sources, carbon footprint could be reduced. A critical issue at this point is the purity of hydrogen; a PEM fuel cell should be at high purity and should contain very little CO and CO_2, otherwise the anode could be deactivated.

Specifically, PEMFC requires very low amount of carbon monoxide in the feed which may require further purification of fuel that is going to be fed. Unlike DMFC, the desired fuel for PEMFC is highly pure hydrogen containing carbon monoxide not more than 100 ppm, which could poison the platinum catalyst on the anode of this fuel cell. (Fierro, et.al, 2002).

Among the other types of fuel cells, low operating temperature (~ 80°C), low weight and quick start-up of PEMFC make them suitable candidates for vehicles. Since storage is problematic, hydrogen can be generated on site by reforming some alcohols. PEMFC utilizes the hydrogen produced by steam reforming of alcohols. The products of steam reforming reactions will vary depending on the operating conditions and the fuel. In this study, hydrogen which has appropriate characteristics to be fed into an on board fuel cell will be produced via steam reforming of methanol. Later on, this produced fuel could be fed into an on board fuel cell if desired.

CHAPTER 2

METHANOL AS HYDROGEN SOURCE AND BIOMETHANOL

Methanol (CH_3OH) is the simplest and the least C containing alcohol ever known. Methanol is liquid under normal conditions due to the existence of carbon-oxygen bond. It is miscible with water and most of the organic solvents. Methanol is an international commodity which can be produced from renewable energy sources such as biomass (animal waste, sewage, etc). Indeed, it has a very large range of sources through which it can be produced: almost any process that can convert carbon containing material into H_2, CO and CO_2 can, in theory, be used to yield methanol (Edlund, 2011). Methanol contains four hydrogen atoms per one carbon atom. It is also called the energy feedstock of future depending on the fact that it can be used to produce hydrogen at low temperatures and has important physical (Table 2) and chemical properties. Chemical reactivity of this alcohol is a peculiar property which provides its usage as liquid feedstock for reformers to produce hydrogen at low to moderate temperatures (250-400°C) (Edlund, 2011).

Table 2: Physical properties of methanol (adapted from Sigma Aldrich, 2018)

Chemical formula	CH_3OH
Molecular weight (g/mol)	32.04
Density at 25°C (kg/m^3)	791
Boiling point (°C)	64.7
Melting point (°C)	-98
Ignition temperature (°C)	470
Vapor pressure at 25°C (kPa)	16.96

Besides the features given in Table 2, methanol is superior to other alcohols due to having very low volatility and minimizing the explosion risk. In addition, its storage and transportation do not become an obstacle when delivering this fuel globally.

Methanol is readily available in today's world but the synthesis of this valuable fuel at commercial scale started in early 1920s, by using a catalyst containing zinc oxide and chromium oxide (developed by BASF) in a high pressure (300 atm) process. Later on, in the light of new researches about catalysts, a better catalyst containing copper, zinc oxide and alumina was introduced to the same system which lowered high pressure and temperature to 50-100 atm and 230-260°C, respectively. Since then, the process became more common in 1960s (Bartholomew, 2006).

Sources used to yield methanol can vary because it can be produced from any hydrocarbons in theory. Being a renewable source of hydrocarbons, solid biomass can be converted into liquid hydrogen feedstocks such as alcohols (bio ethanol, bio methanol, etc.). Among these liquid hydrogen feedstocks, bio methanol captures attention because of easily being degraded into hydrogen in the presence of a reformer (water or air) at low to moderate temperatures. This feature enables methanol to be used in fuel cells as well, where the hydrogen produced via this alcohol could be converted into electrical energy (Shamsul, 2014). Methanol can also be used in vehicles as fuel when mixed with gasoline. Apart from this feature it can be fed to DMFC, and can be used to produce biodiesel and other valuable chemicals.

2.1 Hydrogen Production from Methanol via Steam Reforming of Methanol

Hydrogen is not readily available in nature so it should be produced from hydrogen containing species. Producing hydrogen from alcohols is less expensive than other alternatives such as electrolysis of water or gasification of hydrocarbons.

Alcohols are hydrogen, oxygen and carbon containing chemicals and when reformed by an oxidizing agent (water, air etc.), carbon atoms are oxidized to carbon monoxide or carbon dioxide letting the hydrogen being released. Considering alcohols, methanol is the least carbon containing one but it also has the highest hydrogen to carbon (H/C) ratio as four. Remembering the higher the H/C ratio, the more energy can be obtained from that alcohol, methanol becomes an

appropriate choice to yield hydrogen. The reaction through which hydrogen is produced from methanol is called Steam Reforming of Methanol (SRM) or Methanol Steam Reforming (MSR).

SRM is the reaction in which methanol is reformed under low to moderate temperatures (200-400°C) to yield hydrogen gas as well as some side products like carbon monoxide and carbon dioxide.

$$CH_3OH_{(g)} + H_2O_{(g)} \rightarrow CO_2 + 3H_2 \qquad \Delta H^{\circ}_{298K} = 49.3\ kJ/mol \qquad \text{[R.1]}$$

$$CH_3OH \rightarrow CO + 2H_2 \qquad \Delta H^{\circ}_{298K} = 91\ kJ/mol \qquad \text{[R.2]}$$

$$CO + H_2O \rightarrow CO_2 + H_2 \qquad \Delta H^{\circ}_{298K} = -41\ kJ/mol \qquad \text{[R.3]}$$

Reactions 1 to 3 are the most encountered ones during the steam reforming of methanol and only two of them are independent reactions. Reaction 1 is the steam reforming of methanol which has an endothermic nature. From the stoichiometry of reaction 1, one mole of methanol yields to a hydrogen-rich mixture with three moles of hydrogen. However, steam reforming of methanol is accompanied with some side reactions, like reactions 2 and 3. Methanol decomposition (reaction 2) and water gas shift (WGS) reaction (reaction 3) result in carbon monoxide formation. This gas should be kept at maximum 100 ppm in order to be fed into a PEMFC (Qi, et. al., 2018). Unlike reaction 1, WGS is an exothermic reaction. In overall, the reaction is endothermic leading to higher conversions of methanol under higher temperatures.

In addition to Reactions 1 – 3, some other side reactions could also occur :

$$CO_2 + C \leftrightarrow 2CO \qquad \text{[R.4]}$$

$$C + 2H_2 \leftrightarrow CH_4 \qquad \text{[R.5]}$$

$$CO + 3H_2 \leftrightarrow CH_4 + H_2O \qquad \text{[R.6]}$$

Boudouard reaction (reaction 4) is a reversible and endothermic reaction. At lower temperatures, the reaction shifts towards reactants and coke formation could be

observed. Reactions 5-6 are the ones in which methane is produced. An important point to remind is methane could be formed as a side product. SRM reaction is highly effective when carried out with Cu catalysts. However, Cu catalysts are not that much effective in methanation reactions (Tartakovsky, 2014). Hence, using Cu based catalysts in SRM at low to moderate temperatures (200-400°C), may lead to desired methanol conversion as well as minimal or no methane formation.

SRM is limited with thermochemical boundaries. Considering only Reaction 1, maximum number of hydrogen produced per mole of methanol is limited to three. To achieve this much of hydrogen yield, operating temperature and the catalyst to be used should be well determined.

To determine the operating temperature, thermodynamic analysis was performed with Gaseq. Gaseq is a program calculating the equilibrium data for the specified chemical compounds. It is mainly based on the minimization of Gibbs free energy. Product distribution at equilibrium with respect to temperature change is given below for the SRM reaction (Figure 2).

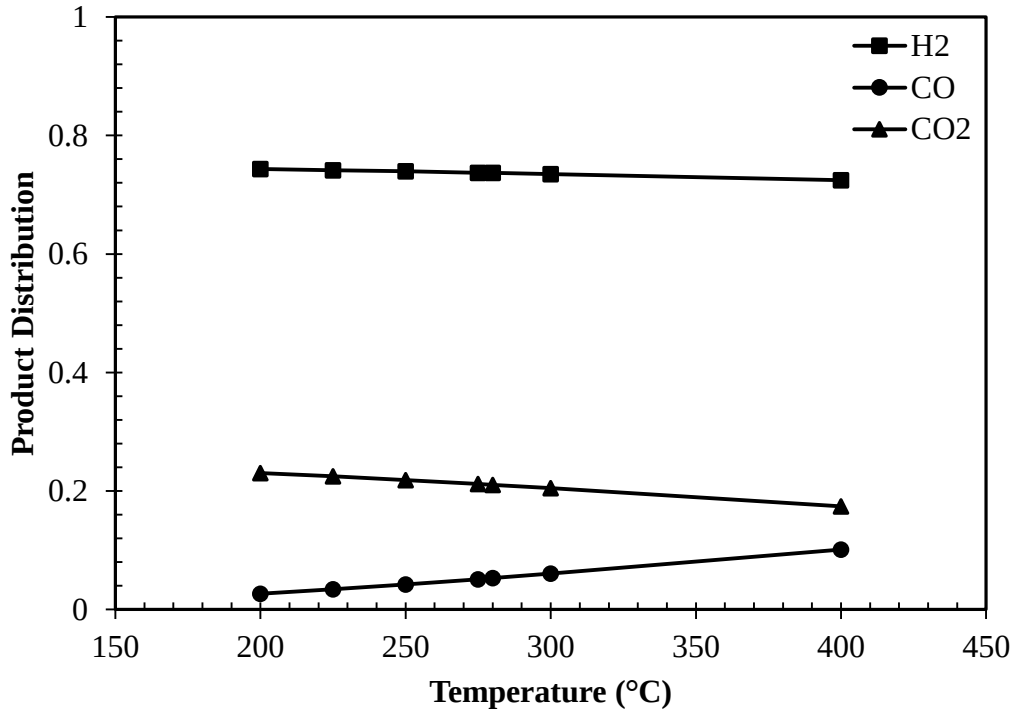

Figure 2: Equilibrium product distribution of SRM reaction at 1 bar and steam to methanol molar ratio of 2.2 calculated by Gaseq

Product distribution graph on dry basis is constructed considering the formation of CO_2, CO and H_2. As can be seen from Figure 2, the product distribution does not get much affected from the change in temperature except CO. As temperature increased from 200 to 300, CO in product stream slightly increased. In between 300 and 400°C, CO increase was distinguishable. CH_3OH and H_2O react to form a hydrogen-rich gas mixture which, on average, consists of 5% CO, 21% CO_2 and 74% H_2, which are in agreement with the literature. In the light of this result and considering the common usage of Cu based catalysts in SRM, reaction temperature was decided as 280°C when the pressure is 1 bar and steam to methanol ratio (S/M) is 2.2.

CHAPTER 3

PROPER CATALYSTS FOR STEAM REFORMING OF METHANOL

Catalysts are materials that reduce the activation energy of the reactions without undergoing persistent chemical changes. Thus, they speed up the reactions which they catalyze. Catalysts are mainly divided into two groups as homogeneous and heterogeneous. Homogeneous catalysts have the same phase as the reactants whereas phases of reactants and the catalyst differ for heterogeneous catalysts. A catalyst can have acidic or basic nature depending on the support material and the metals loaded. A catalyst usually consists of a support material.

According to the definition made by International Union of Purely Applied Chemistry (IUPAC), porous materials are classified into three groups depending on their pore sizes :

Pores which do not exceed 2 nm are called *micropores,*
Pores which are in between 2 to 50 nm are *mesopores* and
Pores having larger diameter than 50 nm are referred to as *macropores*.

Depending on the synthesis route, catalysts can possess different pores. Distribution and connection of the pores in the catalyst plays an important role in determining the activity of the catalyst. If a catalyst has interconnected pores, mass transfer could easily take place. However, pore diameter is an important parameter affecting the mass transfer through the catalyst. Generally if the pore diameter is too small, mass transfer limitations within the catalyst could occur hence the pores could be blocked. In order to minimize the mass transfer limitations, mesoporous materials are frequently preferred as catalysts or catalyst supports.

3.1 Mesoporous Materials

This class of materials has pore diameters ranging from 2 to 50 nm. Mesoporous materials do not necessarily have to have mesopores only; they can also possess micro or macropores but the dominant pore diameter is in mesoporous range. Generally, mesoporous materials capture attention as catalyst support materials. Mobile Composition Matter No. 41 (MCM-41), Santa Barbara Amorphous type of material (SBA-15) and silica aerogels are typically encountered examples of mesoporous catalyst supports.

MCM-41, which is a mesoporous silica, has uniform pore openings in regular hexagonal array. A big advantage of this material is its adjustable pore sizes by altering the length of surfactants. MCM-41 is known as molecular sieve which has a surface area around 1000 m^2/g (Zhao, 1996). MCM-41 is thermally stable but it loses its stability under humid media, in other words, it is not hydrothermally stable. Despite having good features, poor hydrothermal stability of this material limits its usage in steam reforming reactions.

Another mesoporous silica, developed by Zhao et. al in 1998 is SBA-15. This material also has large surface area and well defined pore structure (Santos et al, 2013). Unlike MCM-41, SBA-15 is both thermally and hydrothermally stable which makes it superior to MCM-41 in steam reforming reactions.

On the other hand, silica aerogels, which are a subgroup of aerogels and found out by Kistler in 1932, have outstanding features such as low density (0.003 g/cm^3), high porosity around 80 to 99.8%, high specific surface area around 500-1200 m^2/g and large pore diameter around 11 nm (Dorcheh, 2008). They are thermally stable up to 1000°C and hydrophobic nature of silica aerogels makes them appropriate catalyst supports in steam reforming reactions.

3.1.1 Silica aerogels

Aerogels are the lightest solid material ever known. They are obtained from a gel by replacing the liquid inside the pores with air. Aerogels were first introduced by Kistler et.al in 1932. These groups of materials have some unique features such as high porosity up to 99%, low thermal conductivity (~0.01 W/m.K), high specific surface area (1,000 m^2/g) and large pore volume (~12 nm) (Leventis, 2011). As a result of these properties, aerogels find a variety of usage areas in aerospace industry, thermal insulation, acoustics and catalysts.

The most recognised aerogel is silica aerogel. It has an amorphous and hydrophobic nature. Because of having large specific surface area, large pore diameter, high porosity, being thermally stable up to 1000°C and having a hydrophobic nature, they capture attention for being used as a catalyst support.

Silica aerogels are obtained via sol-gel method. As the name implies, first a solution is formed and then it is turned into a gel by some catalysts. The gel is formed by the hydrolysis and condensation of silicon alkoxides ($Si(OR)_4$). Alkoxides are used as silica precursors and are denoted by OR and R is alkyl, usually methyl (CH_3) or ethyl (C_2H_5) (Leventis, 2011). After the formation of gel, the gel and solution are aged in order to strengthen the silicon skeleton formed in previous step. Aging is effective on the porosity of aerogels. Depending on the concentration of aging time and solution, porosity characteristics can alter (Aravind, 2010). The last and the most important step in silica aerogel formation is drying. This step can be at ambient pressure, by freezing or under supercritical conditions of the solvent used. Drying is the part during which the solvents in the pores of aerogel are exchanged with air. When this change occurs, capillary stresses also occur inevitably which inhibits monolithic aerogel production (Leventis, 2011).

The main idea behind supercritical drying is to go beyond liquid-vapor phases and eliminating the capillary stress effects and shrinkage of the gel. Both the temperature and pressure of medium where aerogel is placed are increased above the critical point of the used solvent, generally liquid CO_2. Apart from CO_2, organic

solvents such as methanol, ethanol, acetone, etc. could also be used for supercritical drying of the wet gel. Even though supercritical drying offers almost no shrinkage and capillary stress, it is a highly energy consuming, expensive and dangerous process. This is why other alternative drying methods are preferred.

In the case of freeze drying, the liquid inside the pores is freezed and then is sublimated under high pressure. This process also resembles supercritical drying in terms of crossing the liquid-gas boundary. The main disadvantage of this drying technique is high pressure and low temperature. Thus, this method is also energy intensive and expensive.

The last technique, ambient pressure drying, is accepted as the most promising drying technique for aerogels for large scale manufacturing processes. This method is based on evaporating the pore liquid in the wet gel simply at atmospheric pressure and temperatures above the boiling point of the solvent used. Hence, this method seems to be the most reasonable one among the others but it should be noted that ambient pressure drying does not prevent capillary stress formation. But in order to compensate the undesired effects of capillary stresses on drying, some surfactants can be used to control pore size, pore volume and even distribution. The key point is to introduce incondensable species (Si-R groups) via sylilation of the gel to promote a spring-back effect.

To conclude, silica aerogels capture attention for being used as the catalyst support. They are appropriate candidates to be used in SRM for being thermally and hydrothermally stable, owing large pore volume and specific surface area. The next step is to load the appropriate metals to this support to make it active enough to be used in SRM reactions.

3.2 Catalysts Used in Steam Reforming of Methanol

Steam reforming of methanol is the desired reaction to yield hydrogen from methanol itself but some other side reactions such as decomposition of methanol

and water gas shift reactions also take place. Therefore, considering the possibility of side reactions as well, a highly active and stable catalyst under reaction conditions, which will also minimize the undesired product formation such as CO, should be determined. In general, catalysts for SRM are divided into two main groups as group 8-10 catalysts and copper based catalysts.

3.2.1 Group 8-10 catalysts

As the name implies, these catalysts are located on the 8^{th}-10^{th} rows of the periodic table and are metal based catalysts. Specifically, Pd based catalysts are the most preferred ones among this group due to their high performances (Sa, 2010). Pd based catalysts' activity strongly depends on the support material (SiO_2, ZnO, ZrO_2, Al_2O_3, MgO, CeO_2, etc.). As reported in the literature, when Pd is supported by ZnO, it shows anomalously high selectivity towards hydrogen due to alloy formation between Pd and Zn (Sa, 2010). Superiority of Pd/ZnO catalyst on other metals such as Ni, Co, Pt and Ru was proven. No alloy formation with Zn was observed for Ni, Co, Ru metals which reduced their methanol conversion and enhanced CO formation in the SRM reaction. Further support of Pd/ZnO has increased its stability in life test: $Pd/ZnO/Al_2O_3$ catalyst has the same activity as $Cu/ZnO/Al_2O_3$ catalyst but with longer stability. In the light of researches made, it is seen that group 8-10 catalysts except Pd, lead to production of CO and H_2 dominantly. In general group 8-10 catalysts result in lower activity than copper based ones with Pd/ZnO exception which forms alloy. Even so, the catalytic activity of Pd/ZnO catalyst did not exceed that of Cu based catalyst unless it is further supported via Al_2O_3.

3.2.2 Copper based catalysts

Copper based catalysts are the most encountered catalysts used for SRM reactions due to their high activity. High dispersion with small particle sizes of copper is the key to higher activity. Again, like group 8-10 catalysts, type of promoter used to support copper affects the nature of catalyst and its properties. Cu promoted by

ZnO, Al_2O_3, Zn/Zr/Al, Cr_2O_3, CeO_2 and SiO_2 are the most common catalysts used in SRM. In addition to these, carbon nanotubes (CNT) are also used as support material in the SRM reaction.

Interaction of copper with the support is vital. One important parameter that can alter these interactions is the preparation route of the catalyst. It was observed that even the preparation of the same catalyst with different methods led the catalysts have different properties resulting in different methanol conversions and CO selectivities in the SRM reaction (Sa, 2010).

Despite all these good features, copper based catalysts have the main problem of being deactivated. This behavior is generally traced to the sintering of catalyst, change in the oxidation state or coke formation (Sa, 2010). In order to minimize the deactivation, steam to carbon ratio (S/C) could be increased with the addition of more water to the feed. By doing so, coke formation could be inhibited and the catalyst could be used for a longer period of time.

To conclude, when comparing group 8-10 catalysts to copper based ones, copper based catalysts have higher activities. In spite of the risk of being deactivated, they yield better results and are appropriate candidates to be used in SRM.

CHAPTER 4

LITERATURE SURVEY

Considering the fast depletion of fossil based resources and related environmental issues, significant research activities were devoted to the development of non-fossil clean energy carriers, in recent decades. Hydrogen is considered as a major alternate to petroleum, due to being a carbon-free energy carrier and having clean combustion properties. CO-free hydrogen has very high potential to be used as a fuel in PEM fuel cells. Thermodynamics of low temperature reforming of methanol favors minimization of CO in the produced synthesis gas. Development of new catalysts which will minimize undesired side products and will show good activity at low temperature reforming reactions is still a challenge in catalysis research.

Silica aerogels captured attention to be used as catalyst supports due to their large surface area, high porosity and interconnected pores. There are many studies related to the synthesis of silica aerogel via ambient pressure drying (APD) method. Ivanov, et. al (2014) worked on the synthesis of silica aerogel by surface modification. They used trimethylchlorosilane (TMCS) as the surfactant molecule to obtain a hydrophobic aerogel at ambient pressure. After the synthesis was complete, FTIR spectra were taken and Si-OH bonds turned out to be Si-$(CH_3)_3$ which showed the hydrophobicity of the aerogel. Another study made by Wua, et. al (2011), silica aerogel was synthesized by sol-gel method which then was followed by two-step surface modification and drying at ambient pressure. The resulting aerogels exhibited high porosity up to 87.7–92.3%, and surface area in between 852 and 1005 m^2/g. The displacement of the water in the pores of aerogel during the surface modification step led the aerogel have higher thermal stability. Drying of the aerogels was performed gradually at ambient pressure; the gels were heated 3 hours at 55°C, 4 hours at 80°C and finally 2 hours at 130°C. The obtained silica aerogels had a pore diameter in the range of 2-50 nm which showed their mesoporosity. The average pore sizes of the aerogels were changing from 6.93 to

10.78 nm which could be altered with the molar ratios of the reactants (TEOS:MTMS:EtOH:H_2O).

Silica aerogels exhibit a number of advantages such as high surface area (500-1000 m^2/g), high porosity (80-99.8%), low thermal conductivity (0.02 W/mK) (Aravind, et. al, 2010) and their densification behavior prevents the sintering (Fricke, 1998). Having these properties, they capture attention for being used in the steam reforming of methanol reaction as the catalyst support (Amiri, et. al, 2016).

In a research made by Amiri and Moghaddas (2014), silica aerogel was used as to support copper in the SRM reaction. The effect of calcination temperature, copper content and the activation method on the catalysts' activity and hydrogen production were investigated. Copper silica aerogel was synthesized by cogelation method and dried catalysts were calcined at 450 or 700°C. It was seen that at constant flow rate and reaction temperature of 300°C, increasing Cu content from 7.7 to 13.3 wt%, also increased the methanol conversion from 63 to 99.4%. It was found out that copper tend to be in cupric ions entrapped into silica matrix when it was at low content. But when the Cu content increased, CuO clusters were formed which increased reactants possibility to access those clusters and yielded better conversion values. The effect of calcination temperature on conversion of methanol was surprising: catalysts calcined at 700°C gave higher conversions than the ones calcined at 450°C under the same conditions. The reason of this was attributed to dispersion of copper in silica: for the samples calcined at 450°C, XRD results revealed copper ions with no diffraction peaks whereas in the patterns of catalysts calcined at 700°C, there was characteristic CuO peaks. Lastly the effect of activation by means of reducing with H_2 prior to reactions at 200, 300 and 400°C was examined. It was found that regardless of the activation temperatures, each catalyst gave almost the same conversion under SRM at 300°C. They reported that due to the low reduction temperatures of copper loaded catalysts around 210-270°C, activation of these catalysts became easy. It was found out that increased copper content inhibited CO formation. Hence, Cu-SiO_2 catalyst was approved to be a suitable catalyst for SRM when compared to Pd/ZnO, CuO/CeO_2, Cu-Zn-Zr or Cu/ZnO/Al_2O_3 catalysts which led to CO formation in the range of 3-20%.

In the work of Matsumura and Ishibe (2009), silica supported copper catalyst was tested in SRM at 250°C. As it was stated by Matsumura and Ishibe, the increase in the pre-reduction temperature from 300 to 400°C caused less activity in the catalyst. However when the catalyst was pre-reduced at 250°C, its activity increased with increasing copper loading up to 40 wt%. When the catalyst amount was doubled, methanol conversion increased from 95% to 97%, together with an increase in CO selectivity from 1.1% to 2%. A comparison in terms of activity was made between Cu/SiO_2 and $Cu/ZnO/Al_2O_3$ and silica supported catalyst was reported to be more active than the commercial catalyst. Lastly when the copper content increased from 20 wt% to 30-50wt%, it was seen that metallic copper particles turned into Cu_2O particles after the reaction. This caused a decrease in activity in 30-50 wt% copper loaded catalysts.

In another study of Matsumura and Ishibe (2009), a SRM byproduct, CO was aimed to be suppressed by the addition of zinc oxide into 30 wt% copper loaded silica. XRD results of the catalysts after reaction were reported to show zinc oxide's interaction with Cu particles to oxidize them to Cu_2O. The addition of 10 wt% ZnO was reported to reduce CO selectivity and increase the catalytic activity because ZnO contributed to the suppression of reverse WGS reaction. Since CO formation was found out to be dependent on conversion, formation of CO was estimated to be due to reverse WGS reaction. Due to the dominancy of Cu^+ particles on catalyst surface, Cu/SiO_2 was found out to be an advantageous catalyst.

In a study of Mrad, et.al, (2011) copper, zinc and alumina containing different types of catalysts were tested in SRM reaction at 350°C. Alumina (Al_2O_3) itself was also tested in SRM in addition to the Cu-Al, Zn-Al and Cu-Zn-Al containing catalysts and it was reported that Al_2O_3 increased CO formation but addition of copper into alumina decreased CO formation up to 0.1%. It was found that the addition of Zn into Cu- Al_2O_3 catalyst increased CO emission from 0.1% to 0.8%. The reason of this was attributed to the partially covering of copper particles by ZnO which enhanced the decomposition of methanol and led more CO formation. As a result, the addition of Al_2O_3 was found to enhance copper oxide dispersion by stabilizing Cu^{+2} ions and methanol conversion and hydrogen yield increased with the addition of 5% copper into alumina.

Park, et. al (2014) studied on the SRM reaction using a $Cu/ZnO/ZrO_2/Al_2O_3$ catalyst having a Cu:Zn:(Al+Zr) molar ratio of 3:3:4 at 473 and 573 K. They found out that an increase in calcination temperature reduced the crystallite size of copper but the increased reduction temperature from 523 to 573 K increased the copper crystallite size. After the SRM reaction, crystallite size of copper increased for all catalyst containing Cu, Zn, Zr and Al which was attributed to the deactivation of the catalysts. The $Cu/ZnO/ZrO_2$ catalyst showed the highest hydrogen formation rate at 473 K in SRM.

In the work of Wu, et. al (2009) the role of the promoter in copper based catalysts was investigated for SRM. ZrO_2 and ZnO promoters were tested in SRM at 260°C. Prior to each reaction, the catalysts were reduced with hydrogen. Steam to methanol ratio was 1.2. Comparing Cu, Cu/ZnO and Cu/ ZrO_2, the least methanol conversion was achieved with copper itself (14% which reduced to 0% after 30 min.) whereas the best performance was achieved with Cu/ ZrO_2 catalyst. The initial conversions of ZnO and ZrO_2 supported Cu catalysts were more than 90% but a sudden decay in conversion observed to 37.9 and 56.1% after 25 min. for ZnO and ZrO_2 promoted catalysts, respectively. ZrO_2 showed higher stability than ZnO. Compared to ZnO, ZrO_2 was thought to stabilize the copper crystallite size and prevent their agglomeration during the reaction because ZrO_2 easily desocciates water and forms OH groups, which maintain surface oxygen for Cu^+ and react with the adsorbed methanol to yield hydrogen and carbon dioxide.

In order to minimize the byproduct formation, adsorbents could be used in SRM reactions. Generating hydrogen in SRM using a catalyst and an adsorbent is called sorption enhanced steam reforming of methanol and it captures attention to obtain hydrogen at a high purity that could be fed into a PEMFC.

In a study of Wu, et. al, (2015) sorption enhaced SRM (SESRM) was performed using a 22% K_2CO_3 promoted hydrotalcite (K-HTl) as adsorbent and a commercial catalyst ($CuO/ZnO/Al_2O_3$) at 230°C with a steam to methanol ratio of 2. When the performance of the commercial catalyst was compared to hydrotalcite promoted commercial catalyst, an increase in the hydrogen concentration more than 20% was reported. Five grams of commercial catalyst was used together with 60 g of K-HTl.

When K-HTl promoted catalyst was tested in SESRM at 230°C, 99.61% H_2 and 0.39% CO were obtained. The same results without adsorbent were 74.42% H_2, with 1.24% CO and remaining CO_2. It was also recorded that as the steam to carbon ratio increased, the breakthrough time for CO_2 adsorption also increased to 10 min.

In a recent study of Qi, et. al (2018), hydrogen production via SESRM using K-HTl promoted commercial $CuO/ZnO/Al_2O_3$ catalyst was performed at 473-573 K with a steam to methanol ratio of 3. The configurations of the catalyst and the adsorbent were tested. One with the catalyst and sorbent mixture, the other with composite sorbent and catalyst in pellet form. Sorbent to catalyst ratio was 4.8/1 for each configuration. In both forms, CO_2 adsorption enhanced the SRM reaction. As it was reported, lower methanol conversion was observed in pellet form due to the basic nature of HTl which reduced the catalytic activity of the catalyst. CO_2 adsorption capacity of K-HTl increased from 0.74 to 0.89 mmol CO_2/g catalyst with the increase in temperature from 573 to 673 K.

In addition to $CuO/ZnO/Al_2O_3$ catalyst, other types of catalysts like ordered mesoporous materials were also used in the SRM reaction. In the study of Eswaramoorthi, (2009), mesoporous SBA-15 supported Pd–Zn catalysts were tested in the SRM reaction at 280°C for five hours. 4.5 wt% Pd together with 6.75 wt% Zn was loaded into SBA-15. It was reported that when steam to methanol ratio increased, the conversion of methanol decreased, unlike hydrogen selectivity. Optimum conversion (86 mol%) was obtained when the steam to methanol molar ratio was 1.12.

In a study made by Abrokwah, (2016), the effect of different metals on MCM-41 support was tested in the SRM reaction environment during hydrogen production. 10 wt% Cu, Pd, Sn, Ni, Zn and Co were loaded into MCM-41 separately. In terms of activity and selectivity, copper loaded catalyst showed the best performance at 250°C with a steam to methanol molar ratio of 3. 100% H_2 and 6% CO selectivities were obtained from this catalyst without any methane formation. Stability of the copper loaded MCM-41 catalyst was also tested for forty hours at 300°C. The conversion dropped only to 74% at the end of forty hours. Even though Pd, Sn and

Zn loaded catalysts showed better activity than copper, they became deactivated in a shorter period of time.

In the study of Deshmane, (2015) different amount of copper was loaded (from 5 wt% to 20 wt%) into MCM-41 and the resulting catalysts were used in the SRM at atmospheric pressure in the temperature range of 200 to 350°C. It was reported that the best result was obtained from 15%Cu-MCM-41 catalyst with 89% methanol conversion, 100% H_2 selectivity and 0.8% CO selectivity at 300°C. When the copper loading exceeded 15%, such as 20%, the surface area of copper was reported to decrease leading to a decrease in copper dispersion. 15%Cu-MCM-41 catalyst maintained its stability for 48 h which showed the significance of the support material used in the SRM.

4.1 Objectives

The main aim of this study is to produce a hydrogen-rich gas mixture from the steam refroming of methanol reaction at low to moderate temperatures (200-300°C) by using a highly active and stable catalyst which will enhance the conversion of methanol and hydrogen yield. To achieve this goal, the scope of this study is to synthesize silica aerogel and silica aerogel supported copper catalysts with different metal percents to be used in the SRM reaction to obtain hydrogen and to reduce the side product formation such as CO and CO_2. In addition, sorption enhanced steam reforming of methanol could also be performed with a suitable sorbent to adsorb CO_2 and reduce CO amount, so that the CO restriction of PEMFC (<100 ppm) could be met.

CHAPTER 5

EXPERIMENTAL

The experimental setup was constructed in Chemical Reaction Engineering Laboratory with the purpose of producing hydrogen in a continuous flow packed column reactor which then could be fed into a fuel cell. Experimental studies could be examined in three parts: synthesis of the catalyst, characterization of the catalyst and hydrogen production experiments. In this study, catalysts were synthesized at different calcination temperatures and calcined with different gases. In addition, different amounts and types of metals were loaded onto the catalyst support. The synthesized catalysts were characterized using X-Ray Diffractometer (XRD), N_2 Adsorption/Desorption, Scanning Electron Microscopy (SEM), Energy Dispersive X-Ray Spectroscopy (EDS), Inductively Coupled Plasma Mass Spectroscopy (ICP-MS), Temperature Programmed Ammonia Desorption (NH_3-TPD), and Thermogravimetric Analysis (TGA) methods. Synthesized catalysts were tested in reaction environment at different temperatures and the side product, CO_2, was captured by using different adsorbents such as huntite and hydrotalcite. Moreover, repeatability experiments were performed. Construction of the experimental setup, synthesis and characterization of the catalysts and the experiments are detailed in the following sections.

5.1 Synthesis of the Catalyst

Synthesis of the catalyst was divided into two sections as the catalyst synthesis studies and synthesis of metal loaded silica aerogels. The route of silica aerogel synthesis was formed by modifying the synthesis procedure of Deshpande, (1996). Different metals were loaded into silica aerogel using wet impregnation method.

5.1.1 Synthesis of silica aerogel

In the synthesis of silica aerogel tetraethylorthosilicate (TEOS, Merck) was used as silica source, trimethyl chlorosilane (TMCS, Merck) was used as surface modifier, distilled water, absolute ethanol (Sigma Aldrich) and hexane (Sigma Aldrich) were used as solvents, hydrochloric acid (HCl, 37% v/v, Merck) was used as acidic catalyst, ammonia (NH_3, 25% v/v, Merck) was used as basic catalyst and ammonium fluoride (NH_4F, Merck) was used as the gelling agent.

1.73 g distilled water, 5.63 g absolute ethanol, 10 g TEOS and 62µL HCl are placed in an airtight beaker, respectively. After that the solution is stirred on a magnetic stirrer at room temperature for 2 hours. Then, 3.8 g distilled water, 9.9 g absolute ethanol and 650 µL NH_3 are added into the same solution, respectively. Gelation is provided by the addition of 800 µL NH_4F into the same solution dropwise and the beaker is shaken gently during the slow addition of NH_4F into the solution to provide uniform gelation. After the formation of gel, it is separated into small pieces by using a spatula, absolute ethanol is added to cover the whole gel and the cap of the beaker is closed to prevent any gas inlet. The gel-ethanol mixture is left at room temperature for 8 hours. At the end of 8 hours, ethanol is poured off from the gel and 30 ml of hexane is added. The gel-hexane mixture is left in a previously prepared water bath at 45°C for 2 hours. Then, hexane is poured off from the gel and 30 ml hexane and 5 g TMCS are added slowly into gel respectively, to provide surface modification and maintain hydrophobicity to aerogel. At this point, water together with HCl vapor comes out. After the HCl vapor diminishes, formed water and hexane solution are taken in a graduated cylinder. The volume of water (the liquid at the bottom of the cylinder) is measured from the cylinder, hexane on top of water is added back into the gel, together with fresh hexane as much as the volume of water left in the graduated cylinder. Hence, the water is eliminated from the gel structure. After that the gel-hexane mixture is left in the water bath at 45°C for 5 hours. This step is repeated once more by pouring off the hexane first and then leaving the gel in the water bath at 45°C for another 5 hours. After taking the mixture from the water bath, the cap of the beaker is opened, hexane is poured off

and the gel is placed in an oven which was already set to 125°C. The gel is left drying in the oven for 2 hours.

5.1.2 Metal loading into silica aerogel

Metal is loaded into silica aerogel support to obtain an active catalyst in the SRM reaction for hydrogen production. Wet impregnation method is used to load metal into silica aerogel. In this study, copper and zinc metals were loaded.

5.1.2.1 Copper loading

Copper nitrate trihydrate ($Cu(NO_3)_2.3H_2O$, Merck) was used as the metal source. One gram silica aerogel is powdered, put in a beaker and placed on a magnetic stirrer to mix with 20 ml absolute ethanol for 20 minutes. In another beaker, 0.4021 g $Cu(NO_3)_2.3H_2O$ is dissolved in 10 ml absolute ethanol and is also placed on a magnetic stirrer for 20 min. After the solutions are mixed homogeneously, copper containing solution is added into silica solution dropwise. The resulting solution is left on a magnetic stirrer for 24 hours. At the end of mixing for 24 hours, the solution is left for drying in a furnace previously set to 60°C. Then the dried gel is powdered. This amount of metal is valid for 10 mole % copper loading. For 15 mole% copper loading, the recipe is the same except the amount of $Cu(NO_3)_2.3H_2O$ which is 0.6030 grams. In this study 10 and 15 mole% copper loaded silica aerogels were synthesized.

5.1.2.2 Copper and zinc loading

The same route with copper loading is followed. The only difference is loading copper and zinc into silica aerogel simultaneously by wet impregnation. Zinc nitrate tetrahydrate ($Zn(NO_3)_2.4H_2O$, Merck) was used as zinc source and $Cu(NO_3)_2.3H_2O$ was used as copper source. 0.1065 g $Zn(NO_3)_2.4H_2O$ dissolved in 10 ml absolute ethanol and 0.6029 g $Cu(NO_3)_2.3H_2O$ dissolved in 10 ml absolute ethanol are added dropwise into 1 g silica aerogel dissolved in 20 ml absolute ethanol dropwise. The

resulting solution is left for mixing for 24 hours on a magnetic stirrer. The mixed solution is then placed in a furnace previously set to 60°C till it becomes dry. When the gel is dried, it is powdered. In this study 15 mole% Cu and 10mole% Zn containing silica aerogel was prepared.

5.1.3 Calcination of the catalyst

Metal loaded silica aerogel catalyst, prepared by wet impregnation technique, is placed in a quartz reactor and heated from room temperature to 280, 450 or 700°C with a heating ramp of 1°C/min at 1.5 bar under air flow at 80 ml/min. When the furnace reaches the desired calcination temperature, the catalyst is kept at that temperature for 4 hours. After 4 hours, air flow is stopped and argon is let flow for 1 hour at the same flow rate (80 ml/min). For the reducing step of the calcined catalyst, hydrogen is passed from the catalyst with a rate of 80 ml/min at 5 bar prior to each experiment for 3.5 hours. After hydrogen passes, argon is let flow over the catalyst for 30 min before starting the experiment. The same procedure is followed for calcination with N_2. The only difference is passing N_2 instead of air and after N_2 flow, no inert gas is passed over the catalyst.

5.1.4 Naming of the synthesized catalysts

Metal loaded silica aerogel catalysts are synthesized. These synthesized catalysts are named in the following format XY-SA Z T(P) where X indicates the metal percent in moles, Y is the metal loaded, SA stands for silica aerogel, Z is the calcination gas, T is the calcination temperature and P is the reaction temperature. For instance 10Cu-SA Air/Ar 700(280) indicates that the catalyst is 10 mole% copper loaded, calcined under Air/Ar at 700°C and is reacted at 280°C.

5.2 Characterization Studies

Metal loaded and calcined silica aerogel catalysts were characterized by several methods in order to obtain further information about their physical and chemical

properties. The characterization techniques used in this study were: X-ray diffraction (XRD), N_2 adsorption/desorption (BET), Inductively coupled plasma mass spectroscopy (ICP-MS), Temperature programmed ammonia desorption (NH_3-TPD), Scanning electron microscopy (SEM) and Thermogravimetric analysis (TGA).

5.2.1 X-ray diffraction method (XRD): This analysis was performed to obtain information about the crystal structure of the synthesized catalysts. The form of the metal in silica aerogel and the particle sizes of metals/metal oxides were calculated using XRD pattern.

X-Ray Diffraction patterns were obtained in between 3-90° with a rate of 0.2°/min. copper filtered CuKα_1 radiation with a wavelength of 1.5406 Å was used to obtain XRD patterns. Rigaku Ultima-IV X-ray Diffraction device in METU Central Lab was used for this analysis.

5.2.2 N_2 adsorption/desorption analysis (BET): This analysis is based on the flowing of N_2 at 77 K from the pores of the catalyst under vacuum. The porous sample first adsorbs nitrogen at high pressures but when the pressure is lowered, the adsorbed nitrogen becomes desorbed by the catalyst. This way, pore structure, pore volume and size and surface are of the catalyst could be determined. Silica aerogel samples were degassed at 110°C for 4 hours before being analyzed. This analysis was performed under the relative pressure range of $0.0001<P/Po<0.99$ with Micromeritics Tristar II 3020 device at METU Department of Chemical Engineering.

5.2.3 Scanning electron microscopy (SEM): This analysis gives information about the surface topography of the catalyst. Before taking SEM images of silica aerogels, the samples were covered with Au/Pd in order to be conductive and interacted with the electrons. SEM images of silica aerogel catalysts were taken at METU Central Lab using QUANTA 400F Field emission high resolution scanning electron microscope having a resolution of 1.2 nm.

5.2.4 Inductively coupled plasma mass spectroscopy (ICP-MS): This analysis gives information about the type of the metal and its weight percent. Perkin Elmer DRC II at the METU Central Lab was used for this analysis. Prior to analysis, the samples were dissolved in HNO_3, HCl and HF.

5.2.5 Thermogravimetric analysis (TGA): This analysis is used to determine the coke formation in the catalyst after reaction. Information about thermal stability of the catalyst could also be learned. The catalysts used in the SRM reaction were heated from room temperature to 900°C with a heating rate of 10°C/min while air was flowing through the sample at a flow rate of 60 ml/min. Shimadzu DTG-60H device was used for this analysis, which is at Department of Chemical Engineering at METU.

5.2.6 Temperature programmed ammonia desorption (NH_3-TPD): Acid capacities of the synthesized catalysts were determined with this technique. The catalyst was degassed with Ar at a flow rate of 50 ml/min at 200°C for an hour. After that it is cooled down to room temperature and 5% NH_3- 95% He (v/v) gas mixture with a flow rate of 50 ml/min was sent over the catalyst for an hour. When the saturation of catalyst with NH_3 was over, the samples were waited under Ar flow for 10 minutes at 25°C and at a flow rate of 50 ml/min. The samples were then heated with He with a flow rate of 50 ml/min and a heating rate of 30°C/min to 125°C. After the samples were waited at 125°C for 10 minutes, the heating rate was changed to 10°C/min and the samples were heated with a flow rate of 50 ml/min from 125 to 600°C. By doing so, ammonia desorption curve is obtained. The analysis was done in the Department od Chemical Engineering at METU using Micromeritics TPx System.

5.3 Activity Tests

5.3.1 The reaction system

Activity tests and the calcination of the catalysts are done in the catalyst activation test system. After silica aerogel was synthesized, different metal loadings were done on this support to prepare a catalyst to be used in the steam reforming of methanol reaction to produce hydrogen. The experimental setup, constructed with this purpose was given in . The feed consisting of equal volumes of methanol and water is fed into the syringe pump and this alcohol-water mixture is evaporized at 130°C in an evaporator. The evaporator is used to vaporize the alcohol which is going to be used in steam reforming reaction. Vaporized methanol-water mixture is carried to the reactor via argon gas. The flow rate of argon is controlled by a mass flow controller device. The reactants (methanol-water) going out from the evaporator are fed into the reactor with the help of a heated pipeline. Thermocouples were placed around these pipelines in order to prevent the condensation of alcohol and water and to maintain its temperature. Reactor is placed inside a tubular furnace which is used to set the temperature of the reactor in which the SRM reaction will take place. The reactor is made up of quartz and has dimensions of 13 mm diameter and 680 mm length. The synthesized catalyst is placed inside the reactor. Argon and methanol-water in gas phase flows over the catalyst to prepare the reaction environment. The exit gas of the reactor follows a heated line and goes into the condenser. The condenser is used to condense the unreacted methanol and water. With this purpose, it is cooled down via a circulated water bath till -10°C. The exit stream of the reactor is which is eliminated from water and methanol is fed into a gas chromatograph, Shimadzu GC Plus 2010, to identify its chemical composition. Argon is also fed into the GC at a flow rate of 30 ml/min at 5 bar simultaneously with the exit stream. The exit stream leaves GC and is sent to ventilation after it passes from the bubblemeter.

Prior to be used in the experiment, the synthesized catalyst is calcined and then reduced with H_2 in order to convert metal oxides into metallic form. During the

calcination of the catalyst, the flow rate of the desired calcination gas (Air/Ar and N_2) is set by using the mass flow controllers. The calibration curves of mass flow controllers of argon and hydrogen gases were given in Appendix A. A bypass line is present in the experimental setup to provide direct entrance of these calcination gases into the reactor without being sent to evaporator. By using this line, the reactor exit stream is directly sent to ventilation instead of passing from the condenser and GC separately.

5.3.2 Experimental setup

Synthesized silica aerogel is placed in a quartz reactor and inserted in a tubular furnace. The reaction temperature is set by using the furnace. Water-methanol mixture (2.2 molar ratio) is fed into the evaporator at 0.9 ml/h via a syringe pump. Water-methanol mixture in the evaporator, which was evaporated at 130°C, is mixed with argon gas and the resulting gas mixture is moved to the reactor. Total flow rate of the gas which was sent to the reactor (argon, methanol and water vapor) is 50 ml/min. The exit stream of the reactor is first passed from the condenser where it is separated from the unreacted water and methanol, and then the gas is sent to GC. There are two thermal conductivity detectors (TCD) in GC both for the liquid and gas analyses. For liquid analysis, a Rt- Q-Bond column with 0.53 mm inside diameter (ID) and 30 m length is used. For gas analysis, a Carboxen 1010 Plot column having the same properties with the liquid column (ID and the length), was used. Helium is fed into the GC when analyzing the liquids and Ar is fed for gas analyses. By using the GC, composition analysis of the reactor exit stream is carried out. A suitable analysis method to detect the chemical composition of the reactor exit stream developed in Schimadzu GC-2010 Plus. The method is given on Table 3. The length of the analysis is 21.85 minutes which can be used both for liquid and gas analysis. In order to obtain the mole numbers of components in the reactor exit stream, beta factors (β) are calculated. Beta factors are calculated by feeding a standard gas mixture consisting of 1% H_2, 1% CO_2, 1% CH_4, 1% CO, 1% C_2H_4 in Ar to the GC for five times.

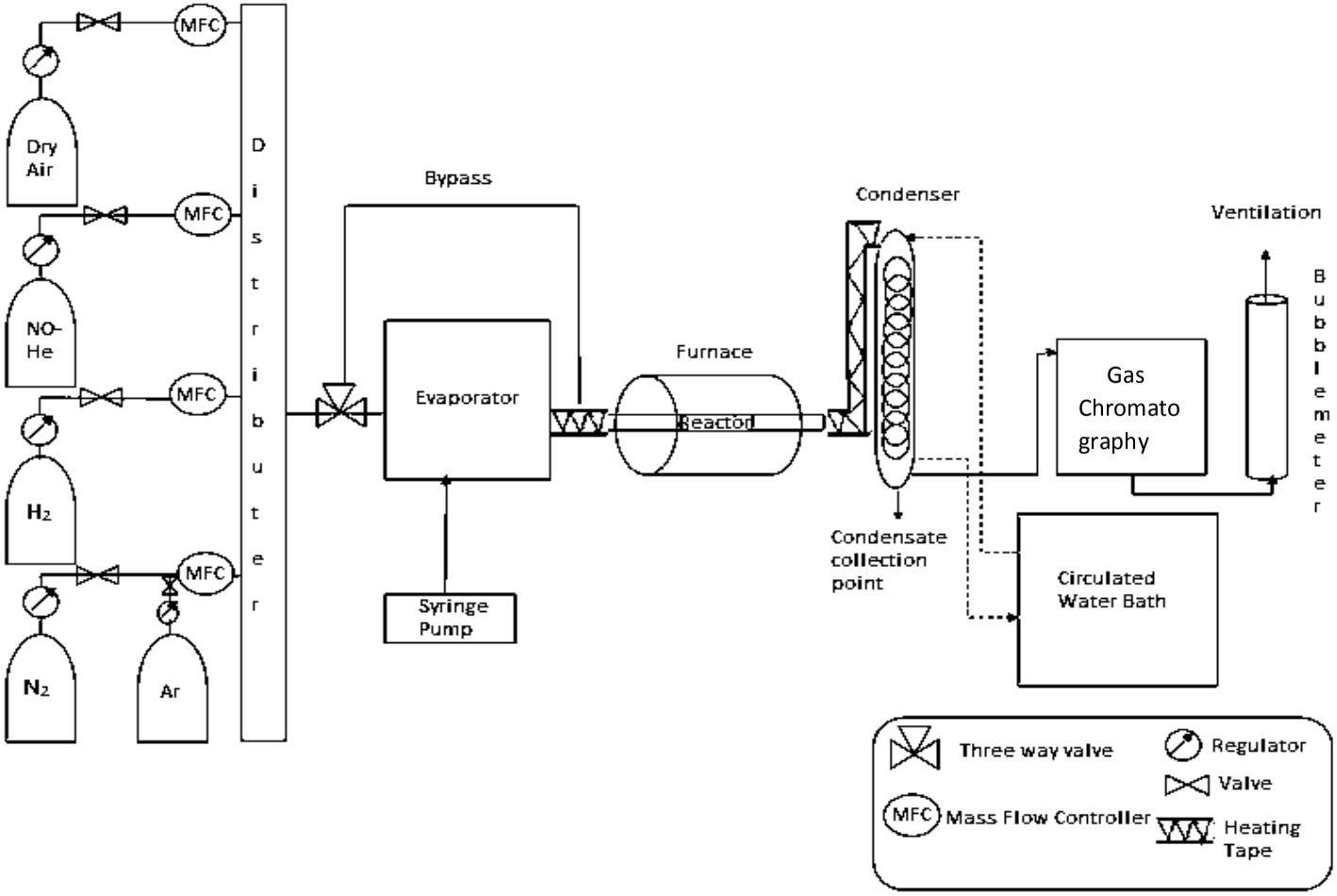

Figure 3: Flow diagram of hydrogen production setup

Table 3: Temperature program used in GC for liquid and gas analysis

Rate (°C/min)	Temperature (°C)	Retention Time (min)
-	35	7.5
23	250	5
21	36	-

5.3.3 Experimental method

Catalyst (0.15 g) is placed inside the quartz reactor and then inserted in a tubular furnace to be used in alcohol reforming reaction. After that the catalyst is reduced. GC is turned on before starting the experiment. Mass flow controller of Ar is set to 30 ml/min and the water bath is set to -10°C to condensate the methanol and water in the reactor exit gas. GC spectrum is taken once while only the carrier gas Argon is passing through the experimental setup. The tubular furnace is set to the desired reaction temperature and is heated from room temperature to that temperature at a heating rate of 7°C/min. After that the syringe pump, containing equal volumes of methanol and water, is turned on and evaporator is set to 130°C. Pipelines at the furnace inlet and outlet are covered with heating tapes which are also set to 130°C. The flow rate of argon and methanol-water vapor mixture is controlled by the soap bubblemeter, which is supposed to be 50 ml/min. After the total flow rate becomes 50 ml/min, the first spectrum of the reaction is taken using GC. Since the coming order of the components in the reactor exit stream is known, identification of these gases (hydrogen, carbon monoxide, carbon dioxide, etc.) is easily made. Steam reforming of methanol is performed under a constant rate of carrier gas (30 ml/min) at 5 bar and constant feed flow rate of 0.9 ml/h. Experimental conditions of all hydrogen production reactions were given on Table 4. Working conditions of the method used in GC for gas and liquid analysis were given on Table 5 and Table 6, respectively.

Table 4: All parameters and catalysts tested in SRM reaction

Catalyst	Calcination Temperature (°C)	Calcination Gas	Metal (mol%)	Reaction Temperature (°C)	Reaction Time (h)	Adsorbent
10Cu-SA Air/Ar 280(280)	280	Air-Ar	Cu (10)	280	5	No
10Cu-SA Air/Ar 450(280)	450	Air-Ar	Cu (10)	280	5	No
10Cu-SA Air/Ar 700(280)	700	Air-Ar	Cu (10)	280	5	No
10Cu-SA N_2 280(280)	280	N_2	Cu (10)	280	5	No
10Cu-SA N_2 450(280)	450	N_2	Cu (10)	280	5	No
10Cu-SA N_2 700(280)	700	N_2	Cu (10)	280	5	No
15Cu-SA Air/Ar 700	700	Air-Ar	Cu (15)	300 280 275 250 225 200	5	No
15Cu-SA Air/Ar 700(280)	700	Air-Ar	Cu (15)	280	22.73	No
15Cu-10Zn-SA Air/Ar 700(280)	700	Air-Ar	Cu (15) Zn(10)	280	5	No
15Cu-SA Air/Ar 700(280)-0.1Huntite	700	Air-Ar	Cu (15)	280	5	Yes
15Cu-SA Air/Ar 700(225)-0.1Huntite	700	Air-Ar	Cu (15)	225	5	Yes
15Cu-SA Air/Ar 700(200)-0.1Huntite	700	Air-Ar	Cu (15)	200	5	Yes
15Cu-SA Air/Ar 700(200)-0.15Huntite	700	Air-Ar	Cu (15)	200	5	Yes
15Cu-SA Air/Ar 700(200)-0.10MgO	700	Air-Ar	Cu (15)	200	5	Yes
15Cu-SA Air/Ar 700(200)0.15 Hydrotalcide	700	Air-Ar	Cu (15)	200	5	Yes
Hifuel R-120	-	-	Cu, Zn, Al, Na	280	5	No

Table 5: Analysis conditions of GC for gaseous products

Furnace Temperature (°C)	250
Injection Temperature (°C)	200
Detector type and temperature (°C)	TCD-250
Column pressure (psi)	3.89
Analysis time (min)	21.85
Carier gas and rate (ml/min)	Ar-50
Split ratio	1/1

Table 6: Analysis conditions of GC for liquid products

Furnace Temperature (°C)	250
Injection Temperature (°C)	200
Detector type and temperature (°C)	TCD-250
Column pressure (psi)	3.89
Analysis time (min)	21.85
Carier gas and rate (ml/min)	He-258
Split ratio	1/50

CHAPTER 6

RESULTS AND DISCUSSION

Characterization results of Cu loaded silica aerogel catalysts with different metal/Si ratios, calcination gases and temperatures are given in Characterization Results of Catalysts part. Performance results of these catalysts in the SRM reaction are given in Activation Test Results part.

6.1 Characterization Results of the Catalysts

Synthesized catalysts were characterized using several techniques. XRD, BET, SEM, ICP, TGA and TPD results of the synthesized catalysts are given in this section.

6.1.1 X-ray diffraction (XRD) results

XRD patterns of 10 mole% Cu loaded silica aerogel catalysts calcined under N_2 flow at different temperatures are given in Figure 4. Each XRD pattern given in Figure 4 exhibits a broad peak around 22.8°, which is a characteristic peak of silica and is in accordance with the literature (Hu, 2016). 10Cu-SA N_2 280 catalyst has shown peaks at 2θ values of 36.50 and 43.44°. 10Cu-SA N_2 450 catalyst has shown peaks at 2θ values of 35.32 and 38.82° (PDF card no: 01-070-6829 given in Appendix B). Lastly, 10Cu-SA N_2 700 catalyst has shown peaks at 2θ values of 35.54, 38.74 and 61° (PDF card no: 01-089-5898 given in Appendix B). All of these peaks belong to copper oxide (CuO). All synthesized catalysts which were not reduced with H_2 contain CuO.

XRD patterns of 10 mole% Cu loaded silica aerogel catalysts calcined under Air/Ar flow at different temperatures are given in Figure 5.

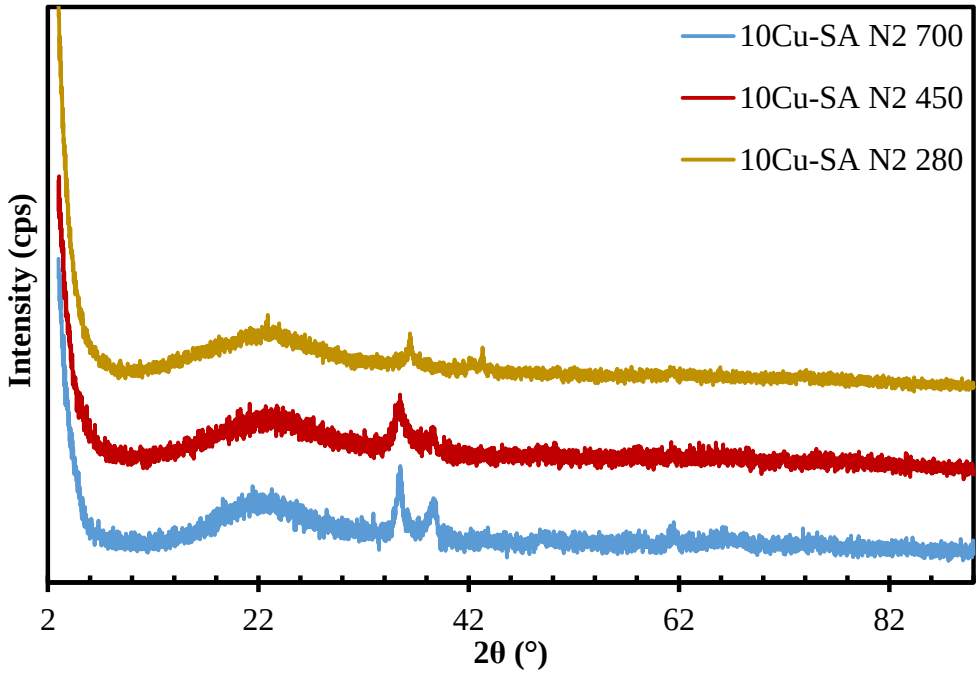

Figure 4: XRD patterns of 10% Cu loaded silica aerogels calcined with N_2 at different temperatures

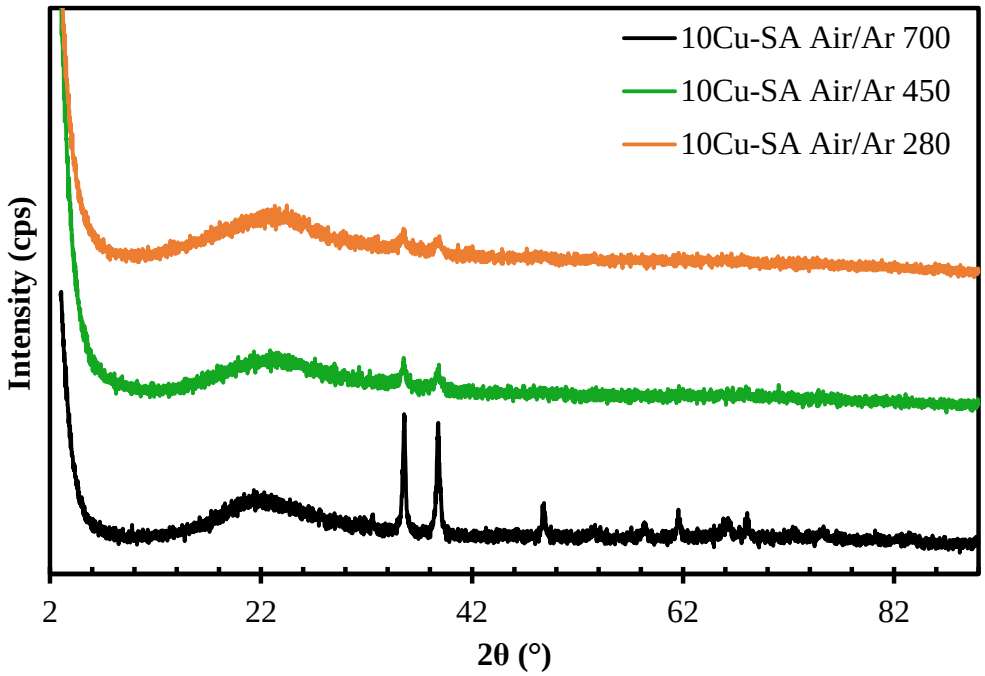

Figure 5: XRD patterns of 10% Cu loaded silica aerogels calcined with Air/Ar at different temperatures

When Figure 5 is examined, 10Cu-SA Air/Ar 280 catalyst has shown peaks at 2θ values of 35.58 and 38.9° whereas 10Cu-SA Air/Ar 450 catalyst has shown peaks at 2θ values of 35.60 and 38.88°. All these peaks belong to CuO (PDF card no: 01-080-0076 given in Appendix B). Lastly, 10Cu-SA Air/Ar 700 catalyst has shown peaks at 2θ values of 36.60, 38.80, 48.78, 58.84, 61.72, 66.26 and 68.08°. Again these peaks are characteristic peaks of CuO (PDF card no: 01-080-0076).

When Figure 4 and 5 are examined together it can be concluded that copper has been successfully loaded into silica aerogel framework. Cu loaded silica aerogels calcined under Air/Ar have a tendency of increasing CuO crystallite size with the increase of calcination temperature. This trend can be seen from the sharpening of d_{100} peaks in Figure 5 from top to bottom.

XRD patterns of pure, 10 mole% and 15 mole% Cu loaded silica aerogel are given in Figure 6.

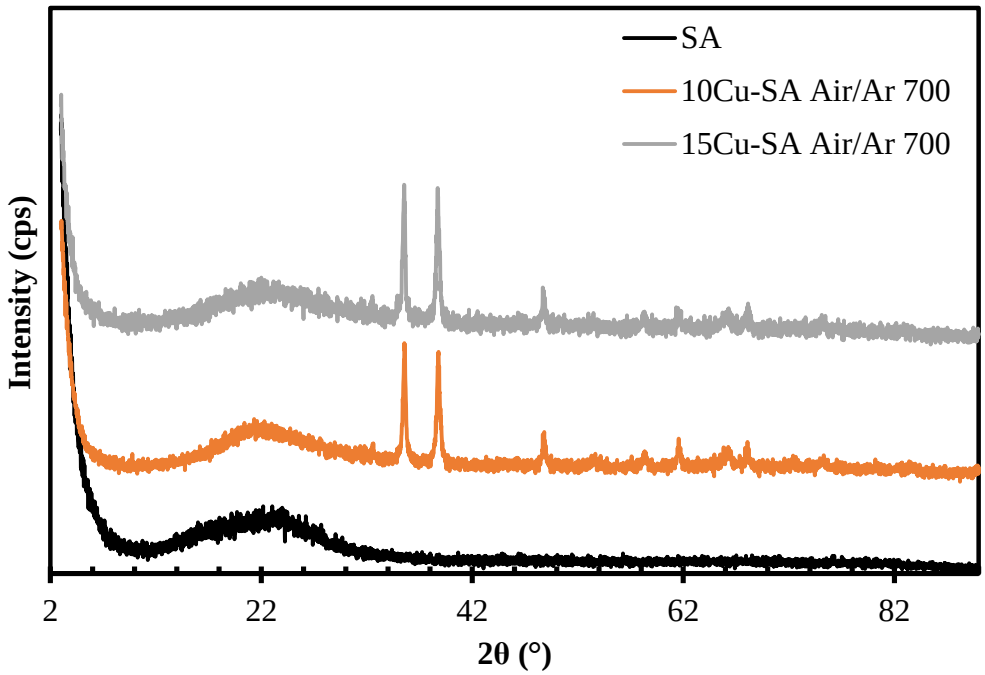

Figure 6: XRD patterns of pure and 10% and 15% Cu loaded silica aerogels calcined with Air/Ar at 700°C

The characteristic broad peak of amorphous silica at 2θ 22.8° is also seen in Figure 6 for all catalysts. This indicates that the structure of aerogel is not disturbed with metal loading. 15Cu-SA Air/Ar 700 catalyst has shown peaks around 2θ values of 35.55, 38.65, 48.74, 58.20, 61.60, 66.20 and 68.07° all of which belong to CuO. XRD data of PDF card no: 01-089-5898 is given in Appendix B. General XRD patterns of 15% and 10% Cu loaded catalysts coincide with each other except the fact that intensity of peaks has increased with the increase in metal loading. XRD paterns of Cu loaded catalysts after the SRM reaction are given in Figure 7.

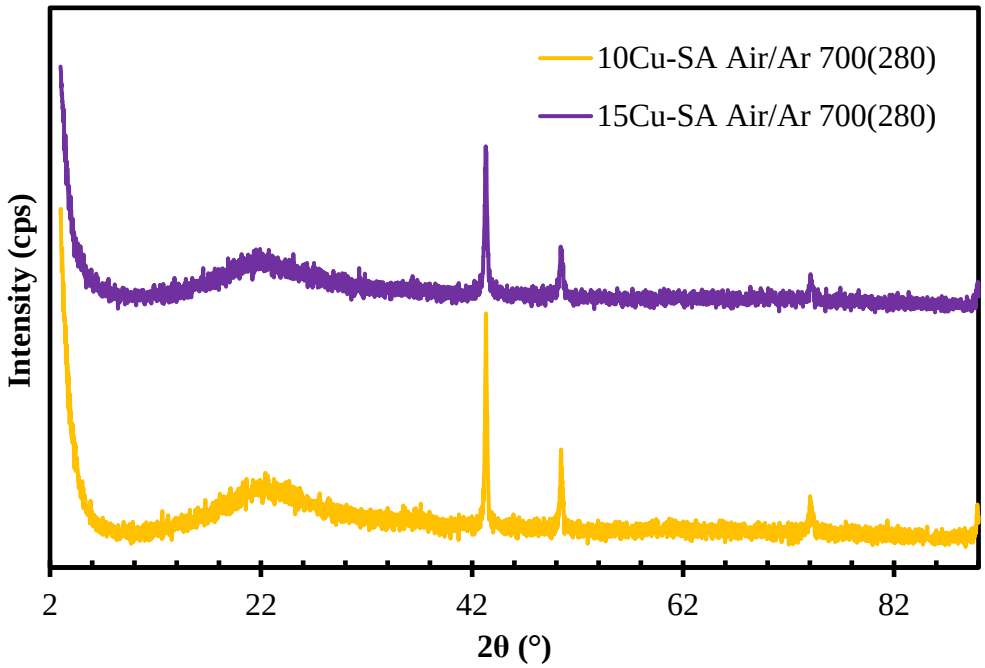

Figure 7: XRD patterns of 10% and 15% Cu loaded silica aerogels after reaction at 280°C.

By looking at Figure 7, the characteristic broad peak of amorphous silica at 2θ 22.8° is maintained in both catalysts. 10Cu-SA Air/Ar 700(280) catalyst has shown peaks around 2θ 43.32, 50.44 and 74.1° whereas 15Cu-SA Air/Ar 700(280) has shown peaks at 2θ 43.34, 50.4 and 74.08°. These two patterns almost coincide with each other except a difference in the intensity and the peaks are attributed to characteristic peaks of Cu (PDF card no: 01-070-3039 given in Appendix B). No CuO particles were detected after reaction because the catalysts were reduced prior to the reaction.

XRD patterns of Cu-Zn loaded catalysts before and after SRM are given in Figure 8.

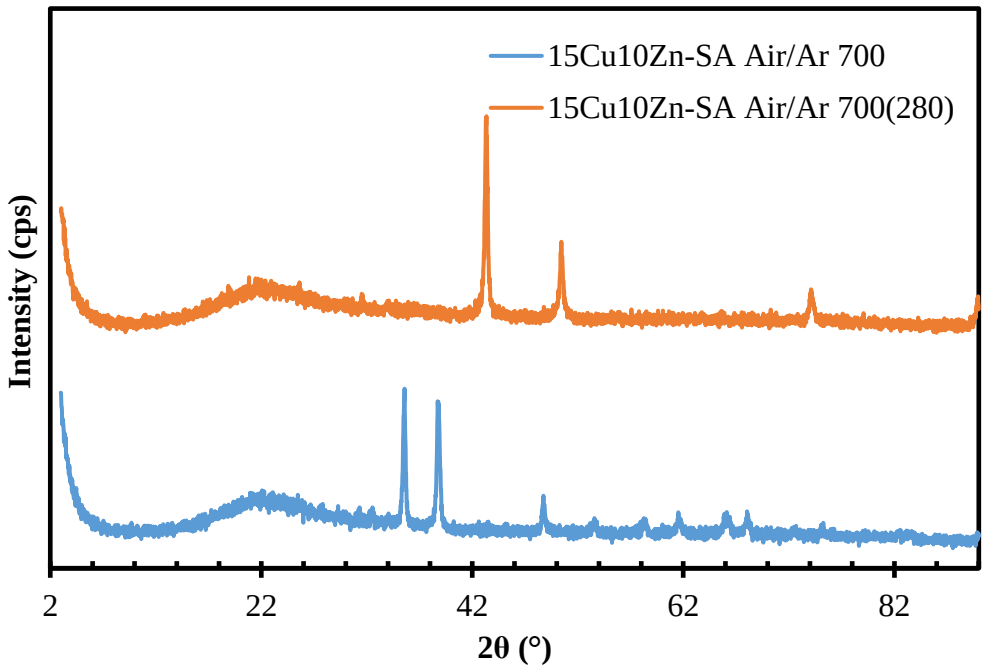

Figure 8: XRD patterns of 15% Cu and 10% Zn loaded silica aerogels before and after reaction at 280°C.

From Figure 8, different peaks were observed for the same catalyst before and after the experiment. In the XRD pattern of 15Cu10Zn-SA Air/Ar 700 catalyst, which represents the fresh catalyst, peaks around 2θ 35.54, 38.74, 48.8, 53.64, 58.46, 61.54, 65.94, 67.96 and 75.26° were observed which are CuO peaks (PDF card no: 01-070-6829). All PDF cards were given in Appendix B. At 2θ 43.3, 50.46 and 74.2°, peaks were observed for 15Cu10Zn-SA Air/Ar 700(280) catalyst. These peaks are indicating the presence of Cu particles. After reaction at 280°C, XRD pattern of the catalyst showed the formation of Cu particles. Even though both catalysts contained Zn, no Zn peaks were observed. The reason of this was attributed to the homogeneous dispersion of Zn within silica aerogel.

Crystallite sizes of metals are calculated by using XRD patterns and Scherrer equation given below :

$$t_{crystallite} = \frac{c\lambda}{B\cos\theta}$$

where c is the crystallite size factor which was taken as 0.89 for all calculations. λ is the wavelength of $CuK_{\alpha 1}$ radiation (0.154 nm). B is the full width at half maximum in radian and 2θ is the Brag angle in radian. Crystallite sizes of CuO particles for Cu loaded silica aerogel catalysts which are calcined under different gases and temperatures are given in Table 7.

Table 7: Crystallite sizes of Cu loaded silica aerogels

Catalyst	CuO Crystallite Size (nm)
10Cu-SA Air/Ar 700	31.01
10Cu-SA Air/Ar 450	14.47
10Cu-SA Air/Ar 280	10.33
10Cu-SA N_2 700	13.09
10Cu-SA N_2 450	6.71
10Cu-SA N_2 280	11.03
15Cu-SA Air/Ar 700	34.37
15Cu10Zn-SA Air/Ar 700	35.11

By looking at Table 7, a directly proportional relation between calcination temperature and crystallite sizes can be seen for the catalysts calcined with Air/Ar. The same relation is not observed for the catalysts calcined with N_2. Crystallite sizes of catalysts calcined with Air/Ar are larger than those calcined with N_2. In addition, similar results were obtained in the crystallite sizes of 15Cu-SA Air/Ar 700 and 15Cu10Zn-SA Air/Ar 700 catalysts after the SRM reaction. 37.74 and 33.54 nm crystallite sizes were obtained from these catalysts, respectively.

6.1.2 N_2 adsorption/desorption results

N_2 adsorption/desorption isotherms of pure and 10% Cu loaded silica aerogels are given in Figure 9. According to Brauner-Deming-Deming-Teller (BDDT)

classification, BET isotherms of all catalyst exhibited a characteristic mesoporous Type IV isotherm. All synthesized catalysts had hysteresis which results from capillary condensation in mesopores and differences in adsorption/desorption mechanisms. Except pure silica aerogel, which had H_3 hysteresis at P/P_0 0.65, all other catalysts show H_1 type of hysteresis. It was seen that pure silica aerogel had micropores at P/P_0 0.02. Total microporosity of pure silica aerogel was 4.78%.

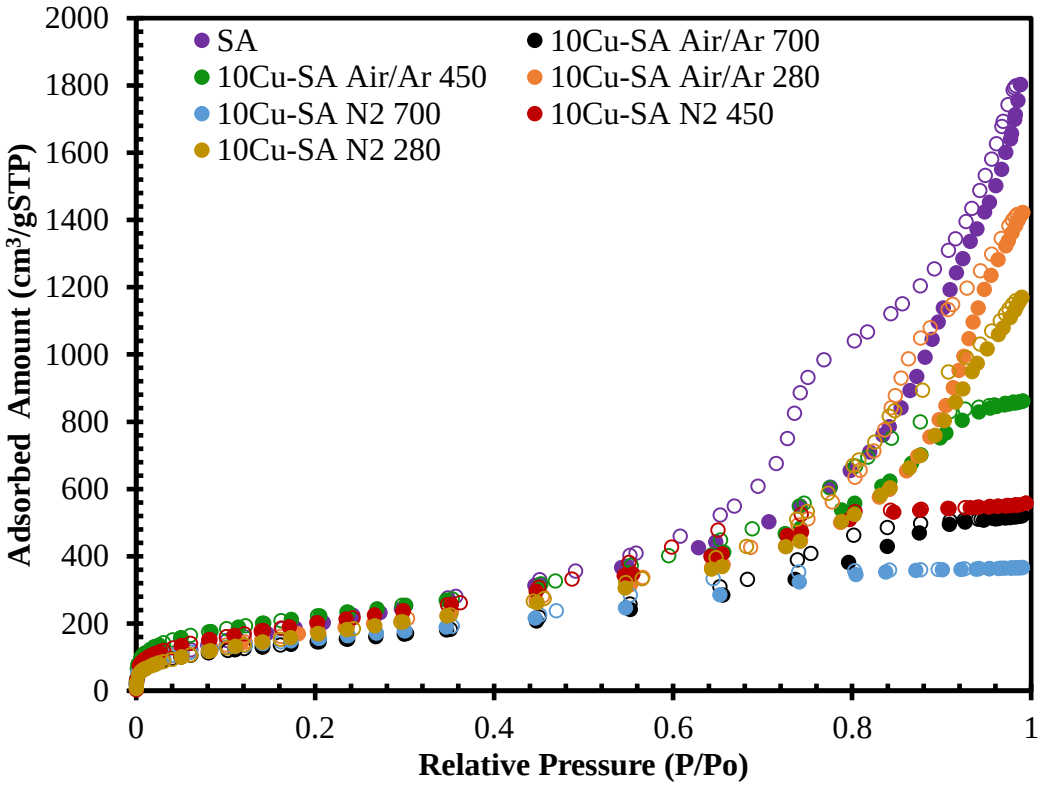

Figure 9: N_2 adsorption/desorption isotherms of pure and 10% Cu loaded silica aerogels (filled points indicate adsorption, empty points indicate desorption branches).

Pore size distribution of pure aerogel was not expected narrow due to the non-parallel array of adsorption/desorption isotherms. On the other hand, pore size distributions of the catalysts with H_1 hysteresis were narrower compared to pure aerogel. This result is in accordance with pore size distribution of Cu loaded catalysts given in Figure 10.

Location of copper particles into mesopores of aerogel resulted in a decrease in mesoporosity percent while triggering an inrease in microporosity. For instance

microporosity of Cu loaded and Air/Ar calcined catalysts has increased from 4.78% to 13.88% while Cu loaded and N_2 calcined catalysts' increase in microporosity was from 4.78% to 21.62%. These results can be seen in Table 8.

Increased calcination temperature caused the pore diameters to shift to the left for both gases. This was due to the enhanced blocking of silica aerogel particles with copper with an increase in the calcination temperature. The location of copper particles was mainly onto meso and macropores of the aerogel which resulted in an increase in the microporosity (Table 8). The hysteresis gap observed in pure silica aerogel also became narrower with copper loading. When physical properties of Cu loaded silica aerogels calcined under different gases and temperatures were compared, it can be said that aerogels calcined with N_2 had more microporosity than Air/Ar calcined catalysts at the same temperature. Surface areas of catalysts calcined with different gases are close to each other. However, there are differences in pore diameters. Surface areas and pore volumes of the catalysts decreased with the copper loading because copper particles might have caused silica pores to be blocked. These results are in accordance with BET isotherms.

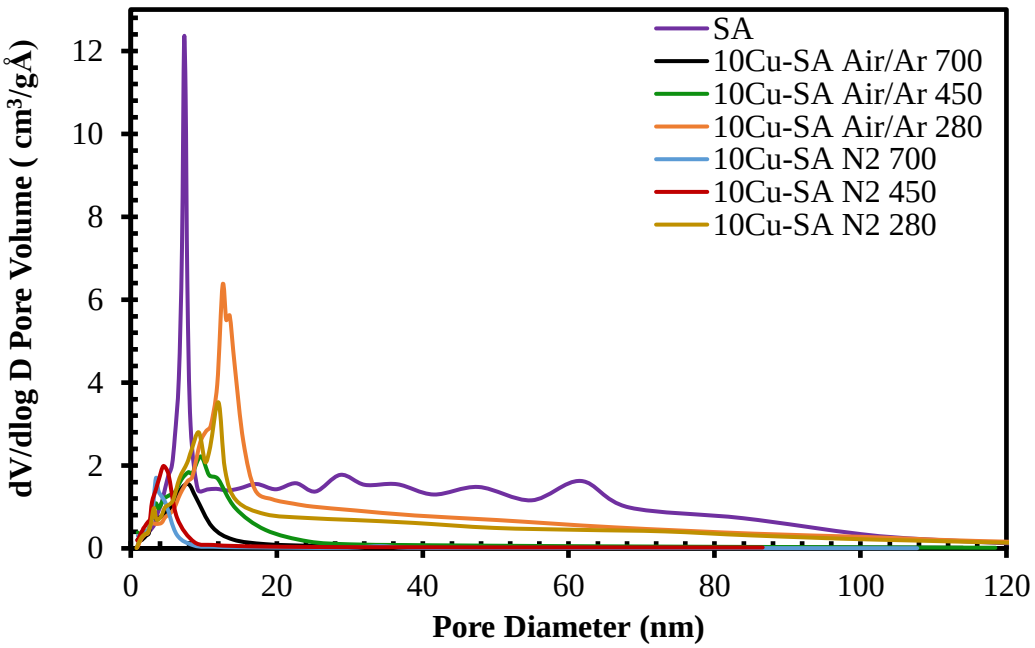

Figure 10: Pore size distributions of pure and 10% Cu loaded silica aerogels

Physical properties of pure and 10% -15% Cu loaded silica aerogels are given in Table 8.

Table 8: Physical properties of pure, 10% and 15% Cu loaded silica aerogels

Catalyst	Multipoint BET Surface Area, (m^2/g)	BJH Desorption Pore Volume, (cc/g)	BJH Desorption Average Pore Diameter, (nm)	Microporosity %
Pure Silica Aerogel	814.66	3.31	8.60	4.78
10Cu-SA Air/Ar 280	696.29	2.20	8.48	6.28
10Cu-SA N_2 280	679.16	1.81	6.94	6.49
10Cu-SA Air/Ar 450	798.92	1.35	9.6	13.37
10Cu-SA N_2 450	761.55	0.87	4.48	17.24
10Cu-SA Air/Ar 700	535.35	0.82	4.16	13.88
10Cu-SA N_2 700	562.90	0.59	5.15	21.62
15Cu-SA Air/Ar 700	568.12	1.24	5.66	9.96

N_2 adsorption/desorption isotherms of pure and 10%-15% Cu loaded Air/Ar calcined catalysts are given in Figure 11.

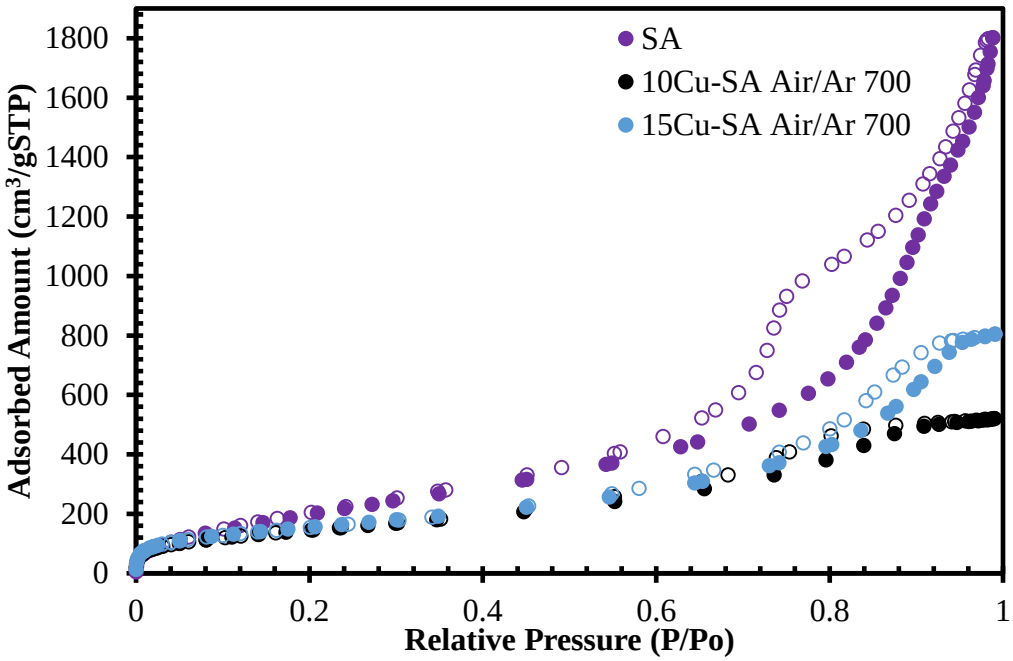

Figure 11: N_2 adsorption/desorption isotherms of pure and 10%-15% Cu loaded Air/Ar calcined catalysts (filled points indicate adsorption, empty points indicate desorption branches).

Type IV isotherm of pure silica aerogel is preserved with metal loading (Figure 11) but a change in Hysteresis from H_3 to H_1 was observed. Compared to silica aerogel, close location of adsorption/desorption isotherms in H_1 type of hysteresis could be a reason of more narrow pore size distribution in metal loaded catalysts. A decrease in the surface area of the catalyst with metal loading is an expected result. BET surface areas of 10 and 15% copper loaded catalysts are close to each other (Table 8). When the microporosity percent of these two catalysts are compared, it is seen that 15% copper loaded catalyst possessed less microporosity percent. This result can be arising from fewer location of CuO particles into meso and macropores in 15% Cu loaded catalyst. Indeed, some of the CuO particles in this catalyst also might be located into micropores.

When the pore size distribution graph of 15% Cu loaded catalyst is examined (Figure 12), two peaks at 4.94 and 13.24 nm are seen. This means that the pore size distribution in this catalyst is not monotype, which is in accordance with the hysteresis gap of 15% Cu loaded catalyst in Figure 11. Pore size distribution peak of 10% Cu loaded catalyst is also bimodal with 3.62 and 9.33 nm. All 10% copper loaded and Air/Ar calcined catalysts exhibited bimodal pore size distribution, like 10Cu-SA N_2 280 catalyst. On average, 15% Cu loaded catalyst has greater pore diameter than 10% Cu loaded catalyst. This result makes us think that copper metal is located into meso and macopores in both catalysts, which is in accordance with Table 8. Average pore diameter of 15% Cu loaded catalyst is 5.66 nm while that of 10% Cu loaded catalyst is 4.16 nm.

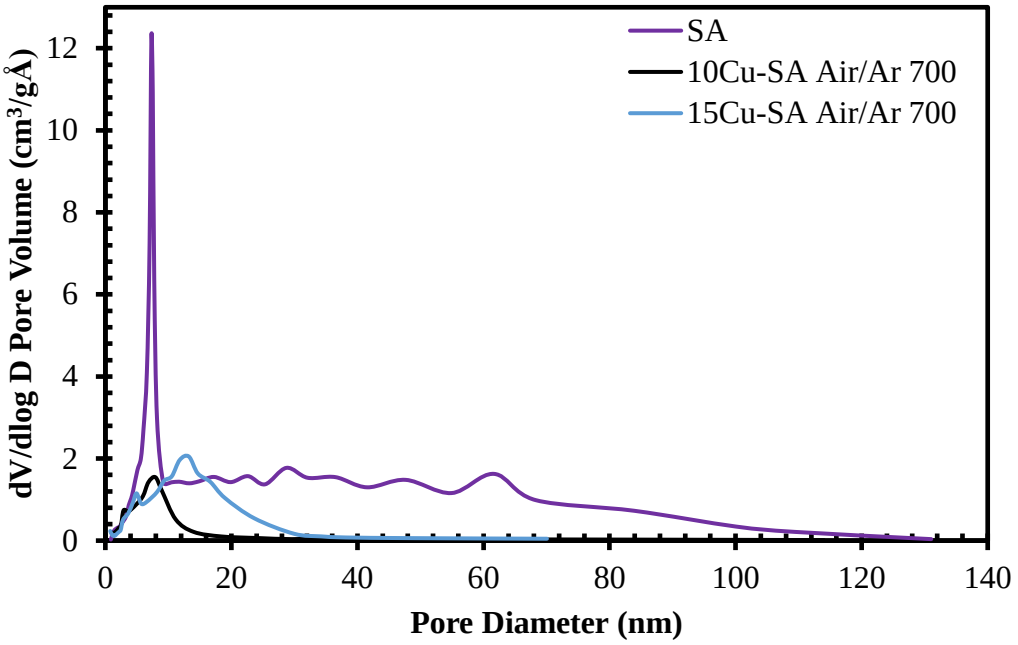

Figure 12: Pore size distributions of pure, 10 and 15% Cu loaded silica aerogels

6.1.3 Scanning electron microscopy (SEM) results

The images formed by transmitting high energy electrons from pure silica aerogel are given in Figure 13.

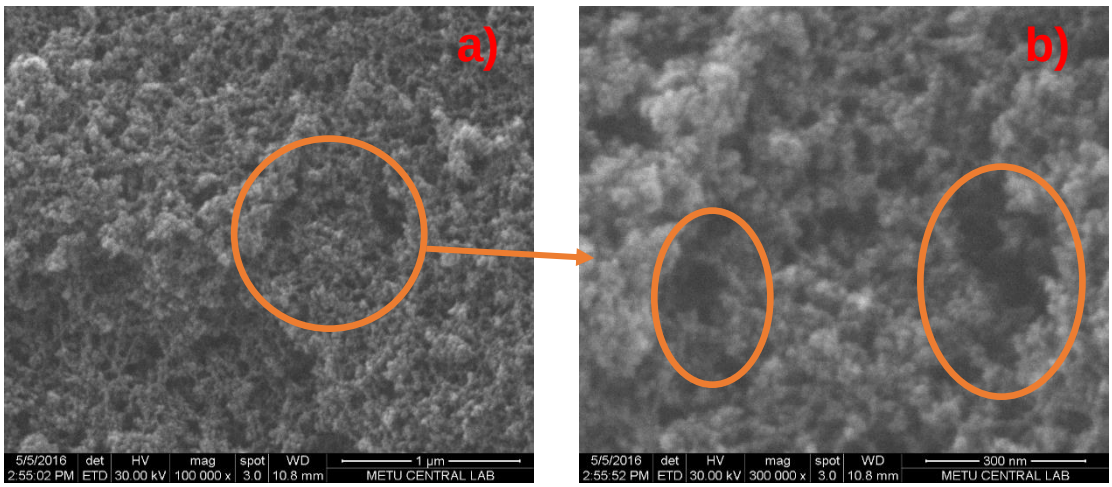

Figure 13: SEM images of pure silica aerogel at 100000X **(a)** and 300000X **(b)** magnifications

Porous morphology of silica aerogel can be seen in Figure 13. The gaps between the pores represent different sized pores in silica aerogel structure and these results match up with the pore size distribution (orange circles in Figure 13b). EDX result

of Figure 13 is given in Figure 14. By looking at Figure 14, it is possible to say that the catalyst contains Si and O elements. Au and Pd elements are also seen due to the covering of the samples before SEM imaging. Carbon element comes from the carbon tape. Silica aerogel has a highly intense Si peak, as can be seen from EDX results.

SEM images of copper loaded silica aerogels calcined with Air/Ar and N_2 at 450°C are given in Figure 15 and Figure 16, respectively.

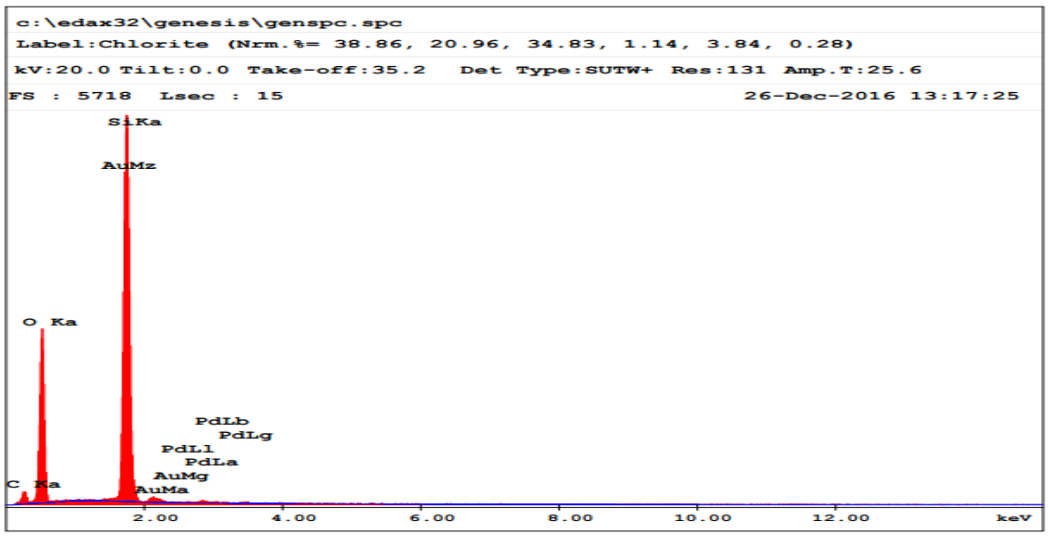

Figure 14: EDX spectrum of pure silica aeogel

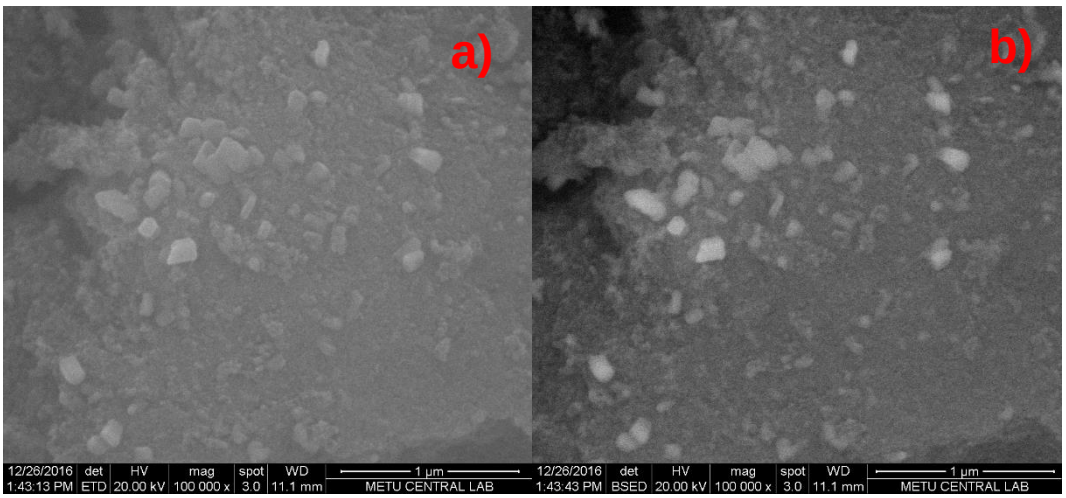

Figure 15: SEM **(a)** and back scattered electron images **(b)** of 10% copper loaded and Air/Ar calcined catalyst at 450°C at 100000X magnification

SEM image of 10% Cu loaded Air/Ar calcined catalyst at 450°C is given in Figure 15a. Back scattered image of this catalyst is given in Figure 15b. The bright areas in Figure 15b are thought to be copper. It could be said that copper distribution was seen in the material. Back scattered images show the non-homogeneous distribution of copper particles.

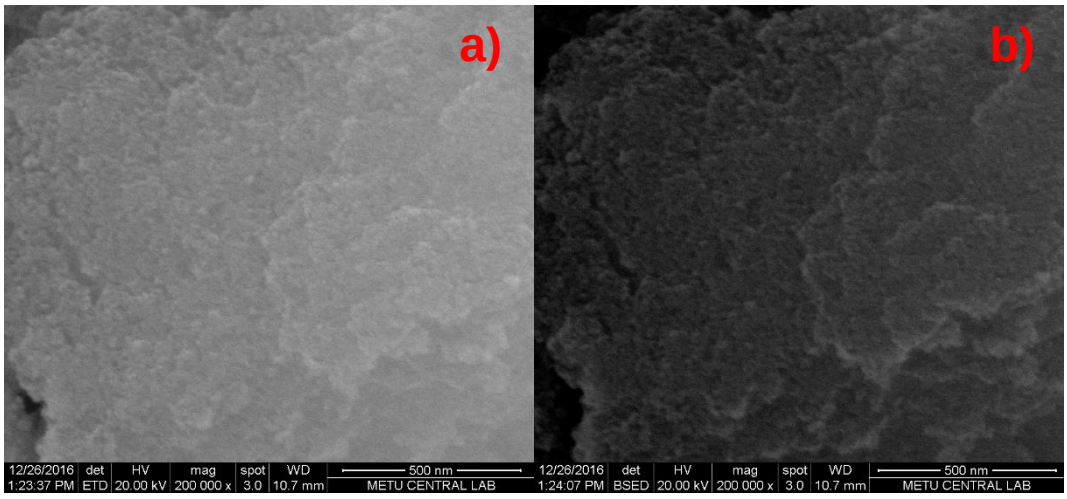

Figure 16: SEM **(a)** and back scattered electron images **(b)** of 10% copper loaded and N_2 calcined catalyst at 450°C at 200000X magnification

When Figures 16a and 16b are examined a layer formation in silica aerogel was observed; in these images copper particles are not obviously distinguishable. EDX spectra of Figures 15a and 16a are given in Figures 17 and 18, respectively.

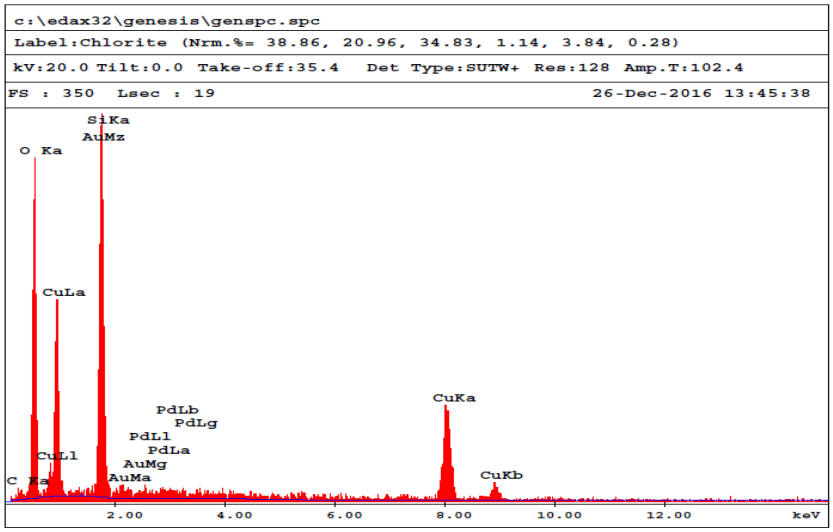

Figure 17: EDX spectrum of 10% copper loaded and Air/Ar calcined catalyst at 450°C.

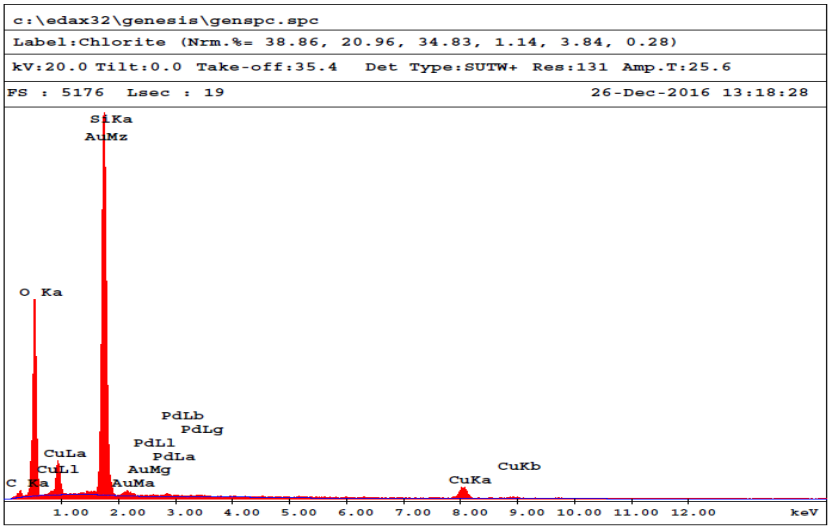

Figure 18: EDX spectrum of 10% copper loaded and N_2 calcined catalyst at 450°C.

Figure 17 points out that the copper peaks are more intense than Figure 18. This could also be supported by SEM images (Figure 16).

Copper peaks in catalysts calcined with N_2 are less distinct than the catalysts calcined with Air/Ar (Figure 18) which shows the non-homogeneous copper dispersion in silica aerogel. SEM and back scattered electron images of the catalysts calcined at 700°C with various gases are given in Figures 19 and 20.

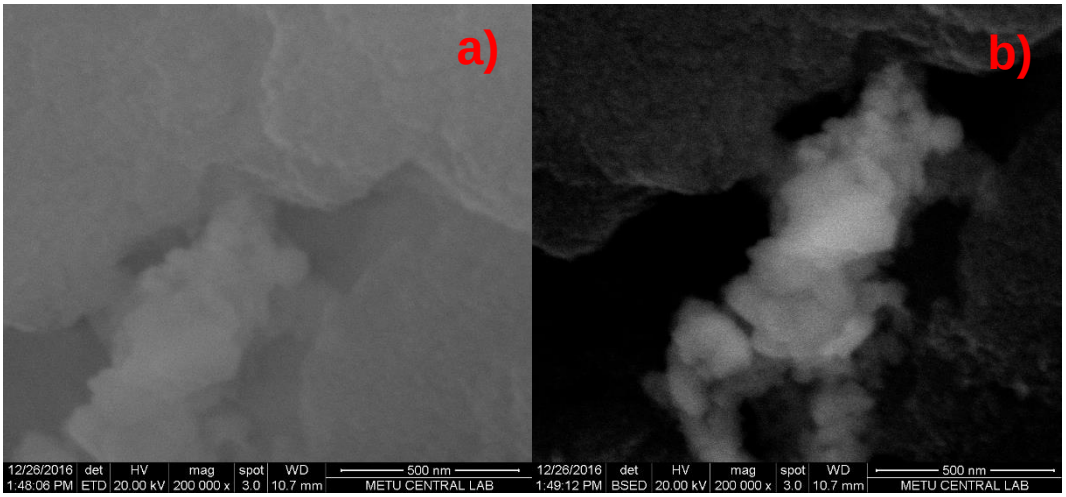

Figure 19: SEM **(a)** and back scattered electron images **(b)** of 10% copper loaded and Air/Ar calcined catalyst at 700°C at 100000X magnification SEM

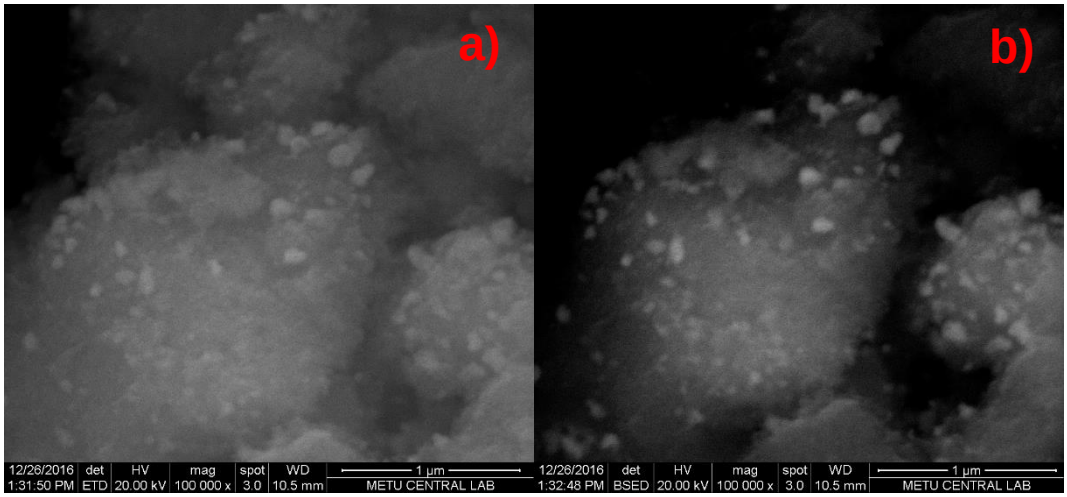

Figure 20: SEM **(a)** and back scattered electron images **(b)** of 10% copper loaded and N_2 calcined catalyst at 700°C at 200000X magnification

As can be seen from Figure 19a and 19b, copper is found as big clusters in silica aerogel. A reason of this can be the sintering of copper at 700°C. Uniform dispersion of copper particles can be seen from Figure 20a and b. EDX spectra of both samples are given in Figures 21 and 22.

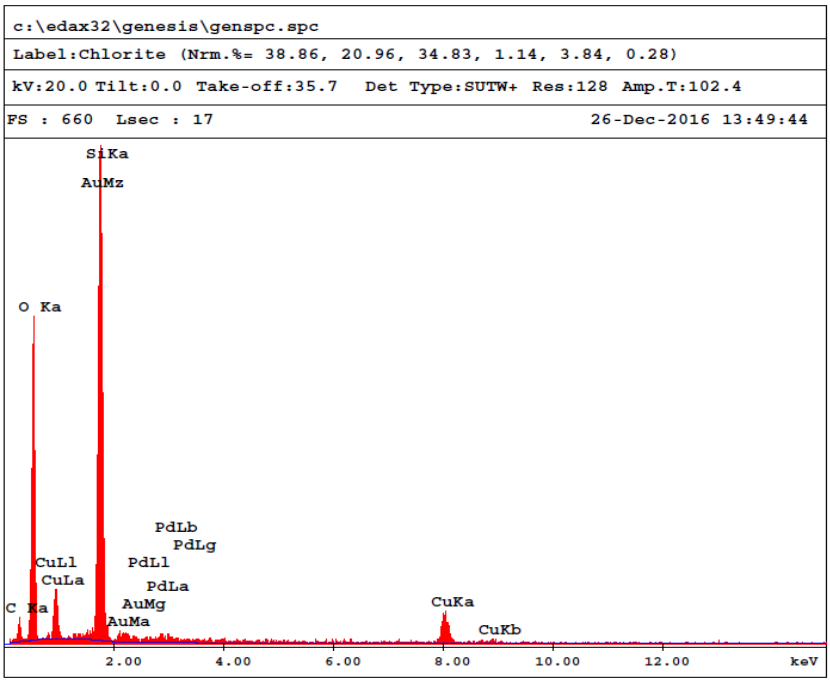

Figure 21: EDX spectrum of 10% copper loaded and Air/Ar calcined catalyst at 700°C.

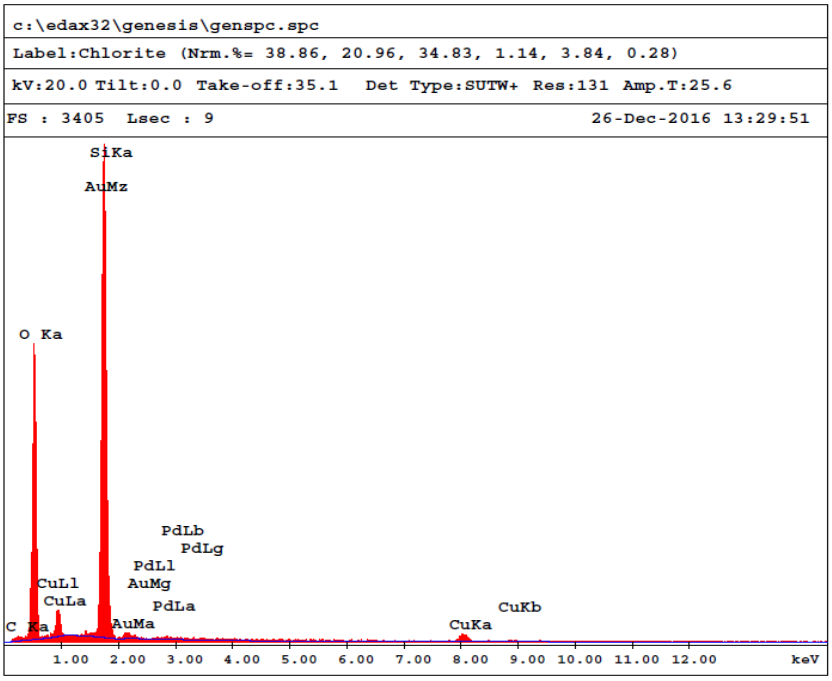

Figure 22: EDX spectrum of 10% copper loaded and N_2 calcined catalyst at 700°C.

When Figures 21 and 22 are compared, copper peak can be seen in both samples which showed that copper was successfully loaded into silica aerogel. SEM images of 10% copper loaded catalysts calcined with N_2 and Air/Ar at 280°C are given in Figures 23 and 24, respectively.

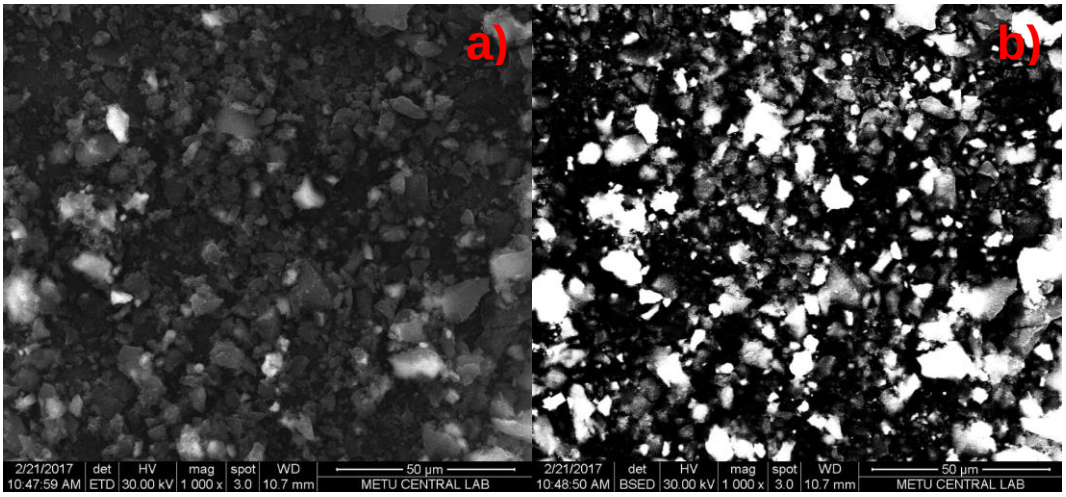

Figure 23: SEM **(a)** and back scattered electron images **(b)** of 10% copper loaded and N_2 calcined catalyst at 280°C at 1000X magnification

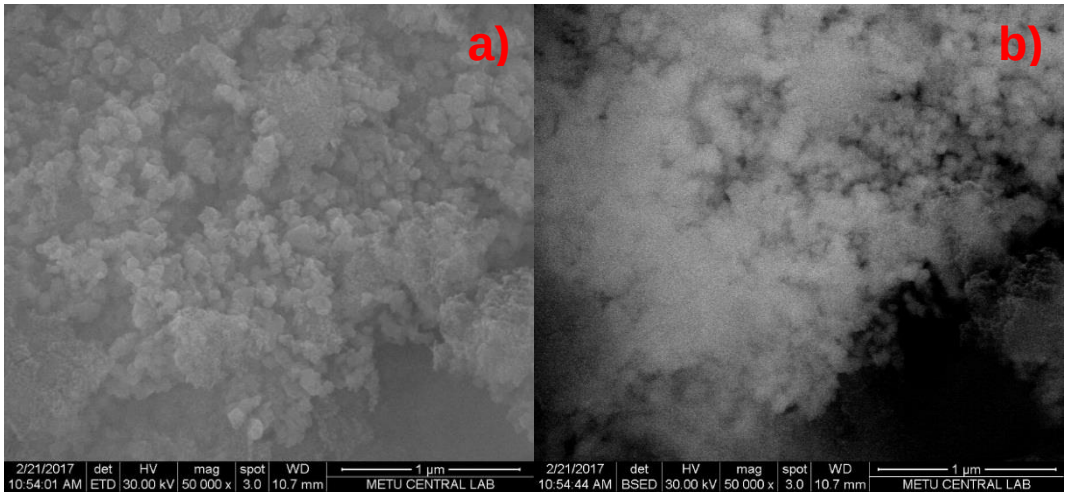

Figure 24: SEM **(a)** and back scattered electron images **(b)** of 10% copper loaded and Air/Ar calcined catalyst at 280°C at 50000X magnification

When Figure 23a and b are examined it is seen that copper is located into silica aerogel framework but has different sizes at different locations. Figure 24a and b reveals the spread of copper metal through the whole aerogel. No change of morphology was observed in silica aerogel. EDX spectra of what is given in Figure 23 a and b are given in Figure 25; Figure 24a and b are in Figure 26.

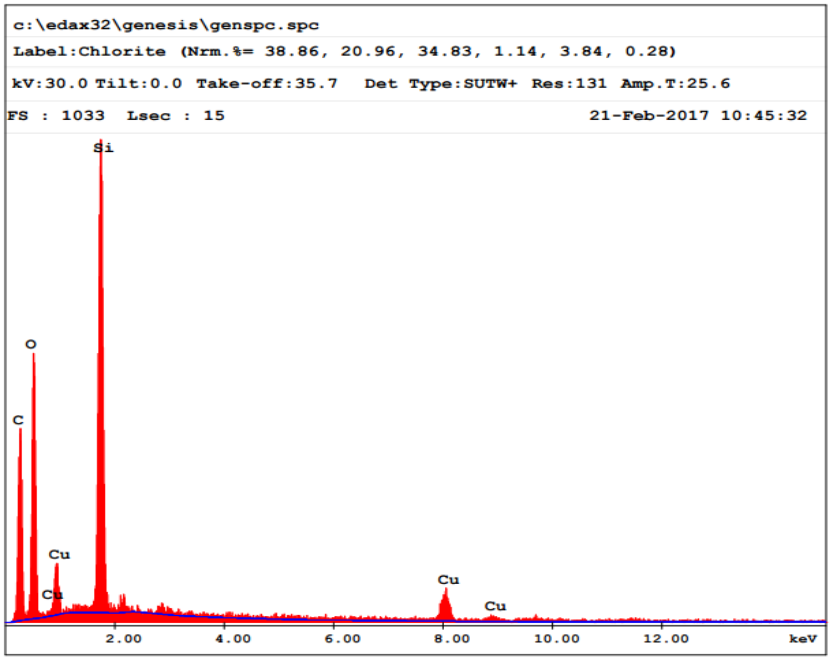

Figure 25: EDX spectrum of 10% copper loaded and N_2 calcined catalyst at 280°C.

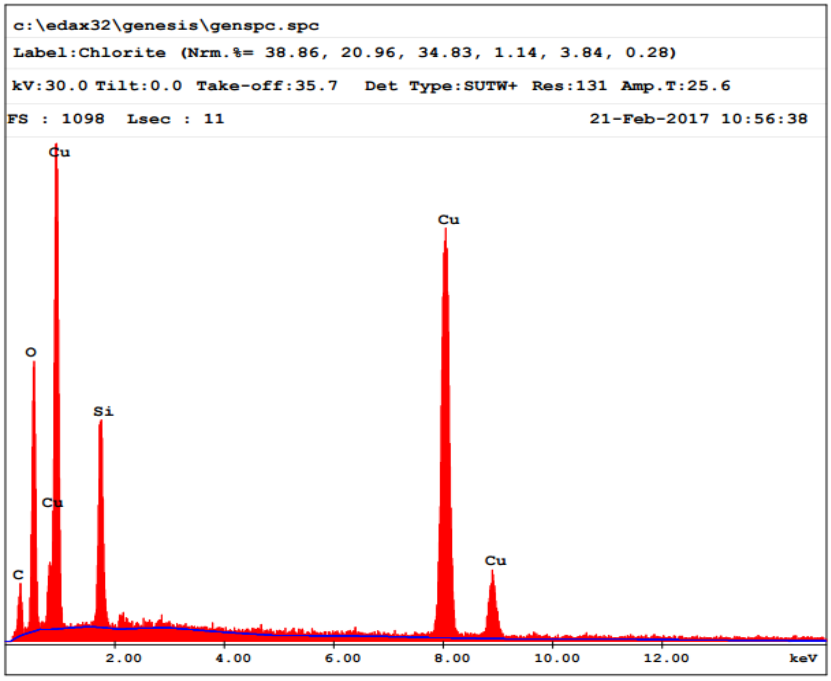

Figure 26: EDX spectrum of 10% copper loaded and Air/Ar calcined catalyst at 280°C.

EDX spectra in Figures 25 and 26 show that copper is successfully loaded into silica aerogel. SEM images of 15% Cu loaded and calcined silica aerogel under Air/Ar at 700°C are given in Figure 27. The clustered groups are found out to be copper. Three times magnified version of the SEM image (orange circle) in Figure 27a is given in 27c. In this image black regions show the pores within silica aerogel whereas white regions are copper. SEM and back scattered electron images of 15Cu-SA Air/Ar 700 catalyst are given in Figure 28. Figure 28a and b shows copper clusters in a different rod-like shape and silica aerogel. Gathered copper particles formed a cluster most probably due to the sintering at 700°C.

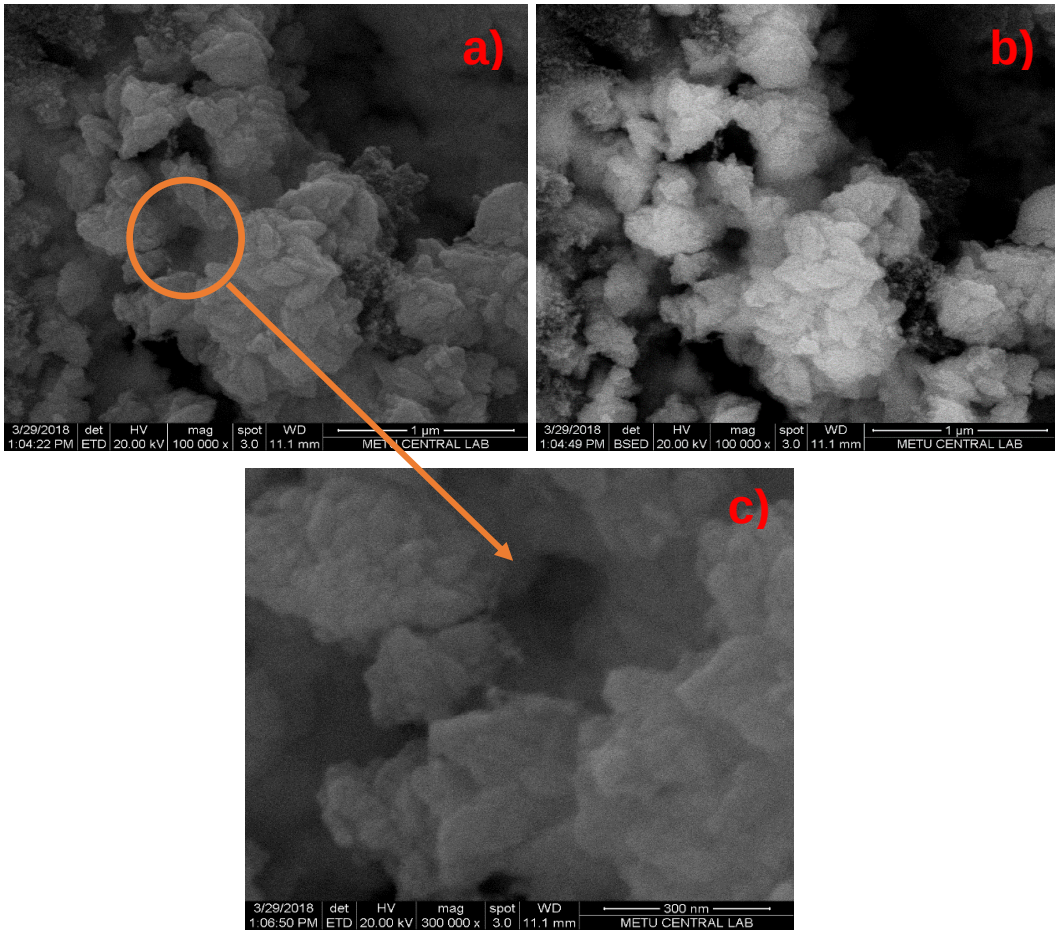

Figure 27: SEM **(a,c)** and back scattered electron images **(b)** of 15%Cu loaded and Air/Ar calcined catalysts at 700°C at 100000X and 300000X magnification

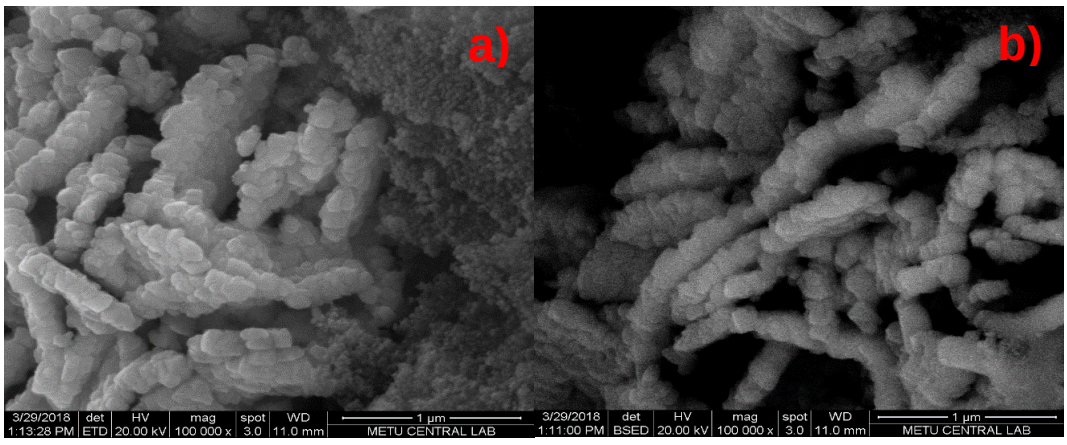

Figure 28: SEM **(a)** and back scattered electron images **(b)** of 15%Cu loaded and Air/Ar calcined catalysts at 700°C at 100000X magnification

SEM image and EDX mapping of 15Cu-SA Air/Ar 700 catalyst was given in Figure 29.

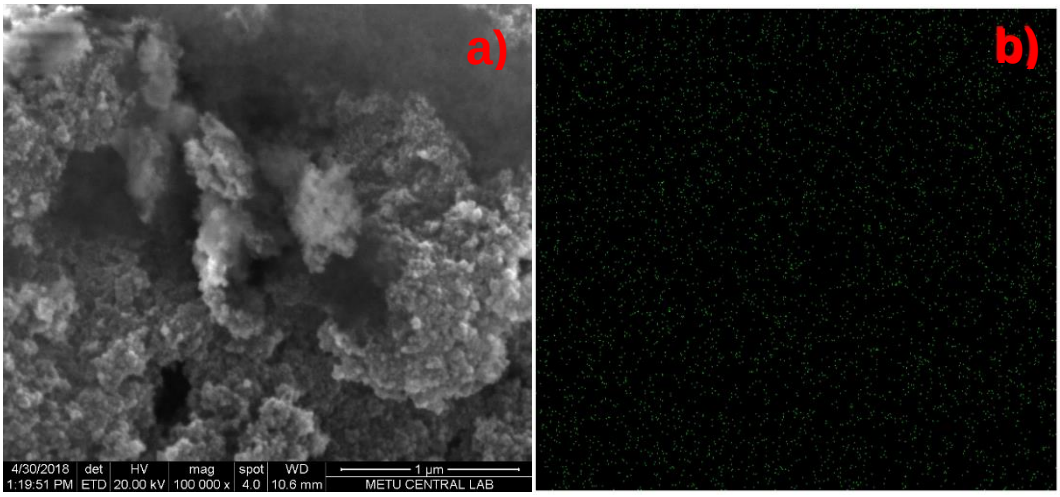

Figure 29: SEM **(a)** and EDX mapping **(b)** of 15%Cu loaded and Air/Ar calcined catalysts at 700°C at 100000X magnification

Green dots in Figure 29b show the dispersion of copper given in Figure 29a in the silica aerogel. By looking at Figure 29b it could be said that copper was uniformly distributed on the silica aerogel catalyst.

SEM and back scattered electron images of 15Cu10Zn-SA Air/Ar 700 catalyst are given in Figure 30.

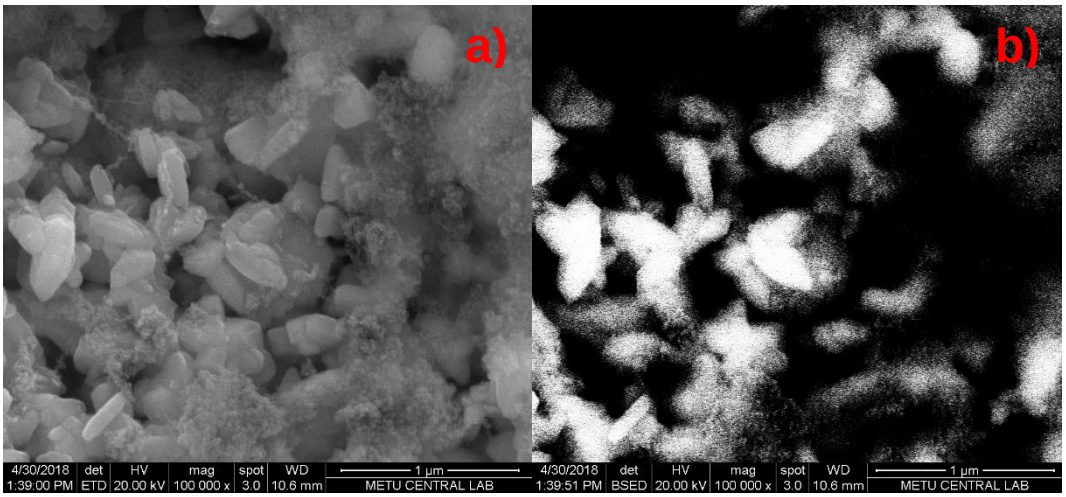

Figure 30: SEM **(a)** and back scattered electron images **(b)** of 15%Cu - 10%Zn loaded and Air/Ar calcined catalysts at 700°C at 100000X magnification

From Figure 30a change in the topography of the catalyst was observed. Silica aerogel was spread around the metals. By looking at Figure 30b it is hard to distinguish if the shiny white particles are copper or zinc. In order to prove the existence of Zn in Cu loaded silica aerogel, EDX of this catalyst was done. EDX results of 15Cu10Zn-SA Air/Ar 700 catalyst was given in Figure 31.

From Figure 31, the existence of zinc metal was detected. Hence it could be said that zinc was successfully loaded into silica aerogel.

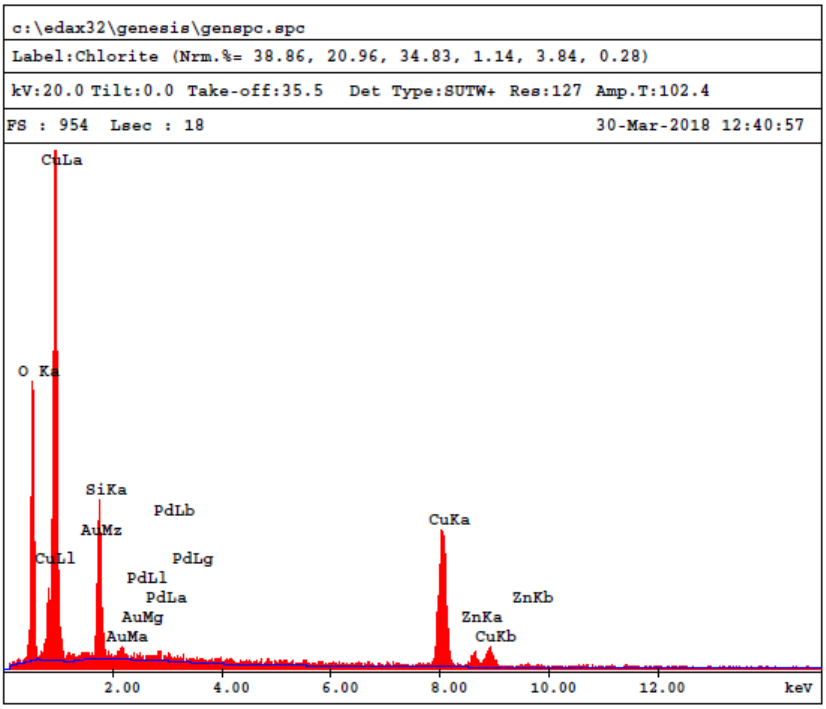

Figure 31: EDX spectrum of 15% copper and 10% zinc loaded and Air/Ar calcined catalyst at 700°C.

6.1.4 Inductively coupled plasma mass spectroscopy (ICP-MS) results

Quantitative analysis was performed in ICP-MS for silica aerogels to which different amounts of copper was loaded. ICP results of catalysts synthesized except the Zn loaded are given in Table 9.

Table 9: Amont of copper in the synthesized catalysts

Element	Weight %						
	10Cu-SA N_2 700	**10Cu-SA N_2 450**	**10Cu-SA N_2 280**	**10Cu-SA Air/Ar 700**	**10Cu-SA Air/Ar 450**	**10Cu-SA Air/Ar 280**	**15Cu-SA Air/Ar 700**
Si	36.9 ± 0.2	33.3 ± 0.5	28.4 ± 0.1	35.2 ± 0.4	34.4 ± 0.1	29.0 ± 0.3	34.7 ± 0.5
Cu	11.5 ± 0.2	11.1 ± 0.3	10.3 ± 0.1	10.5 ± 0.1	9.7 ± 0.1	10.4 ± 0.1	13.0 ± 0.2

By looking at Table 9, it could be concluded that copper was successfully loaded into silica aerogel, which is in accordance with EDX results. Copper contents of 10% copper loaded catalysts were found to be matching with the metal actually loaded; 10 mole% Cu corresponds to 11 wt% and this result is in consistency with the ICP results. Cu loading in 15Cu-SA Air/Ar 700 catalyst was found to be 13 wt% which is a little less than 15 mole%, corresponding to 16 wt%**.**

6.1.5 Temperature programmed ammonia desorption (NH_3-TPD) results

NH_3-TPD analysis results of copper loaded silica aerogel catalysts are given in Figure 32. The sharp peak ending around 115°C, which is present in all catalysts, is the physisorption peak of NH_3 indicating weak acidity. The peaks starting from 125°C show chemically desorbed NH_3 indicating strong acidity.

In Figure 32, NH_3-TPD results of copper loaded silica aerogels which were calcined with Air/Ar are given. According to this figure, 10Cu-SA Air/Ar 700, 450 and 280 catalysts showed major peaks at 330, 298 and 200°C, respectively. However, 15Cu-SA Air/Ar 700 and 15Cu-10Zn-SA Air/Ar 700 catalysts showed major peaks at 265 and 328°C, respectively.

NH_3-TPD results of copper loaded silica aerogels calcined with N_2 are given in Figure 33. According to this figure, 10Cu-SA N_2 700, 450 and 280 catalysts showed major peaks at 282, 548 and 494°C, respectively. In the literature, it was reported that the peaks between 200-400°C are attributed to moderate acidity whereas peaks after 400°C indicate strong acidity (Llanos. 2008; Srinivas. 2016). When Figures 32 and 33 are examined together the catalyst having the strongest acidity could be found as 10Cu-SA N_2 280.

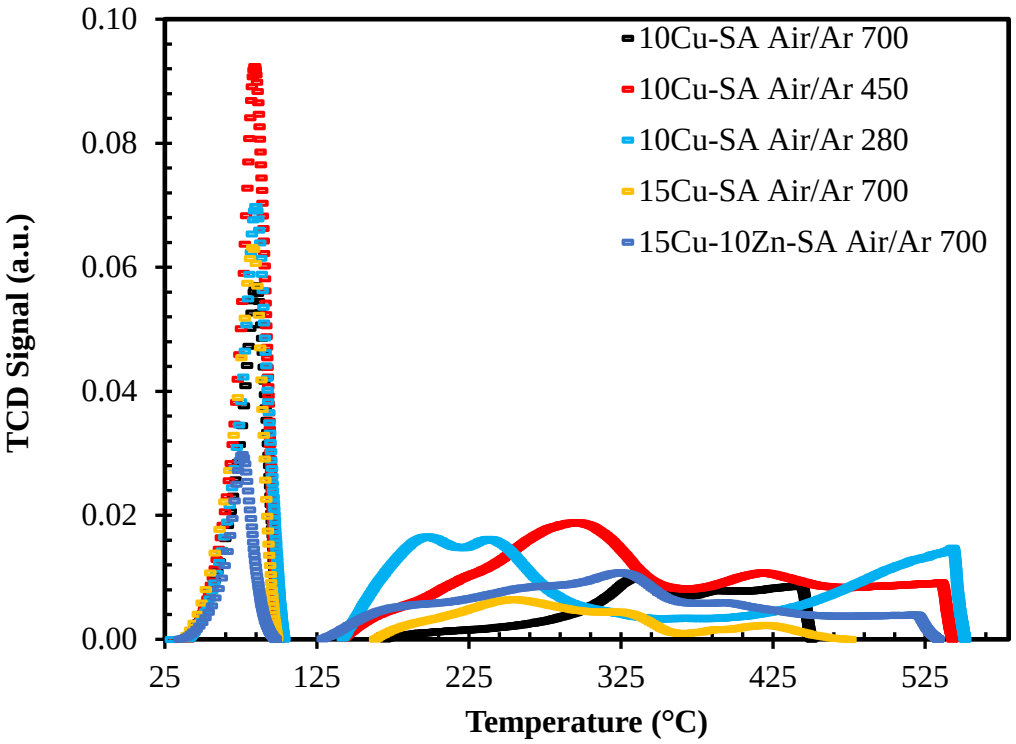

Figure 32: NH_3-TPD graphs of the synthesized and copper loaded catalysts which are calcined with Air/Ar

Total acid capacity of each catalyst was found from the areas under signal-temperatue graphs which are due to ammonia adsorption and desorption. Total acid capacities of the synthesized catalysts are given in Table 10.

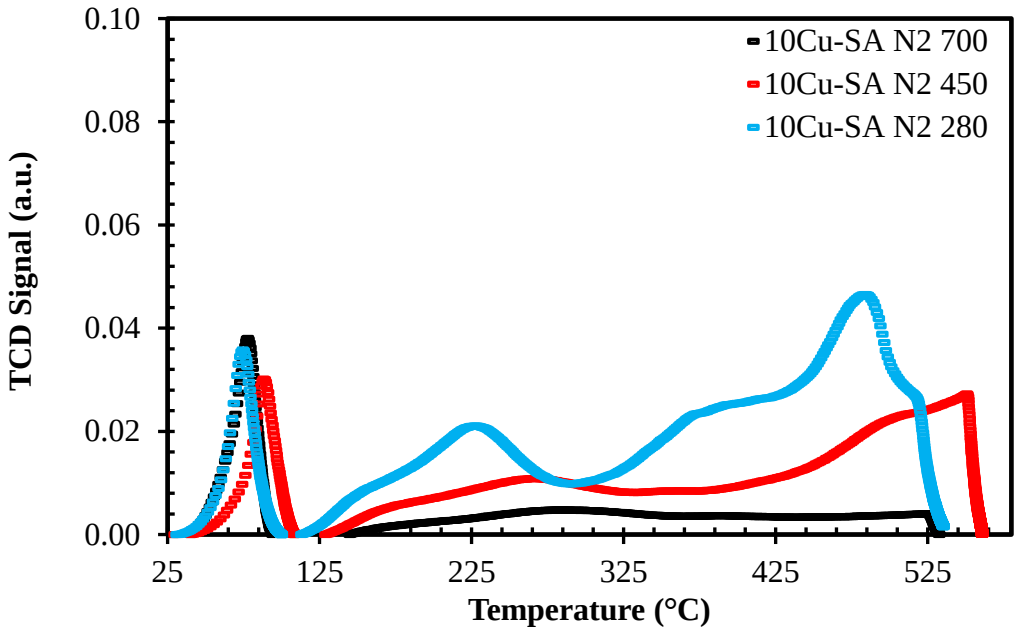

Figure 33: NH_3-TPD graphs of the synthesized and copper loaded catalysts which are calcined with N_2 .

Table 10: Acid capacities of the synthesized catalysts

Catalyst	Total acid capacity, mmol/g
10Cu-SA Air/Ar 280	1.18
10Cu-SA N_2 280	1.84
10Cu-SA Air/Ar 450	1.42
10Cu-SA N_2 450	1.29
10Cu-SA Air/Ar 700	0.31
10Cu-SA N_2 700	0.62
15Cu-SA Air/Ar 700	0.56
15Cu-10Zn-SA Air/Ar 700	0.16

When Figures 32 and 33 are examined together with Table 10, acid capacities in descending order were found to be : 10Cu-SA N_2 280 > 10Cu-SA Air/Ar 450 > 10Cu-SA N_2 450 > 10Cu-SA Air/Ar 280 > 10Cu-SA N_2 700 > 15Cu-SA Air/Ar 700 > 10Cu-SA Air/Ar 700 > 15Cu-10Zn-SA Air/Ar 700.

6.2 Catalytic Activity Results

Activity tests of the catalysts were performed in a continuous flow packed column reactor system. Reactions were perfomed at atmospheric pressure at a temperature interval of 200-300°C, under constant argon flow rate (30 ml/min) and constant alcohol/water feed rate (0.9 ml/h). Prior to each experiment, reduction was carried out to the catalysts to convert metal oxides into metallic form to be used in the SRM reaction. Composition of the outlet reactor stream was determined using a gas chromatograph (GC). Amounts of products were calculated using beta factors of each product and areas obtained from GC. Beta factor calculation is given in Appendix C. Conversion of methanol and hydrogen selectivity were calculated and their graphs were drawn to evaluate data obtained from catalytic activity tests. Mole fractions of the compounds, methanol converison, hydrogen selectivity and hydrogen yield are calculated using the data obtained from GC. These calculations are given in Appendix D.

In this study, hydrogen rich gas was produced from methanol at atmospheric pressure and various reaction temperatures using different amounts of copper loaded catalysts which were calcined under different gases and temperatures. Effects of changing calcination gases and temperatures, metal percent and reaction temperatures on hydrogen production were investigated and evaluated in terms of methanol conversion, hydrogen yield and selectivity.

In order to test the reliability of the experiments for hydrogen production, studies were carried out using a commercial catalyst (HifuelR-120), 10Cu-SA Air/Ar 280 and 10Cu-SA Air/Ar 700 catalysts. The results are given in the sections below.

6.2.1 Repeatability results of the catalysts

6.2.1.1 SRM reaction results performed with Hifuel R-120 commercial catalyst

Steam reforming of methanol reaction was performed at different times under the same conditions. The reaction was carried out with Hifuel R-120 catalyst at 280°C and atmospheric pressure under constant feed (0.9 ml/h) and argon (30 ml/min) flow rates. Analysis of the reactor outlet stream revealed the presence of hydrogen, carbon monoxide and carbon dioxide gases. Formation of these gases showed the occurence of SRM (R.1) and methanol decomposition (R.2) reactions :

$$CH_3OH + H_2O \rightarrow CO_2 + 3H_2 \qquad [R.1]$$

$$CH_3OH \rightarrow CO + 2H_2 \qquad [R.2]$$

Conversion and product distribution of the two experiments performed at different times under the same conditions were given in Figure 34 and 35, respectively. The system reached to a steady state starting from thirtieth minute (Figure 34).

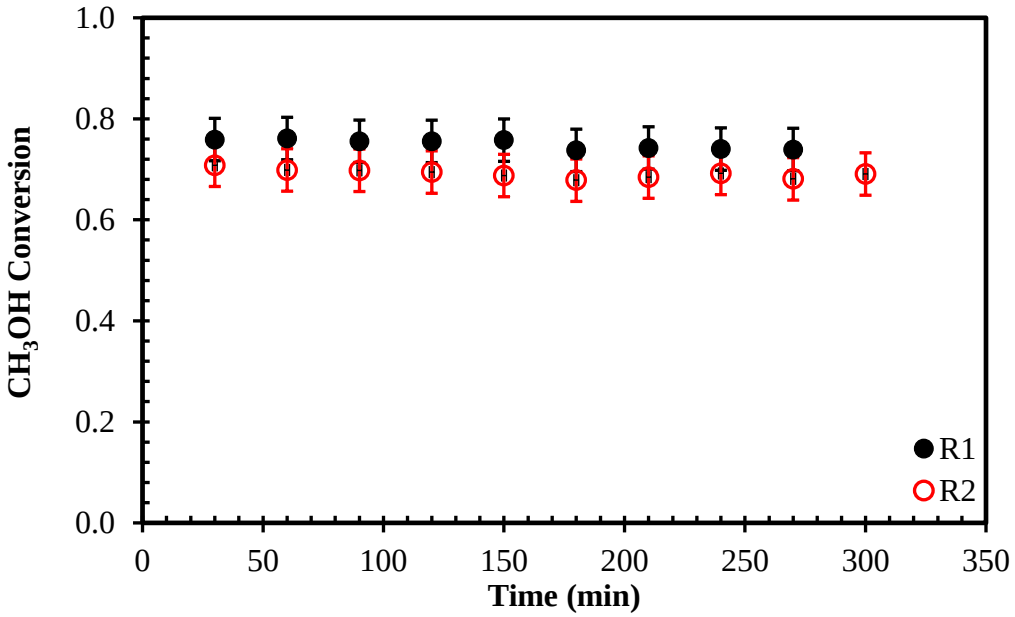

Figure 34: Comparison of two SRM repeatability experiments' methanol conversions (P:1.013 bar, T:280°C, H_2O/CH_3OH = 2.2, Catalyst: HifuelR-120) (R1: 1st run, R2 : 2nd run)

Average methanol conversion of the first experiment was 75% and that of the second experiment was 69.1% which indicates the consistency and repeatability of the results (Figure 34).

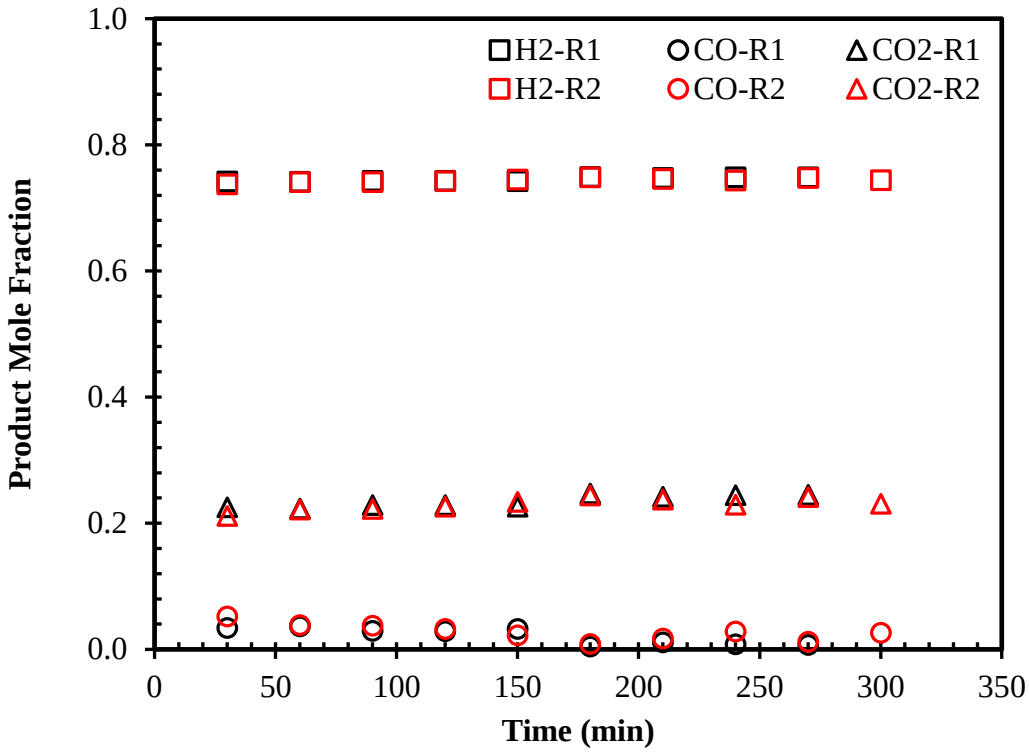

Figure 35: Comparison of two SRM repeatability experiments' product distributions (P:1.013 bar, T:280°C, H_2O/CH_3OH = 2.2, Catalyst: HifuelR-120)

The results of repeated experiments are in agreement with each other (Figure 35). Formation of the same products was observed. Reactor outlet gas composition was a hydrogen rich gas mixture with ~74% H_2, ~24% CO_2 and 2% CO.

Hydrogen yields of the two repeatability experiments using the commercial catalyst are given in Figure 36. The average hydrogen yield was 72.9% and 66.7% in the first and the second experiments, respectively. These results are in consistency.

Hydrogen selectivities of the two repeatability experiments using the commercial catalyst are given in Figure 37.

The average hydrogen selectivity was 97.27% in the first experiment and 96.49% in the second experiment, which are close to each other (Figure 37).

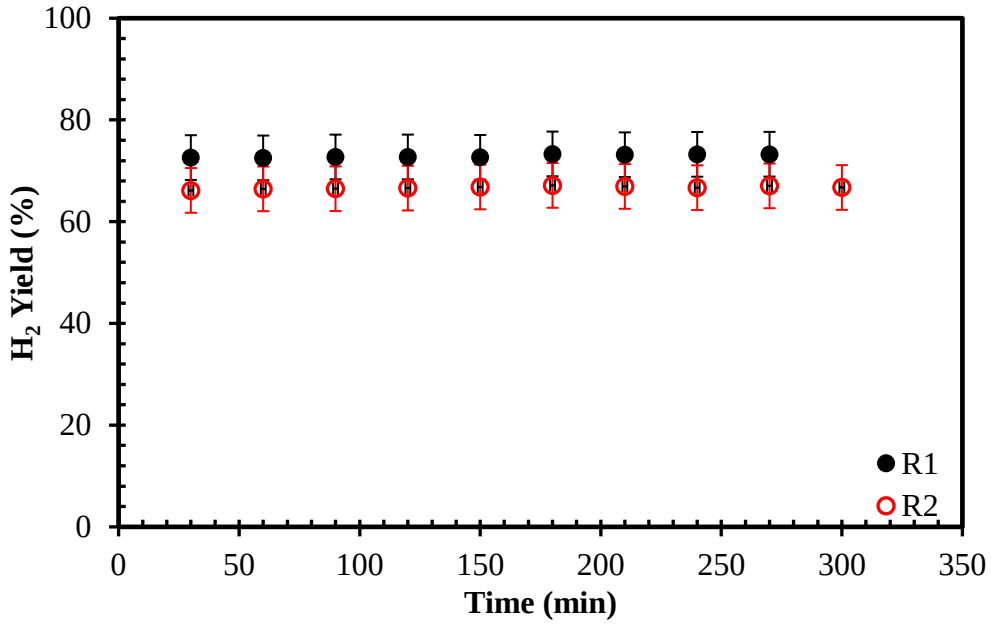

Figure 36: Comparison of two SRM repeatability experiments' hydrogen yields (P:1.013 bar, T:280°C, H_2O/CH_3OH = 2.2, Catalyst: HifuelR-120)

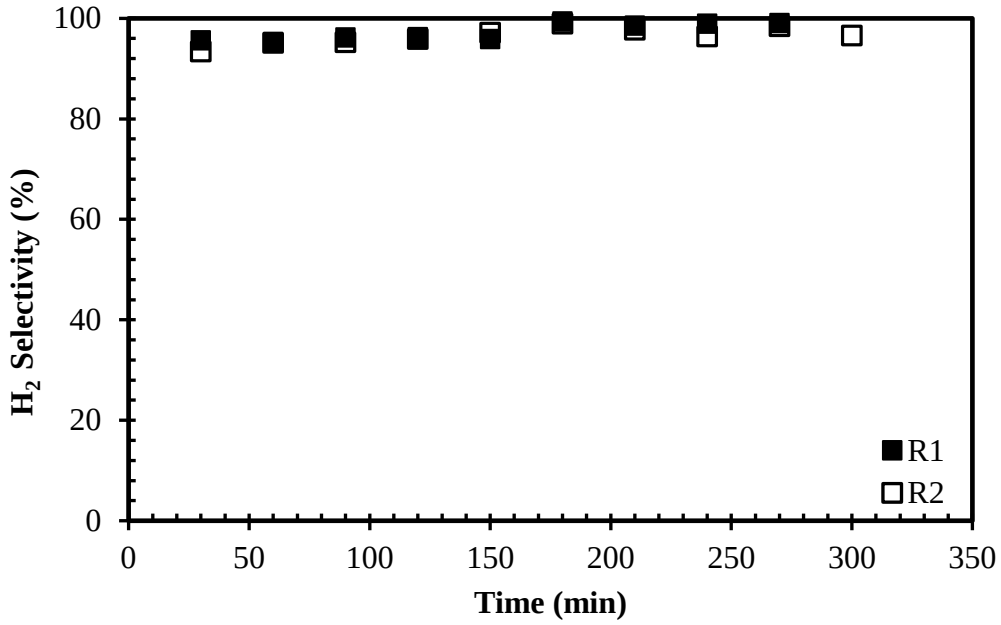

Figure 37: Comparison of two SRM repeatability experiments' hydrogen selectivities (P:1.013 bar, T:280°C, H_2O/CH_3OH = 2.2, Catalyst: HifuelR-120)

6.2.2 SRM reaction results performed with 10Cu-SA Air/Ar 280 and 10Cu-SA Air/Ar 700 catalysts

The experiments were performed with 10Cu-SA Air/Ar 280 and 10Cu-SA Air/Ar 700 catalysts at atmospheric pressure, at 280°C, under constant rate of carrier gas (30ml/min) and constant feed flow rate (0.9 ml/h). As in the case of Hifuel R-120, the outlet stream of reactor also consisted of hydrogen, carbon monoxide and carbon dioxide.

The results of the repeatability experiments done at different times under the same conditions with 10Cu-SA Air/Ar 700 is given in Figure 38.

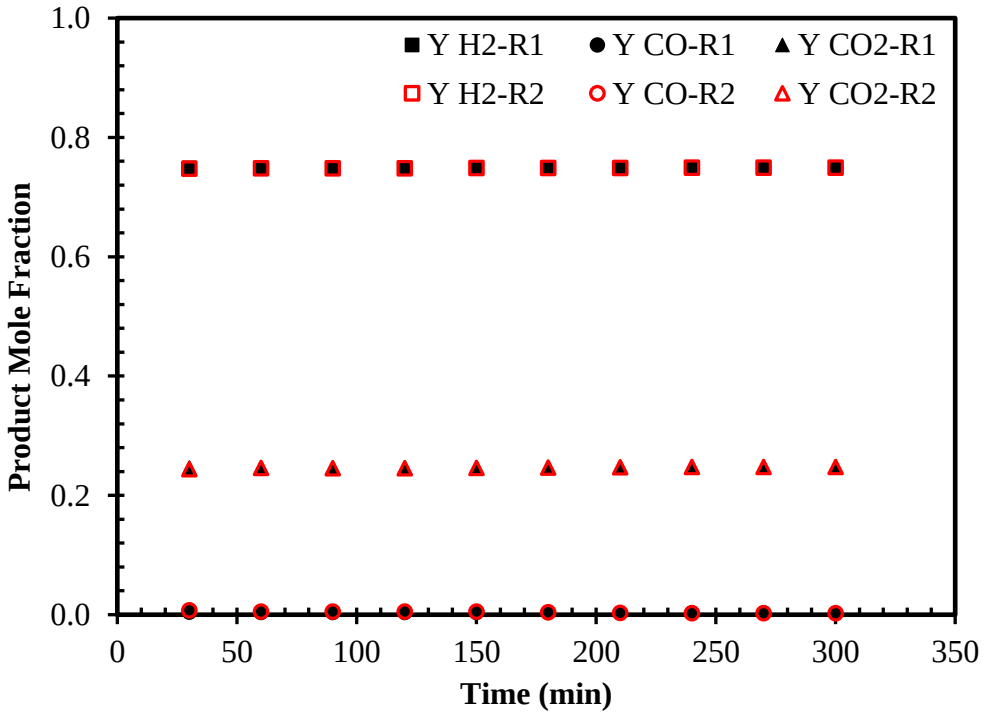

Figure 38: Comparison of two SRM repeatability experiments' product distributions (P:1.013 bar, T:280°C, H_2O/CH_3OH = 2.2, Catalyst: 10Cu-SA Air/Ar 700)

The results of the repeatability experiments done at different times under the same conditions with 10Cu-SA Air/Ar 280 is given in Figure 39.

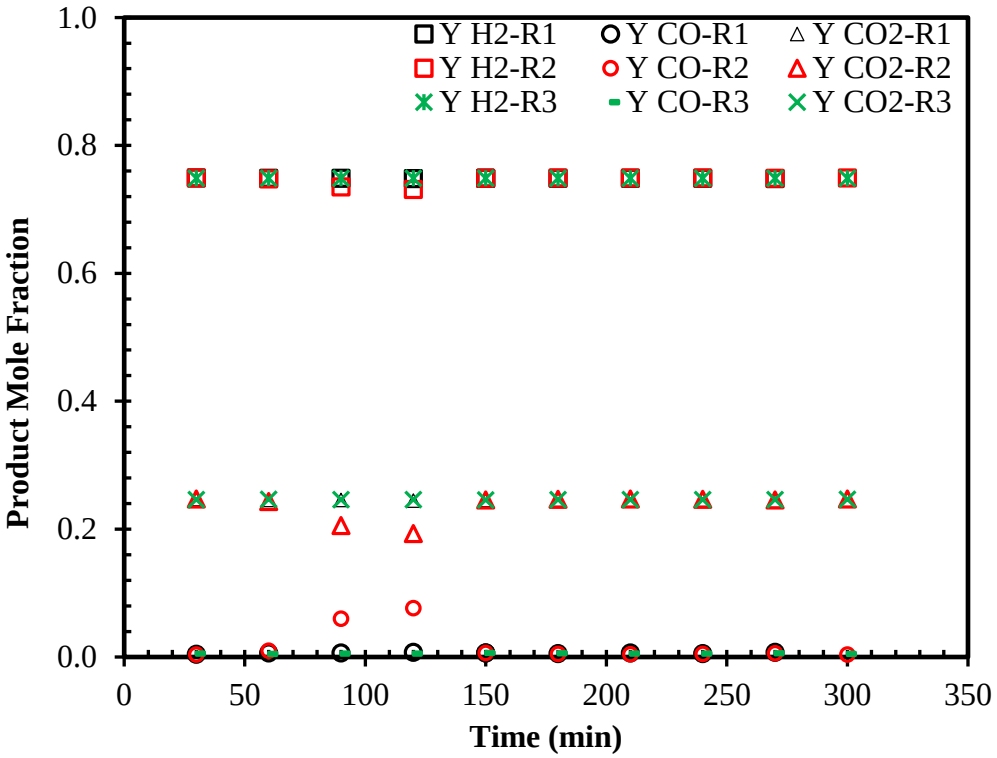

Figure 39: Comparison of three SRM repeatability experiments' product distributions (P:1.013 bar, T:280°C, H_2O/CH_3OH = 2.2, Catalyst: 10Cu-SA Air/Ar 280)

The experiments performed with two different catalysts both showed that the product gas composition was rich in terms of hydrogen. At the end of the experiments done with 10Cu-SA Air/Ar 700, the average composition of products was 74.9% H_2, 0.4% CO and 24.7% CO_2. At the end of the first experiment done with 10Cu-SA Air/Ar 280, the average composition of products were 74.9% H_2, 0.6% CO and 24.5% CO_2. The results of the second and third repeatability experiments were as follows : 74.6% H_2, 1.8% CO, 23.6% CO_2 and 74.9% H_2, 0.5% CO and 24.6% CO_2, respectively.

Repeatability results of 10Cu-SA Air/Ar 700 and 10Cu-SA Air/Ar 280 catalysts in terms of methanol conversions are given in Figures 40 and 41, respectively.

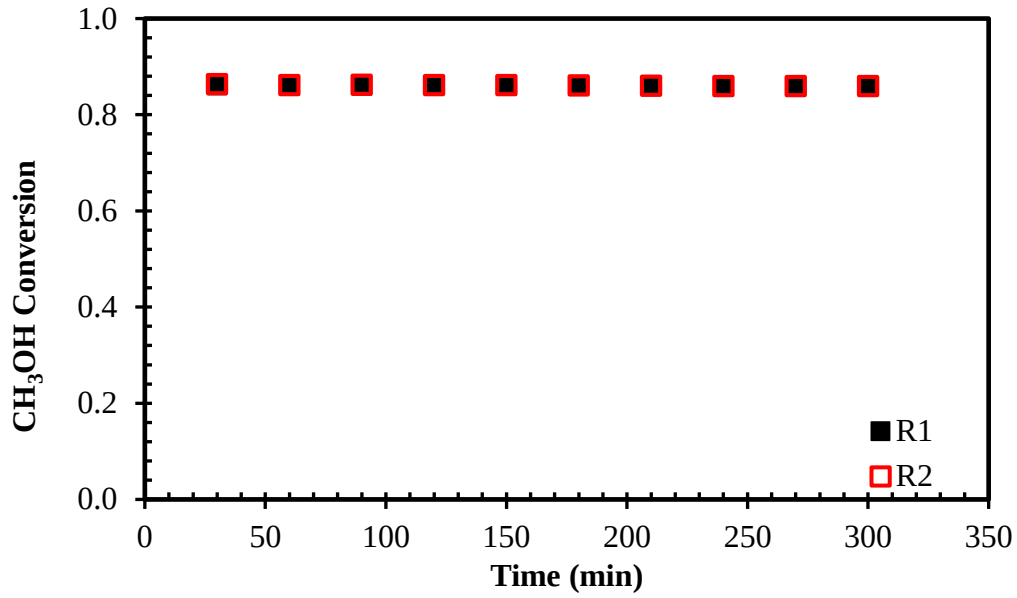

Figure 40: Comparison of two SRM repeatability experiments' methanol conversions (P:1.013 bar, T:280°C, H_2O/CH_3OH = 2.2, Catalyst: 10Cu-SA Air/Ar 700)

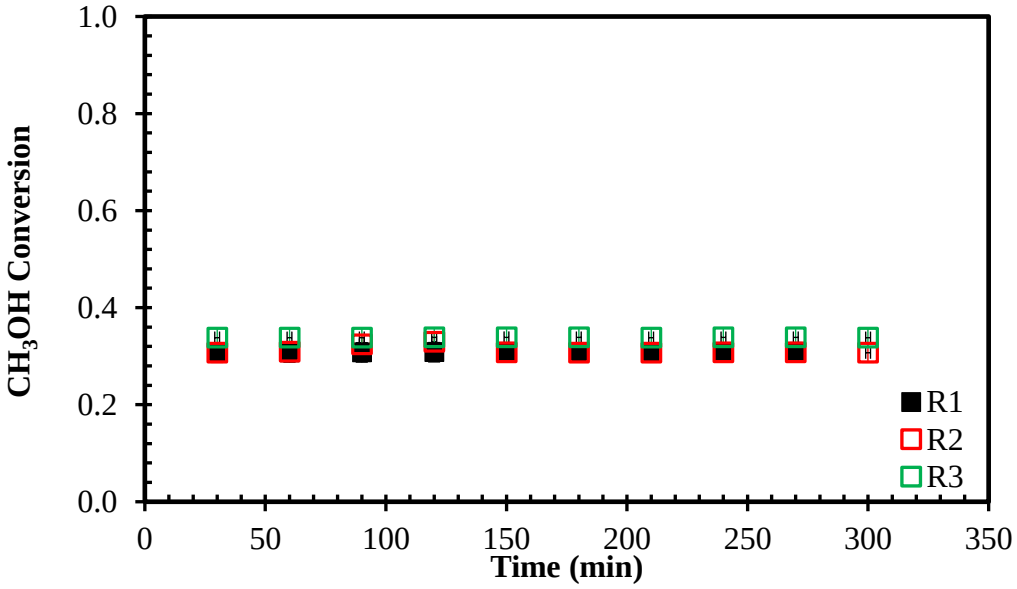

Figure 41: Comparison of three SRM repeatability experiments' methanol conversions (P:1.013 bar, T:280°C, H_2O/CH_3OH = 2.2, Catalyst: 10Cu-SA Air/Ar 280)

86% of the methanol was converted into hydrogen, carbon monoxide and carbon dioxide gases in both of the experiments in the presence of 10Cu-SA Air/Ar 700 catalyst (Figure 40). However, in the repeatability experiments done within the presence of 10Cu-SA Air/Ar 280 catalyst, 30.8% , 31.1% and 31.9% methanol conversions were obtained (Figure 41). Hydrogen yields at the end of each repeatability experiment with these catalysts were given in Figures 42 and 43. Hydrogen selectivities at the end of each repeatability experiment done with these catalysts are given in Figures 44 and 45.

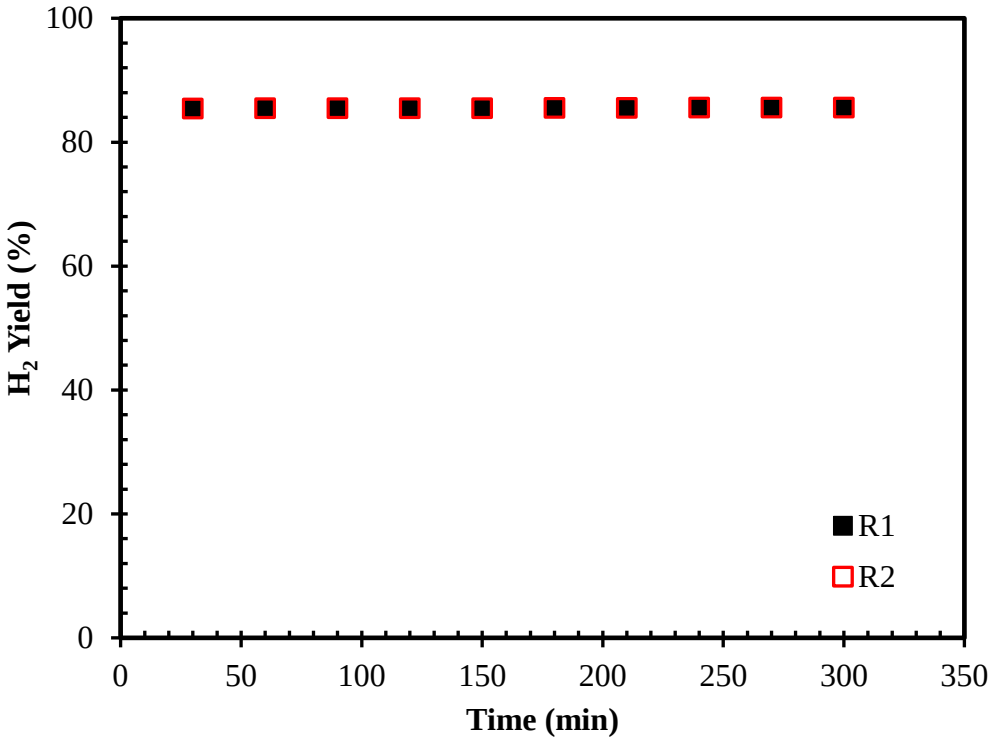

Figure 42: Comparison of two SRM repeatability experiments' hydrogen yields (P:1.013 bar, T:280°C, H_2O/CH_3OH = 2.2, Catalyst: 10Cu-SA Air/Ar 700)

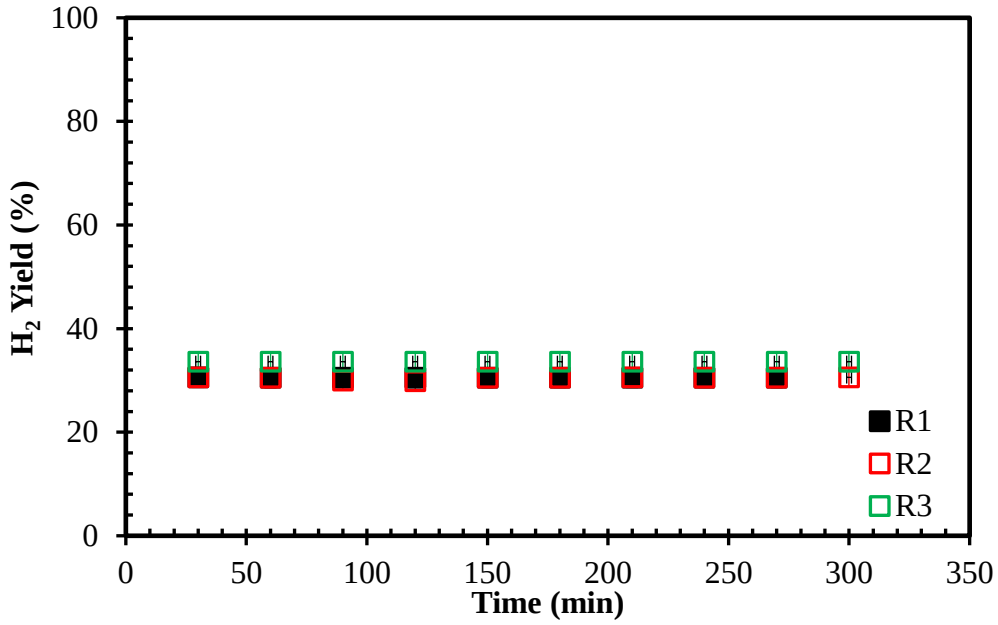

Figure 43: Comparison of three SRM repeatability experiments' hydrogen yields (P:1.013 bar, T:280°C, H_2O/CH_3OH = 2.2, Catalyst: 10Cu-SA Air/Ar 280)

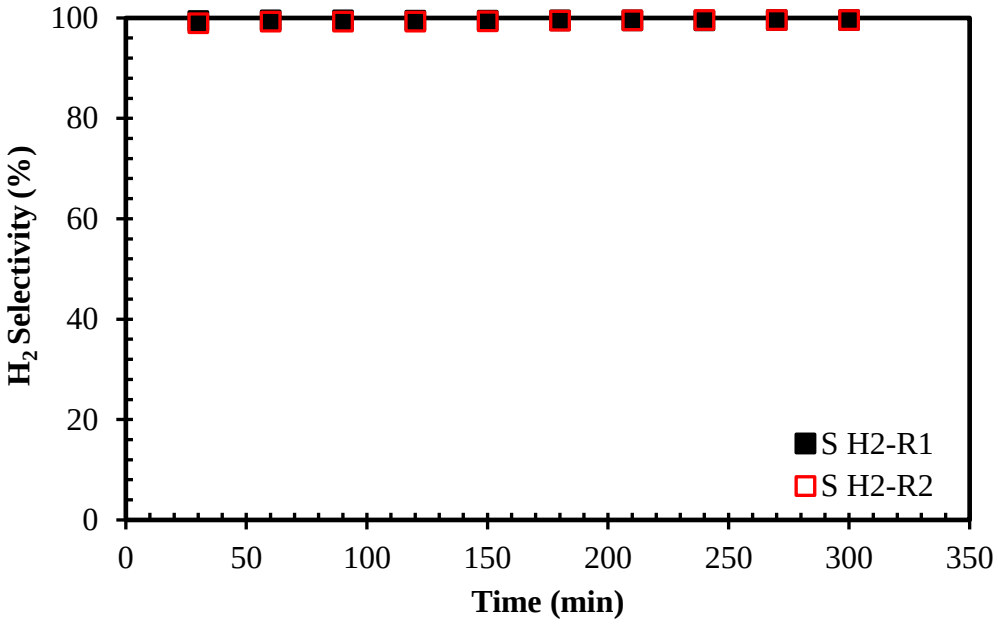

Figure 44: Comparison of two SRM repeatability experiments' hydrogen selectivities (P:1.013 bar, T:280°C, H_2O/CH_3OH = 2.2, Catalyst: 10Cu-SA Air/Ar 700)

In the repeatability experiments with 10Cu-SA Air/Ar 700 catalyst, 85.57% and 85.54% hydrogen yield were obtained. Compared to 10Cu-SA Air/Ar 700 catalyst, lower hydrogen yields were obtained from 10Cu-SA Air/Ar 280 catalyst. 30.54%, 30.41% and 33.60% hydrogen yields were obtained from the repeatability experiments of 10Cu-SA Air/Ar 280.

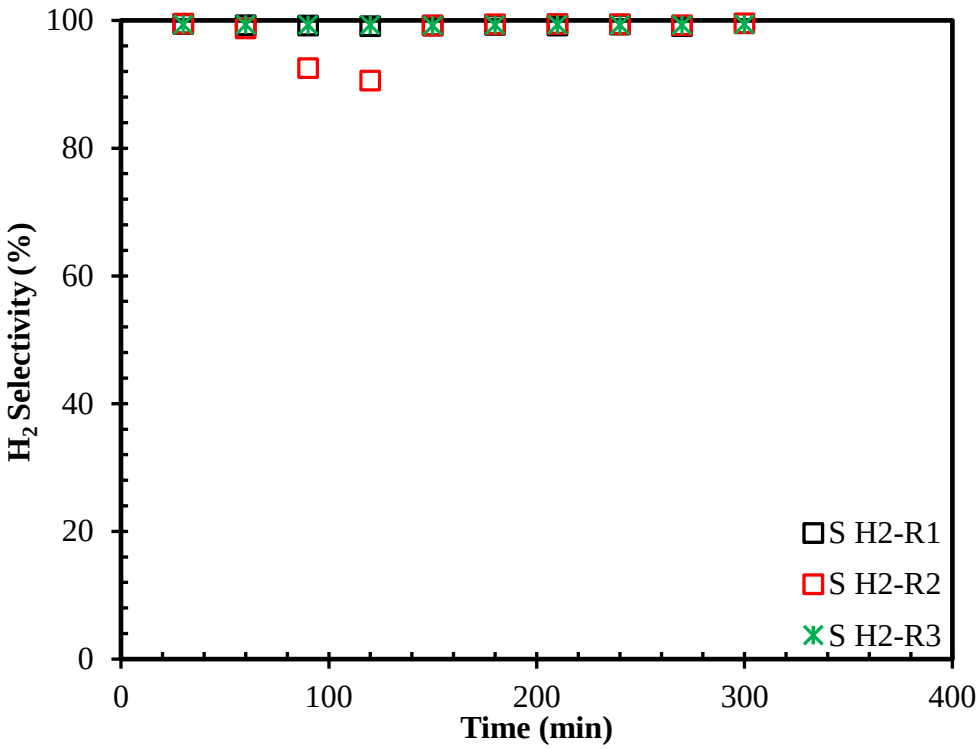

Figure 45: Comparison of three SRM repeatability experiments' hydrogen selectivities (P:1.013 bar, T:280°C, H_2O/CH_3OH = 2.2, Catalyst: 10Cu-SA Air/Ar 280)

In Figure 44, hydrogen selectivities on average were 99.52% and 99.40% whereas these values were 99.21%, 97.74% and 99.29% in Figure 45 indicating that hydrogen selectivity was independent from the calcination temperature of the catalysts. The data obtained in each figure are in agreement with each other.

Consequently, similar results in terms of product distribution, methanol conversion, hydrogen yield and selectivity were obtained from the SRM repeatability experiments performed with different catalysts under the same conditions. These results indicate the reliability and repeatability of the experiments.

6.2.3 Effect of calcination gas and temperature on hydrogen production from the SRM

Effects of calcination gases (Air/Ar and N_2) and calcination temperatures (280, 450 and 700°C) on hydrogen production in SRM in the presence of 10% Cu loaded silica aerogel catalysts were evaluated in terms of product distribution, methanol conversion, hydrogen yield and selectivity. The product distribution obtained from the experiments in which Air/Ar and N_2 calcined catalysts are used are given in Figure 46.

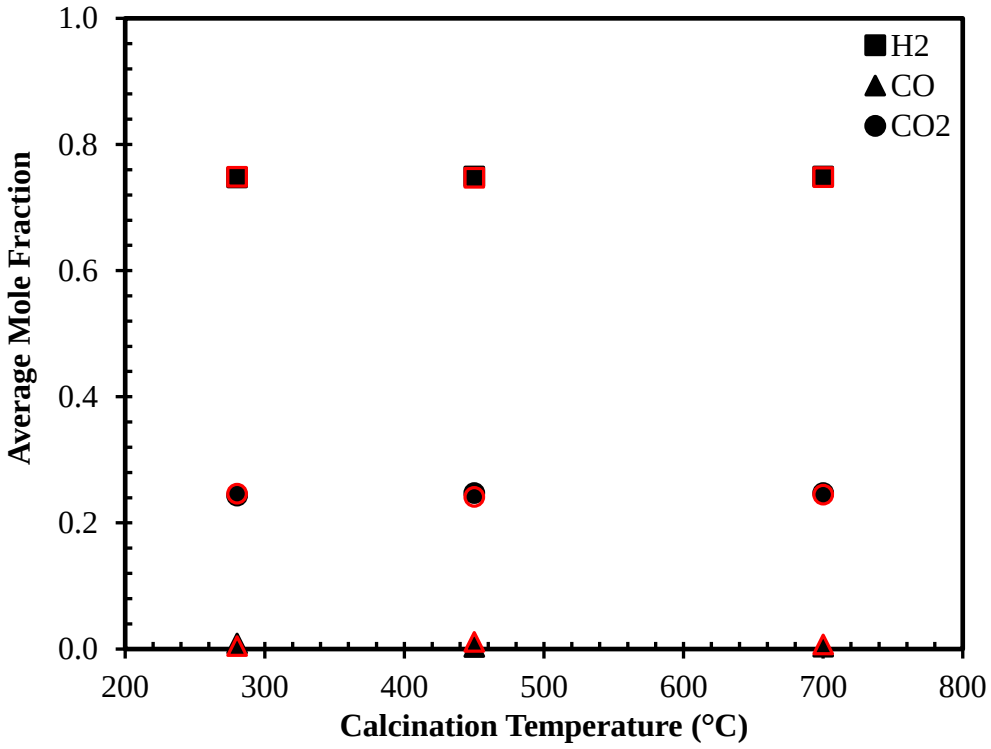

Figure 46: Product distributions of catalysts used in SRM which are calcined with Air/Ar and N_2 at different temperatures (P:1.013 bar, T:280°C, H_2O/CH_3OH = 2.2) (Filled black points : Air/Ar , empty red points : N_2)

It could be said that the product gas of SRM carried out with catalysts calcined with different gases and at different temperatures was rich in hydrogen. In addition to hydrogen, there were carbon monoxide (0.5%) and carbon dioxide (25%) in the

product gas. Regardless of various calcination gases and temperatures, the product distributions of the catalysts were similar.

Methanol conversions of the catalysts used in SRM at 280°C are given in Figure 47. Each point on this graph was formed by taking the average of at least two repeatability experiments and showing their devaiations from this average. It was seen that the increasing calcination temperature led to an increase in methanol conversion for both of the calcination gases, like it was stated in the literature (Amiri, 2014). Even though an increase in the crystallite size of CuO with the increasing temperature was observed for the catalysts calcined with Air/Ar (Table 7), methanol conversion also showed an increase with increasing crystallite size. In adition, moderate acidity enhanced the activity of the catalysts (Table 10).

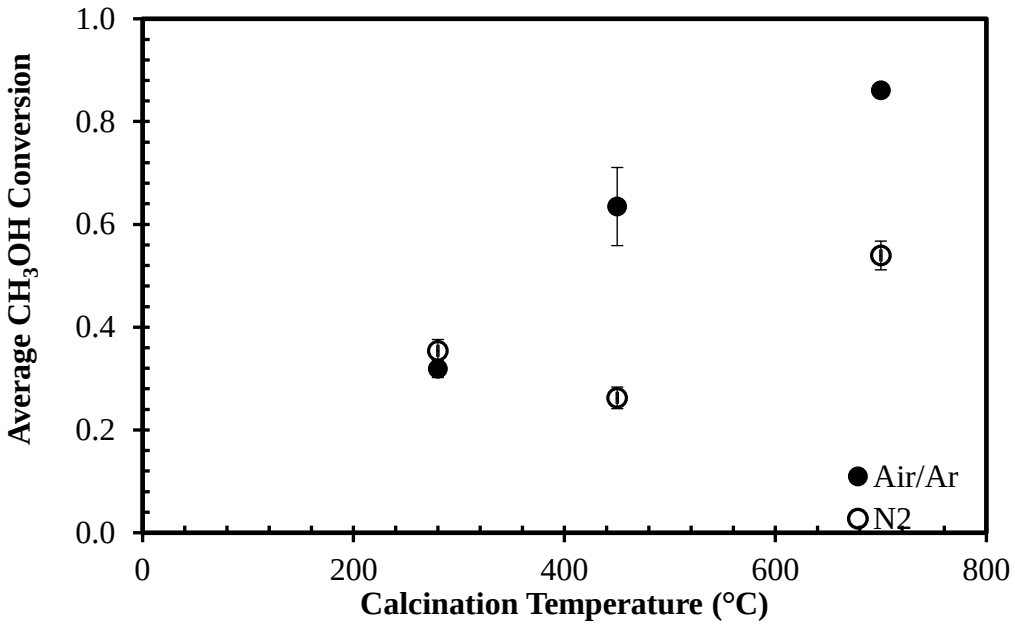

Figure 47: Methanol conversions of 10% Cu loaded silica aerogel catalysts calcined with Air/Ar and N_2 at different temperatures (P:1.013 bar, T:280°C, $H_2O/CH_3OH = 2.2$)

Methanol conversions of catalysts calcined with Air/Ar were thought to be higher than the ones calcined with N_2 due to large pore volumes, pore diameters and better dispersion of Cu metal in Air/Ar calcined catalysts.

Hydrogen yields of the catalysts calcined with different gases at different temperatures are given in Figure 48. Hydrogen yield was observed to increase with increasing calcination temperature. Even though the size of CuO particles increased, hydrogen yield also increased with this change. When the calcination gases are compared, better results in hydrogen yield and methanol conversion were obtained from the catalysts calcined with Air/Ar rather than N_2. This could be seen from Figures 47 and 48.

Among different calcination gases and temperatues the best result obtained from Air/Ar calcined catalysts was at 700°C with an average hydrogen yield of 85.53%. The best result obtained from the catalysts calcined with N_2 was also at 700°C with an average hydrogen yield of 53.41%.

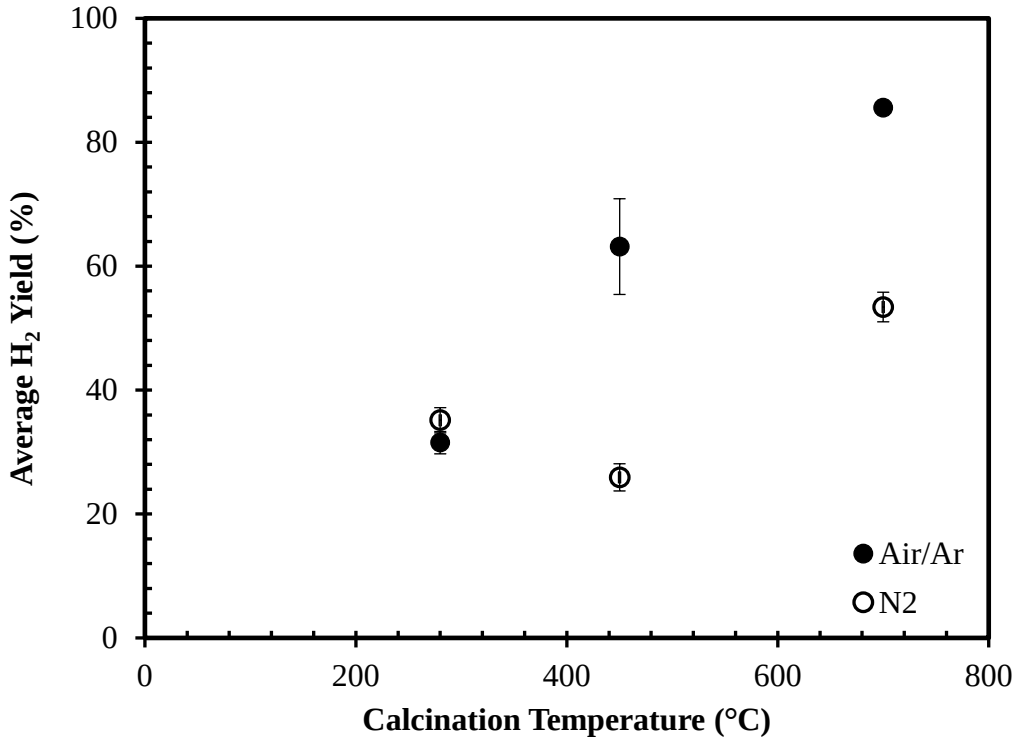

Figure 48: Hydrogen yields of 10% Cu loaded silica aerogel catalysts calcined with Air/Ar and N_2 at different temperatures (P:1.013 bar, T:280°C, H_2O/CH_3OH = 2.2)

The effect of calcination gas and temperature on hydrogen selectivity was given in Figure 49. It was seen that the hydrogen selectivity was independent from calcination gas and temperature.

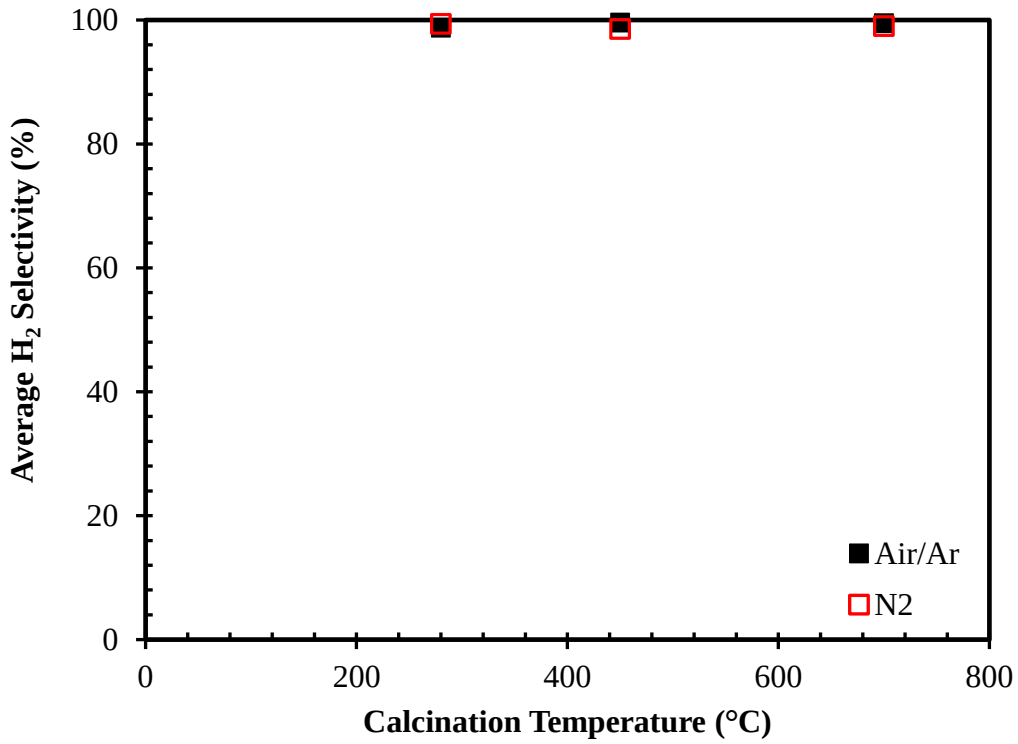

Figure 49: Hydrogen selecitivities of 10% Cu loaded silica aerogel catalysts calcined with Air/Ar and N_2 at different temperatures (P:1.013 bar, T:280°C, H_2O/CH_3OH = 2.2)

Hydrogen selectivities of the catalysts calcined with different gases and at different temperatures were found to be similar with each other. The reason of this was attributed to the similar product distributions.

To conclude, when Figures 46-49 are examined and the calcination temperatures are considered, it could be said that the increasing calcination temperature also increased methanol conversion and hydrogen yield. When Figures 47-48 are examined, it could be seen that Air/Ar led to higher methanol conversion and hydrogen yield than N_2. Condisering all these, the best catalyst was determined as 10Cu-SA Air/Ar 700.

6.2.4 Effect of usage of different metal and metal amount on hydrogen production from the SRM

It was aimed to further improve the best catalyst (10Cu-SA Air/Ar 700) by increasing its copper amount. In line with this purpose, silica aerogel supported and 15 mole% copper loaded catalysts were synthesized, calcined with Air/Ar and finally were tested in SRM at 280°C.

10 mole% Zn was added into silica aerogel support with 15 mole% Cu in order to enhance copper dispersion within the gel and to observe if the metals were going to form a synergistic effect when they gathered. Cu-Zn loaded catalyst was calcined with Air/Ar at 700°C and then used in SRM at 280°C. Comparative results of the catalysts are given in Table 11.

Table 11: Average hydrogen production results in the presence of Cu and Cu-Zn loaded catalysts

Catalyst	Gas Composition			H_2 Yield, %	CH_3OH Conversion	H_2 Selectivity, %
	y_{H2}, %	y_{CO}, %	y_{CO2}, %			
10Cu-SA Air/Ar 700 (280)	0.749	0.004	0.247	82.5	0.83	99.5
15Cu-SA Air/Ar 700 (280)	0.749	0.003	0.247	91.7	0.92	99.6
15Cu 10Zn-SA Air/Ar 700 (280)	0.749	0.002	0.248	82.6	0.83	99.7

Hydrogen yield of 10% Cu loaded catalyst increased from 82.5% to 91.7% with increased copper loading (Table 11). In a similar manner, methanol conversion also increased from 0.83 to 0.92 when additional metal was added into silica aerogel. The best catalyst, which was determined as 10Cu-SA Air/Ar 700, was further improved by 15 mole% Cu loading in total. Increase in the copper content of the

catalyst resulted in an increase in the acidity of the catalyst which provided better conversion and hydrogen yield (Table 11). When the results of Zn loaded and Zn-free catalysts were examined it was realized that Cu-Zn loaded catalyst possessed similar conversion, yield and selectivity values as 10% Cu loaded catalyst. The acidity of Cu-Zn loaded catalyst was less than 15% Cu loaded catalyst which is why the activity of the former was less than the latter. By looking at Table 11, the best catalyst could be chosen as 15Cu-SA Air/Ar 700 (280).

6.2.5 Effect of reaction temperature on hydrogen production from the SRM reaction

In this section of the study, the effect of reaction temperature in between 200-300°C on the hydrogen production from methanol by using the new best catalyst, 15Cu-SA Air/Ar 700, was tested. Effects of reaction temperature on the product distribution, methanol conversion, hydrogen yield and selectivity are given in Figures 50- 53.

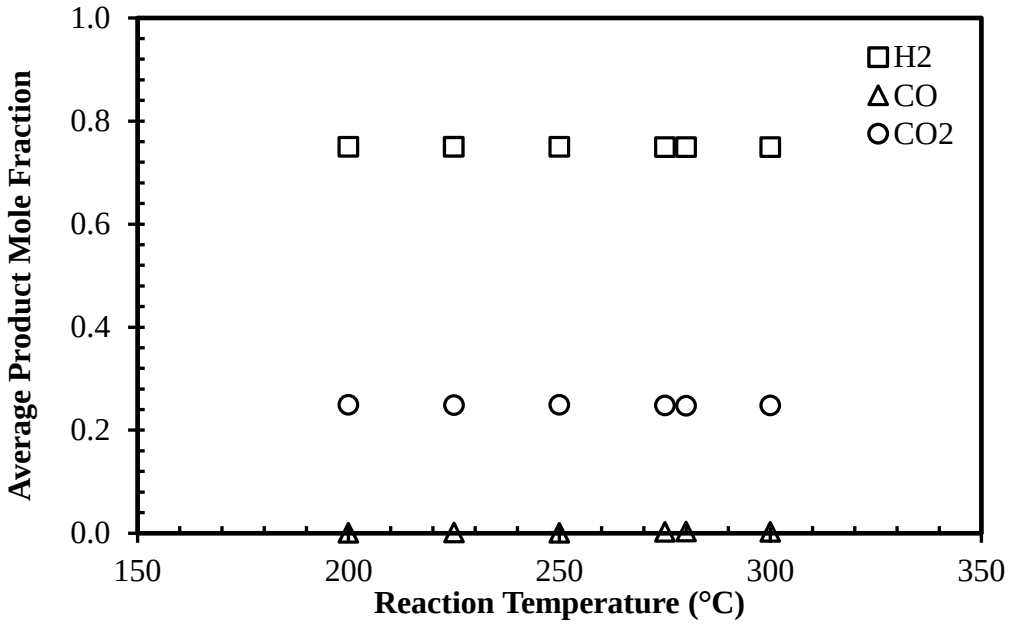

Figure 50: Effect of reaction temperature on average product distribution (P:1.013 bar, T:200-300°C, H_2O/CH_3OH = 2.2, Catalyst : 15Cu-SA Air/Ar 700)

As can be seen from Figure 50, products consisted of 75% hydrogen, 24% carbon dioxide and around 1% carbon monoxide. Despite a change in the reaction temperature, no change in the product distribution was observed. Formation of these gases showed that SRM and methanol decomposition reactions occurred.

Effect of reaction temperature on methanol conversion was given in Figure 51. It was observed that methanol conversion first increased as the temperature increased, after that the conversion became constant. Main reason of this case is the endothermic SRM reaction. Moreover, methanol decomposition reaction results in carbon monoxide and hydrogen formation.

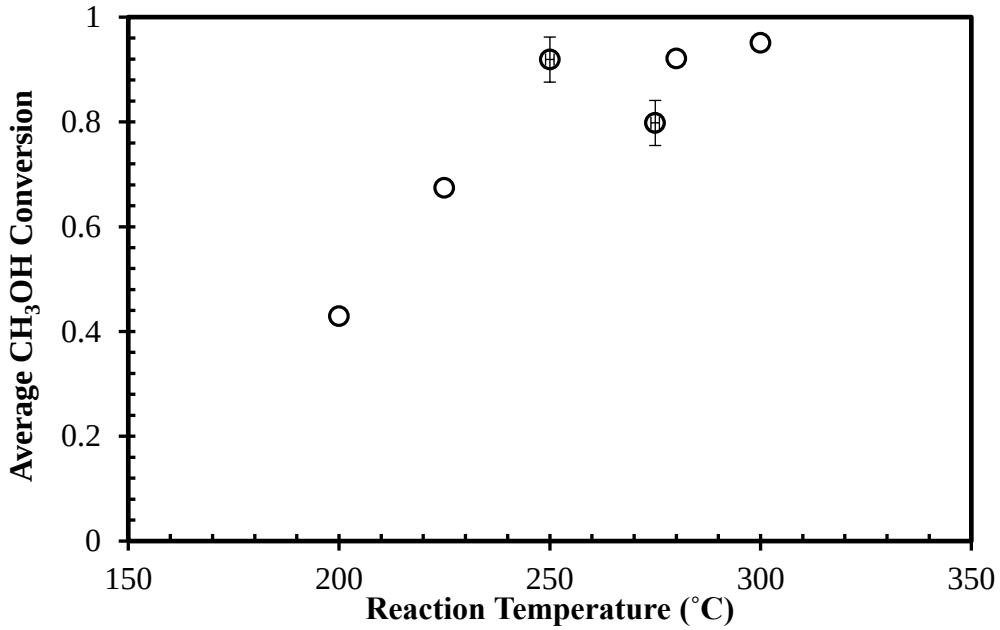

Figure 51: Effect of reaction temperature on average methanol conversion (P:1.013 bar, T:200-300°C, H_2O/CH_3OH = 2.2, Catalyst : 15Cu-SA Air/Ar 700)

The maximum hydrogen yield that can be obtained from SRM is three moles of hydrogen per mole of methanol. In other words. maximum theoretical hydrogen yield is limited to 3. Hydrogen yield as a function of reaction temperature is given in Figure 52. When the percentage is converted into numeric values, it could be said that the maximum point in Figure 52 at 300°C (94.67%) corresponds to 2.84 out of 3. As can be seen from Figure 52, hydrogen yield had an increasing trend with increasing temperature till 280°C. After this temperature, rate of increase in the

hydrogen yield slowed down and became constant around 300°C. This means that the maximum temperature that SRM could be performed was 300°C. Hydrogen yield at 280°C was 2.75 out of 3. The change in the average hydrogen yield of hydrogen is very little in between 280 and 300°C which is due to the sintering of copper.

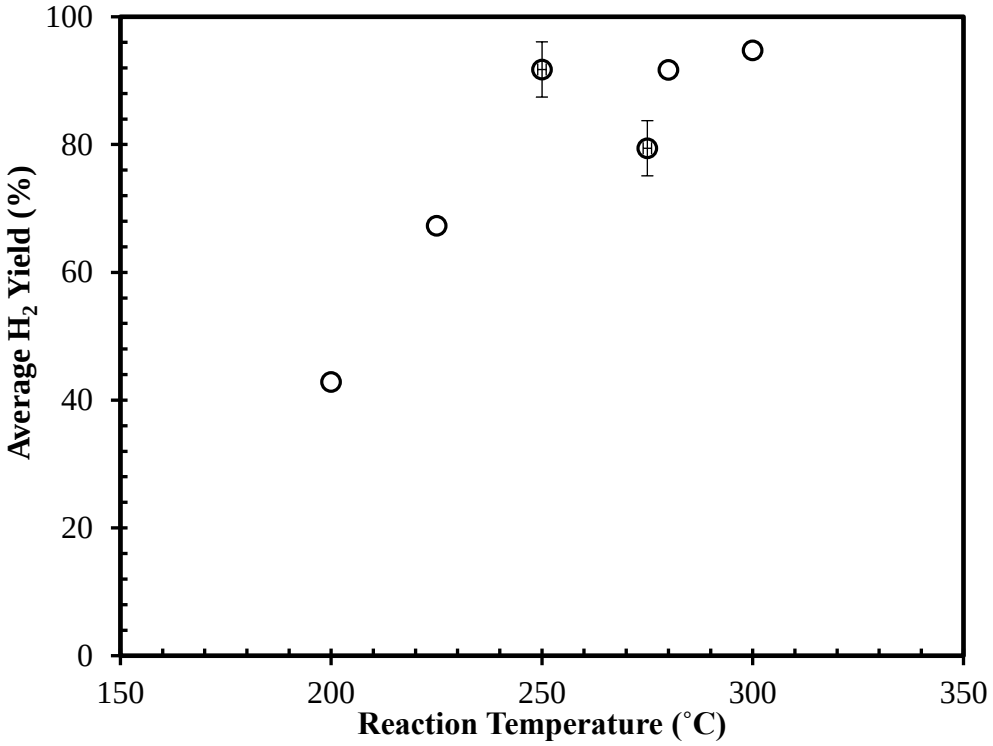

Figure 52: Effect of reaction temperature on average hydrogen yield (P:1.013 bar, T:200-300°C, H_2O/CH_3OH = 2.2, Catalyst : 15Cu-SA Air/Ar 700)

The effect of reaction temperature on average hydrogen selectivity is given in Figure 53. Regardless of different reaction temperatures, the average hydrogen selectivity was found to be 99% from Figure 53. As a result of the experiments done with 15Cu-SA Air/Ar 700 catalyst, it was observed that both the conversion and hydrogen yield increased with an increase in temperature till 280°C, after which the increase turned into a constant point. The point at which the increase in methanol conversion and hydrogen yield became stable around, 280°C, was chosen as the optimum reaction temperature. The experimental results are in accordance with literature in terms of the product composition, methanol conversion under similar

steam to methanol molar ratio, copper percent and reaction temperature (Amiri, 2014, 2016).

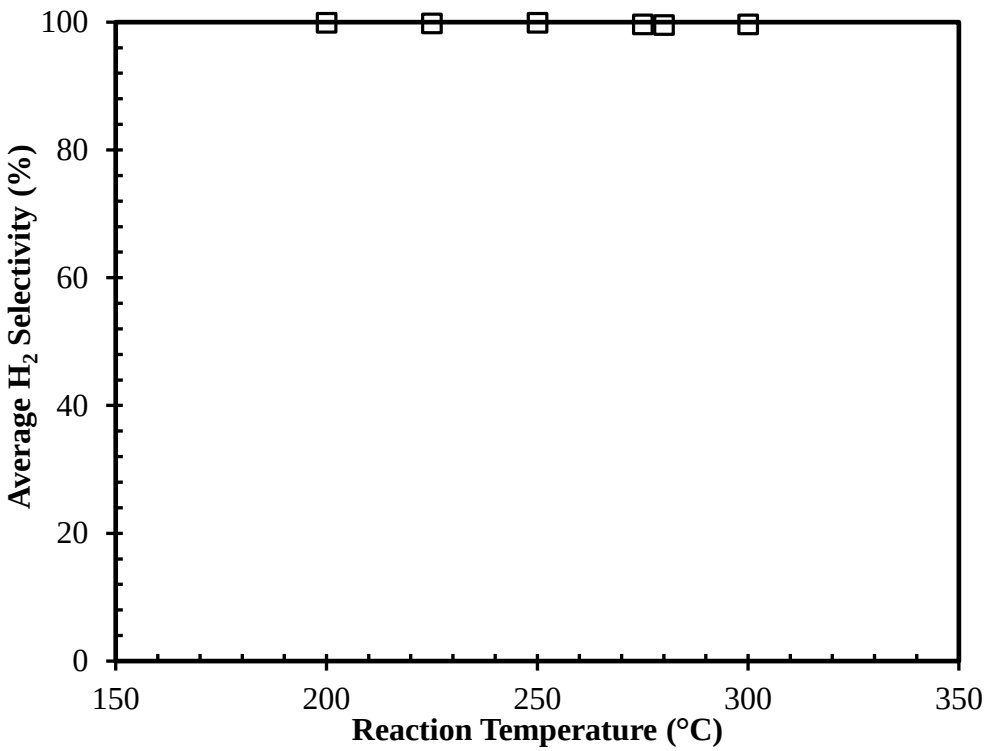

Figure 53: Effect of reaction temperature on average hydrogen selectivity (P:1.013 bar, T:200-300°C, H_2O/CH_3OH = 2.2, Catalyst : 15Cu-SA Air/Ar 700)

Thermogravimetric analysis (TGA) result of the catalyst used in SRM is given in Figure 54. Since the weight lost by the catalyst means the carbon deposited on the catalyst, TGA result was given in terms of coke deposition percent. The first weight loss around 49-178°C was due to water in the sample. Amorphous carbon loss occured around 350-500°C. A slow weight gain around 440°C was attributed to the oxidation of copper. During the SRM reaction, Boudouard reaction could also have occured. Boudouard reaction occurs at low temperatures. In the reactor, cold zones could have been formed due to the radial changes in temperature. These cold zones were the places where Boudouard reaction may take place. Hence, coke formation was observed in the catalyst.

All catalysts tested in SRM showed the same carbon deposition trend as in Figure 54.

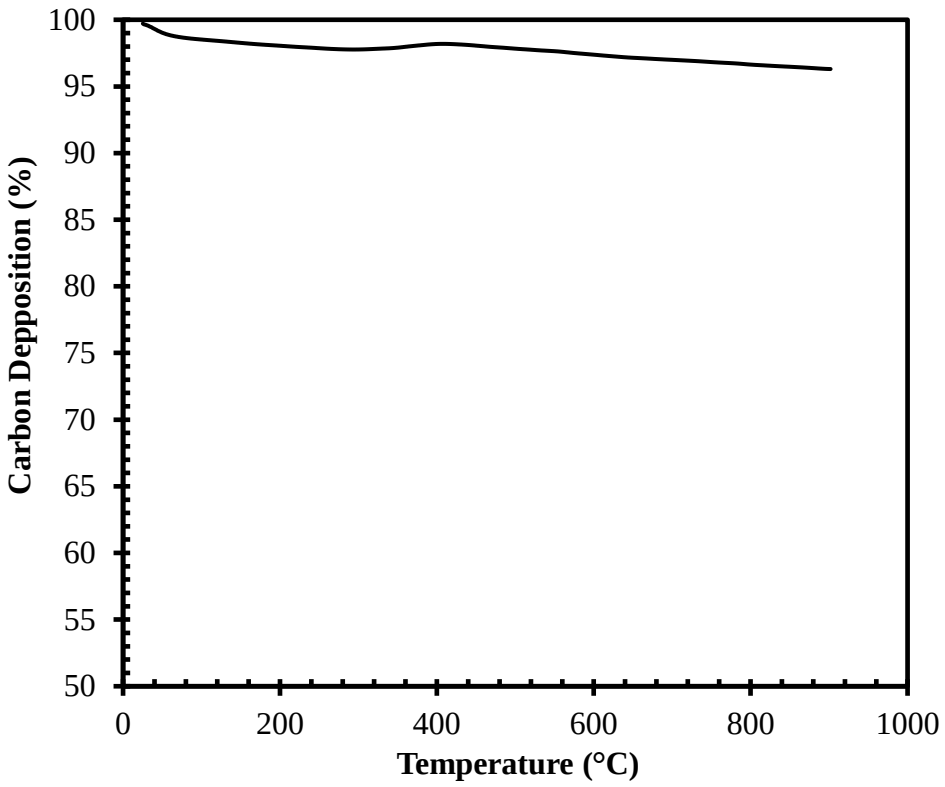

Figure 54: TGA result of catalyst used in SRM (P:1.013 bar, T:280°C, H_2O/CH_3OH = 2.2, Catalyst : 15Cu-SA Air/Ar 700)

Percentage of coke formation for all the catalysts is given in Table 12. Coke formation is very little. As can be seen from Table 12, among 15 mole% copper loaded catalysts, the least coke formation was in 15CuSA Air/Ar (225) catalyst, 1.14%. The most coke formation occured on 15Cu-SA Air/Ar (250) catalyst, 3.75%. In addition, coke formation of 10 mole% copper loaded catalysts calcined with Air/Ar was more than that of 15 mole% copper loaded catalysts.

Table 12: Coke formation in catalysts used in reactions at different temperatures

Catalyst	Reaction Temperature (^{0}C)	Carbon Deposition (%)
15Cu-SA Air/Ar 700 (200)	200	2.62
15Cu-SA Air/Ar 700 (225)	225	1.14
15Cu-SA Air/Ar 700 (250)	250	3.75
15Cu-SA Air/Ar 700 (275)	275	3.45
15Cu-SA Air/Ar 700 (280)	280	3.41
15Cu-SA Air/Ar 700 (300)	300	2.72
10Cu-SA Air/Ar 700 (280)	280	4.42
10Cu-SA Air/Ar 450 (280)	280	8.99
10Cu-SA Air/Ar 280 (280)	280	9.40
10Cu-SA N_2 700 (280)	280	4.60
10Cu-SA N_2 450 (280)	280	4.61
10Cu-SA N_2 280 (280)	280	8.07

6.2.6 Effect of adsorbent usage on hydrogen production in the SRM reaction

After the determination of the optimum catalyst and reaction temperature, it was aimed to reduce the side product formation, namely CO_2. By doing so, the formation of CO could also be lessened (reverse WGS reaction) and hydrogen could be obtained at a higher purity. With this purpose, the best catalyst was mixed with different adsorbents. Amount of adsorbent added into the catalyst was 15 times of the weight of the catalyst used. Huntite ($CaMg_3(CO_3)_4$) and hydrotalcite ($Mg_6Al_2(CO_3)(OH)_{16}.4(H_2O)$) were used to eliminate CO_2 in the reaction medium.

The effect of huntite and hydrotalcite on the product distribution is given in Figure 55a and 55b, respectively.

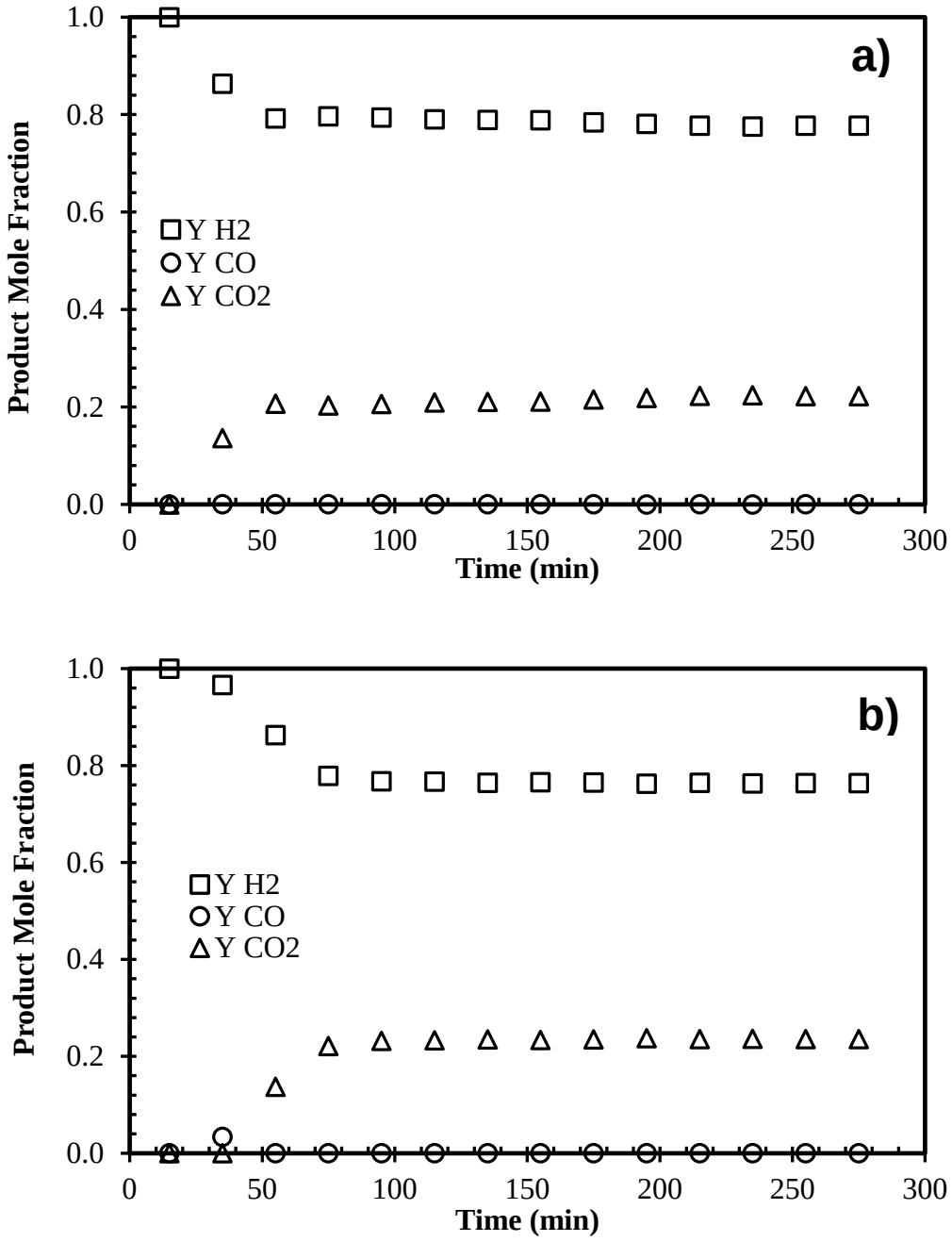

Figure 55: Effect of huntite **(a)** and hydrotalcite **(b)** on the product distribution (P:1.013 bar, T:200°C, H_2O/CH_3OH = 2.2, Catalyst : 15Cu-SA Air/Ar 700)

From Figure 55a, it was seen that formation of CO_2 started around the 35^{th} minute, which means that after the 35^{th} minute, huntite became saturated to CO_2 and started

releasing the excess CO_2 into the reaction medium. CO_2 amount started to increase from the 35th minute till the 55th minute. After this time, CO_2 level remained constant (25%) at 200°C.

In Figure 55b, same reaction was performed with hydrotalcite. When the results are examined it was seen that CO_2 was captured by hydrotalcite for 55 minutes. After this time, as in the case of huntite, the level of CO_2 started to increase and became constant (25%) around the 75th minute. When the two adsorbents are compared, it could be said that huntite captured CO_2 for 35 minutes whereas hydrotalcite captured CO_2 for 55 minutes. This difference arises from the differences in the phyical nature of the adsorbents: before being used in the reaction, both adsorbents were calcined but the removal of water from hydrotalcite was thought to leave more free space to capture CO_2, which was why hydrotalcite became saturated to CO_2 later than huntite.

Hydrotalcite was calcined at 550°C prior to reaction in order to convert carbonates into oxides. The reaction rate of magnesium oxide and carbon dioxide was slow at reaction temperature (200°C) (Ficicilar, 2006). With the addition of hydrotalcite at the exit of reactor and heating that zone to higher temperatures (450°C) could further enhance the sorption capacity of this adsorbent by increasing the reaction rate.

6.2.7 Determination of the catalyst life

In this section. stability results of the best catalyst under optimum reaction conditions (P:1.013 bar, T: 280°C, H_2O/CH_3OH = 2.2) were given. Stability of the catalyst under the reaction conditions was examined with a 23 hour SRM experiment (activity test). The stability result of the catalyst was then compared to two cyclic experiments. Each cyclic experiment lasted for 5 hours and was performed after the activity test by regenerating the catalyst prior to each experiment. Regeneration of the used catalyst was done by calcining the catalyst with air flow at 80 ml/min from room temperature to 700°C with a heating rate of 1°C/min. When the desired temperature (700°C) was reached, the catalyst was kept

at that temperature for 2 hours and 1 hour of argon was let flow over the catalyst, which was then let cool down to be used in cyclic experiments. Activity tests were examined in terms of product distributon, methanol conversion, hydrogen yield and selectivity. Related figures are given in Figures 56- 58.

Product distributions of the activity test and the cyclic experiments are given in Figure 56. Formation of the same products; hydrogen, carbon monoxide and carbon dioxide, at similar amounts was observed. The outlet gas from the reactor is rich in hydrogen, contains carbon dioxide and very little carbon monoxide.

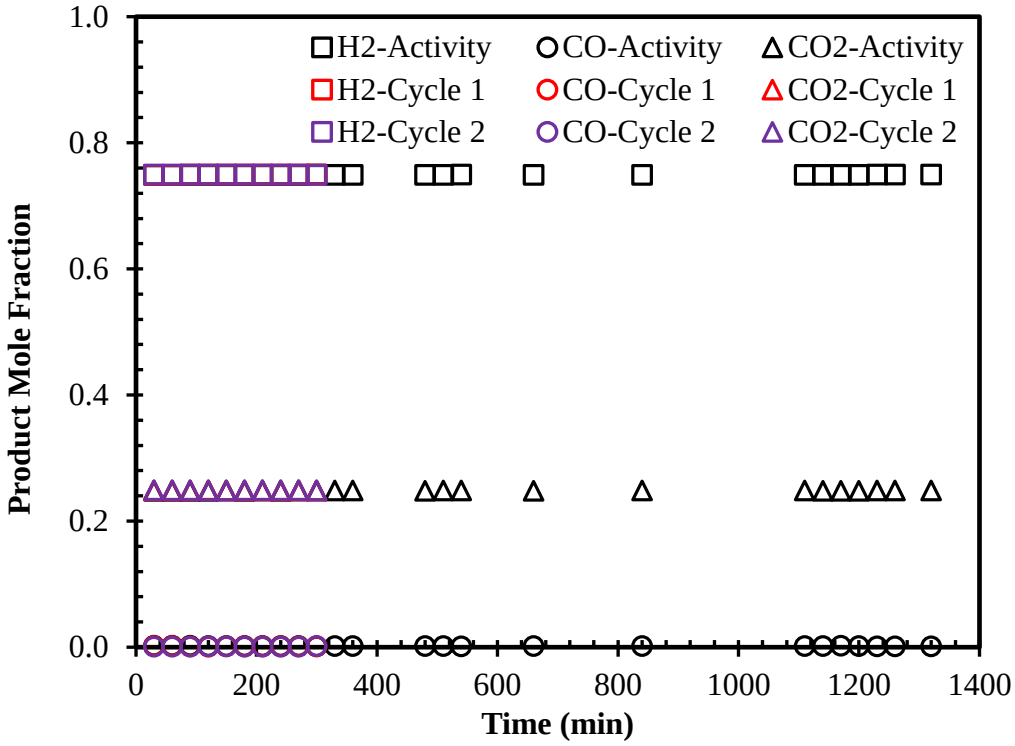

Figure 56: Product distribution of activity test and cyclic experiments (P:1.013 bar, T:280°C, H_2O/CH_3OH = 2.2, Catalyst : 15Cu-SA Air/Ar 700)

Methanol conversion obtained from the activity test and cyclic experiments are given in Figure 57. From Figure 57 it was seen that no significant drop in methanol conversion occurred within the first 14.5 hours. These conversion values were close to complete conversion. However, after 14.5 hours, the conversion started to decrease and at the end of 23 hours, the conversion dropped to 61.3%. This decrease showed the deactivation of copper loaded catalyst, in other words formation of

coke. After the activity test, the catalyst was regenerated with calcination which enhanced its methanol conversion to almost complete conversion. Almost complete conversion was maintained with the two cyclic experiments as well. Hydrogen yield of the activity test and cyclic experiments are given in Figure 58.

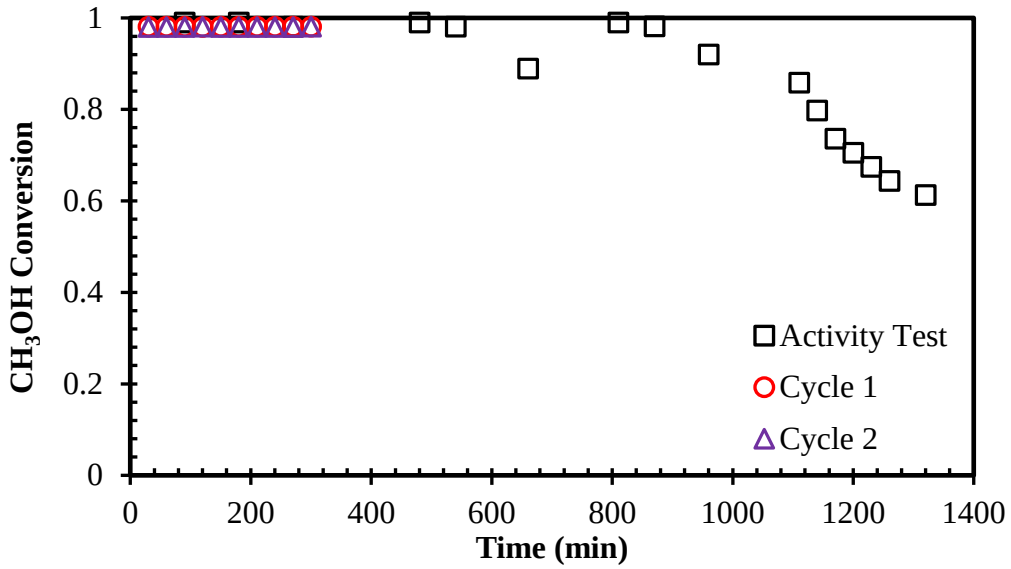

Figure 57: Methanol conversion of activity test and cyclic experiments (P:1.013 bar, T:280°C, H_2O/CH_3OH = 2.2, Catalyst : 15Cu-SA Air/Ar 700)

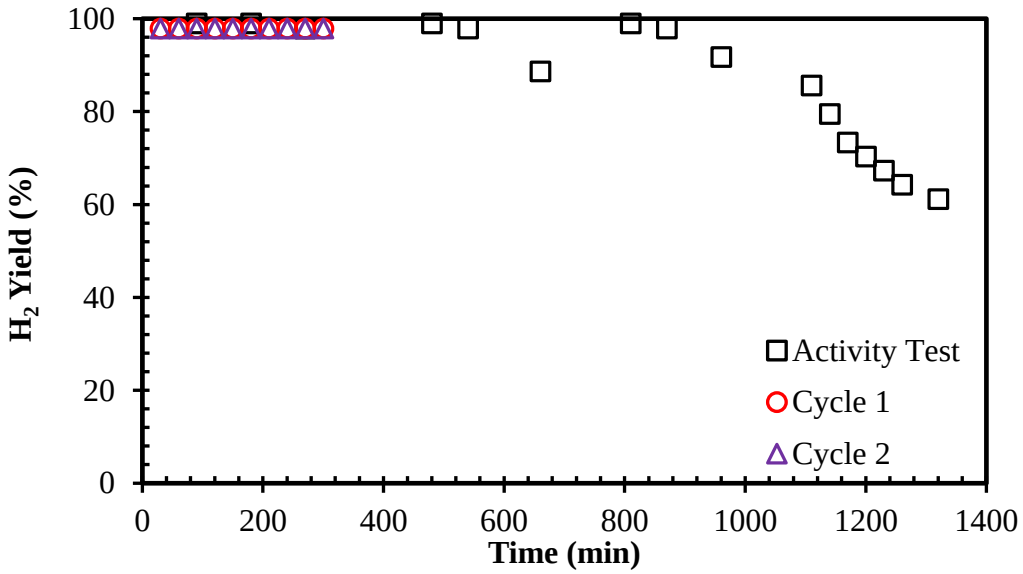

Figure 58: Hydrogen yield of activity test and cyclic experiments (P:1.013 bar, T:280°C, H_2O/CH_3OH = 2.2, Catalyst : 15Cu-SA Air/Ar 700)

The trend in hydrogen yield (Figure 58) was the same as Figure 57; at the end of 23 hours hydrogen yield dropped to 61.2% whereas at the end of the first cyclic experiments this value was 97.9% and it was maintained in the second cyclic experiment. Hydrogen selectivities of the catalysts in activity test and cyclic experiments were maintained around 99% throughout the experiment.

To conclude, during the activity tests performed with 15Cu-SA Air Ar 700 (P:1.013 bar, T:280°C, H_2O/CH_3OH = 2.2, Feed Flow rate : 0.9 ml/h) to determine the life of catalyst, it was observed that the catalyst maintained its stability for 14.5 hours (870 min). After the activity test, the catalyst gained its properties again and became active in cyclic experiments.

CHAPTER 7

CONCLUSIONS AND RECOMMENDATIONS

Experiments were carried out with metal (Cu and Zn) loaded silica aerogel catalysts. Some of the experiments were performed with adsorbents and the catalysts were intended to be stable and active which provide hydrogen gas production with low carbon content. The results obtained in the light of this purpose were given below:

- Mesoporous and metal loaded silica aerogel catalysts were successfully synthesized. These catalysts possessed high surface area and exhibited Type IV isotherms with H_1 hysteresis.

- Effect of the calcination gas and temperature on the crystallite size of metal was found out. An increase in calcination temperature also increased the crystallite size of the metal. Besides, the crystallite sizes of catalysts calcined with Air/Ar are relatively higher than the ones calcined with N_2.

- Acidity of synthesized catalysts were found out to be in this descending order: 10-SA N_2 280 > 10Cu-SA Air/Ar 450 > 10Cu-SA N_2 450 > 10Cu-SA Air/Ar 280 > 10Cu-SA N_2 700 > 15Cu-SA Air/Ar 700 > 10Cu-SA Air/Ar 700 > 15Cu-10Zn-SA Air/Ar 700.

- Methanol conversion and hydrogen yield of the catalysts in SRM were increased from 82.9% to 92.1% and from 82.5% to 91.7%, respectively. The reason of this increase was the increased copper loading from 10 to 15 mole%. The increased metal loading also enhanced the acitiy of the catalysts.

- It was seen that 15CuSA Air/Ar 700 was a stable and regenerable catalyst.

- The catalyst giving the best results was found to be 15Cu-SA Air/Ar 700 which led to a hydrogen yield of 2.75, 92.1% methanol conversion and 3.6% coke formation in SRM at 280°C.

- Capturing the side product CO_2 from the reactor outlet gas was performed the best with hydrotalcite as 55 minutes. The sorption capacity of hydrotalcite could be increased with the addition of hydrotalcite at the exit of reactor and heating that zone to higher temperatures (450°C).

REFERENCES

Abrokwah, R. Y., Deshmane, V. G., Kuila, D., "Comparative performance of M-MCM-41 (M: Cu, Co, Ni, Pd, Zn and Sn) catalysts for steam reforming of methanol", Journal of Molecular Catalysis A: Chemical, 425, 10–20, 2016.

Amiri, T. Y., Moghaddas, J. S., "Performance Evaluation of Cu-SiO_2 Aerogel Catalyst in Methanol Steam Reforming", Iranian Journal of Chemical Engineering. 11 (3), 37-44, 2014.

Amiri, T. Y., Moghaddas, J., Khajeh, S. R., "Silica aerogel-supported copper catalyst prepared via ambient pressure drying process",Journal of Sol-Gel Technology, 77, 627-635, 2016.

Aravind, P. R., Shajesh, P., Soraru, G. D., Warrier, K. G. K.,"Ambient pressure drying: a successful approach for the preparation of silica and silica based mixed oxide aerogels", Journal of Sol-Gel Science Technology, 54, 105-117, 2010.

Bartholomew, C.H., Farrauto, R.J., "Fundamentals of Industrial Catalytic Processes", 2nd Edition, Chapter 6, 390, 2006.

Deshmane, V. G., Abrokwah, R. Y., Kuila, D., "Synthesis of stable Cu-MCM-41 nanocatalysts for H_2 production with high selectivity via steam reforming of methanol", International Journal of Hydrogen Energy, 40, 10439-10452, 2015.

Deshpande, R., Smith, D., Brinker, C.J., US patent No.5, 565, 142, 1996.

Dorcheh, A. S., Abbasi, M. H., "Silica aerogel; synthesis, properties and characterization", Journal of Materials Processing Technology, 199, 10-26, 2008.

Edlund. D.,"Methanol Fuel Cell Systems Advancing Towards Commercialization", Pan Stanford, 2, 29-30, 52, 2011.

Erdener, H., Erkan, S., Eroğlu, E., Gür, N., Şengül, E., Baç, N., "Sürdürülebilir Enerji ve Hidrojen", ODTÜ Yayıncılık, 2013

Eswaramoorthi, I., Dalai, A. K., “A comparative study on the performance of mesoporous SBA-15 supported Pd–Zn catalysts in partial oxidation and steam reforming of methanol for hydrogen production”, International Journal of Hydrogen Energy, 34, 2580–2590, 2009.

Ficicilar, B., Dogu, T., “Breakthrough analysis for CO_2 removal by activated hydrotalcite and soda ash”, Catalysis Today, 115, 274-278, 2006.

Fierro, V., Akdimb, O., Provendier, H., Mirodatos, C.,” Ethanol oxidative steam reforming over Ni-based catalysts”, Journal of Power Sources, 145, 659–666, 2005.

Florida Solar Energy Center, http://www.fsec.ucf.edu/en/consumer/hydrogen/basics/production.htm, last visited on May 2018

Fricke, J., Emmerling, A., “Aerogels- Recent Progress in Production Techniques and Novel Applicatins”, Journal of Sol—Gel Science and Technology, 13, 299-303, 1998.

Ghenciu, A.F., “Review of fuel processing catalyst for hydrogen produciton in PEM fuel cell systems”, Solid State &Materials Science, 6, 389-399, 2002.

Gurav, L.J., Nadargi, Y.D., Rao, A.V.,“Effect of mixed Catalysts system on TEOS based silica aerogels dried at ambient pressure”, Applied Surface Science, 255, 3019– 3027, 2008.

Hu, W., Li, M., Chen, W., Zhang, N., Li, B., Wang, M., ” Preparation of hydrophobic silica aerogel with caolin dried at ambient pressure”, Colloids and Surfaces A: Physicochemical Engineering Aspects, 501, 83-91, 2016.

Ivanov, P., Hristov, Y., Bogdanov, B. I., Pashev, P., “Synthesis of silica aerogel by surface modification”, научни трудове на русенския университет, 10.1, 53, 2014.

Leventis, N., Aegerter, M.A., “Aerogel Handbook”, 1st Edition, Springer, London, 2011.

Llanos, A., Melo, L., Avendano, F., Montes, A., Brito, J. L., “Synthesis and characterization of HPW/MCM-41 (Si) and HPW/MCM-41 (Si/Al) catalysts:

Activity for toluene alkylation with 1-dodecene", Catalysis Today, 133–135, 20–27, 2008.

Matsumura, Y., Ishibe, H., "Selective steam reforming of methanol over silica-supported catalyst prepared by sol-gel method", Applied Catalysis B: Environmental, 86, 114-120, 2009.

Matsumura, Y., Ishibe, H., "Suppression of CO by-production in steam reforming of methanol by addition of zinc oxide to silica supported catalyst", Journal of Catalysis, 268, 282-289, 2009.

Mrad, M., Gennequin, C., Aboukais, A., Aaad, E. A.," Cu/Zn-based catalysts for H_2 production via steam reforming of methanol", Catalysis Today, 1176, 88-92, 2011.

Nikolaidis, P., Poullikkas, A.,"A comperative overview of hydrogen production processes", Renewable and Sustainable Energy Reviews, 67, 597–611, 2017.

Park, J. E., Yim, S. D., Kim, C.S., Park, E. D., "Steam reforming of methanol over $Cu/ZnO/ZrO_2/Al_2O_3$ catalyst", International Journal of Hydrogen Energy, 39, 11517-11527, 2014.

Qi, T., Yang, Y., Wu, Y., Wang, J., Li, P., Yu, J., "Sorption-enhanced methanol steam reforming for hydrogen production by combined copper-based catalysts with hydrotalcites", Chemical Engineering & Processing : Process Intensification, 127, 72-82, 2018.

Rao, A. P., Pajonk, G., Rao, A. V., "Effect of preparation conditions on the physical and hydrophobic properties of two step processed ambient pressure dried silica aerogels", Journal of Materials Science, 40(13), 3481–3489, 2005.

Republic of Turkey, Ministry of Energy and Natural Resources, http://www.yegm.gov.tr/teknoloji/h_depolanmasi.aspx, last visited on May 2018.

Sa, S., Silva, H., Brandao, L., Sousa, J. M., Mendes, A., "Catalysts for methanol steam reforming- A review", Applied Catalysis B: Environmental, 99, 43-57, 2010.

Santos, S. M. L., Nogueira, K. A. B., Gama, M. S., Lima, J. D. F., Júnior, J. S., Azevedo. D. C. S., "Synthesis and characterization of ordered mesoporous silica (SBA-15 and SBA-16) for adsorption of biomolecules", Microporous and Mesoporous Materials, 180, 284–292, 2013.

Shamsul, N.S., Kamarudin, S.K., Rahman, N.A., Kofil, N.T., “An overview on the production of bio-methanol as potential renewable energy”, Renewable and Sustainable Energy Reviews, 33, 578–588, 2014.

Shi, F., Wang, L., Liu, J.,“Synthesis and characterization of silica aerogels by a novel fast ambient pressure drying process”, Materials Letters, 60, 3718–3722, 2006.

Sigma Aldrich, https://www.sigmaaldrich.com/chemistry/solvents/methanol-center.html, last visited on May 2018.

Srinivas, M., Raveendra, G., Parameswaram, G., Sai Prasad, P.S., Lingaiah, N., “Cesium exchanged tungstophosphoric acid supported on tin oxide: An efficient solid acid catalyst for etherification of glycerol with tert-butanol to synthesize biofuel additives”, Journal of Molecular Catalysis A: Chemical, 413, 7–14, 2016.

Takewaza, N., Iwasa, N., “Steam reforming and dehydrogenation of methanol : Difference in the catalytic functions of copper and group VIII metals”, Catalysis Today, 36, 45-56, 1997.

Tartakovsky, L., Baibikov, V., Veinblat, M., “Modeling Methanol Steam Reforming for Internal Combustion Engine”, Energy and Power, 4 (1A), 50-56, 2014.

Toshiba, https://www.toshiba.co.jp/csr/en/highlight/2015/pdf/enr_pdf.pdf, last visited on May 2018.

World Energy Outlook. International Energy Agency, 2014

Wu, G. S., Mao, D. S., Lu, G. Z., Cao, Y., Fan, K. N.,” The Role of the Promoters in Cu Based Catalysts for Methanol Steam Reforming”, Catalysis Letters, 130, 177-184, 2009.

Wu, X., Wu, S., “Production of high-purity hydrogen by sorption-enhanced steam reforming process of methanol”, Journal of Energy Chemistry, 24, 315-321, 2015.

Wua, G., Yua, Y., Chenga, X., Zhang, Y.,” Preparation and surface modification mechanism of silica aerogels via ambient pressure drying”, Materials Chemistry and Physics, 129, 308-314, 2011.

Zhao, S.X., Lu, G.Q., Millar, G.J.," Advances in Mesoporous Molecular Sieve MCM-41", Industrial and Engineering Chemistry Research, 35(7), 2075-2090, 1996.

APPENDIX A

CALIBRATION OF THE MASS FLOW CONTROLLERS FOR ARGON AND HYDROGEN GASES

Calibration of the mass flow controllers of Ar and H_2 were done in order to feed these gases at the desired rates into the reaction system. Related calibration curves are given in Figures A.1 and A.2

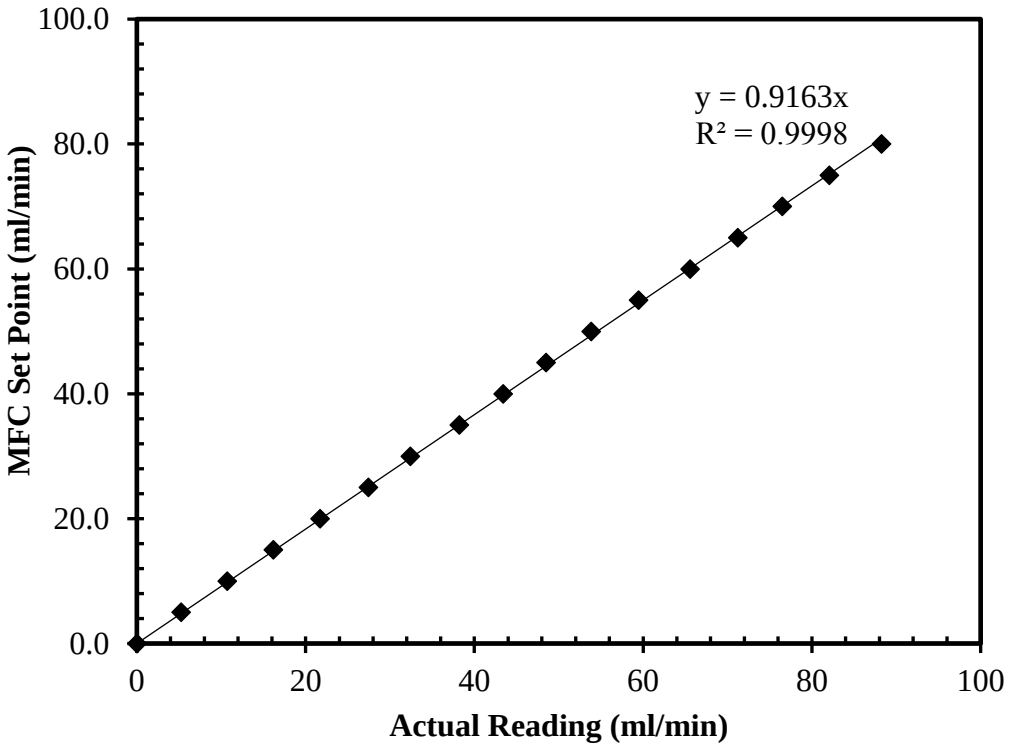

Figure A.1: Calibration curve for the mass flow controller of argon at 5 Bar

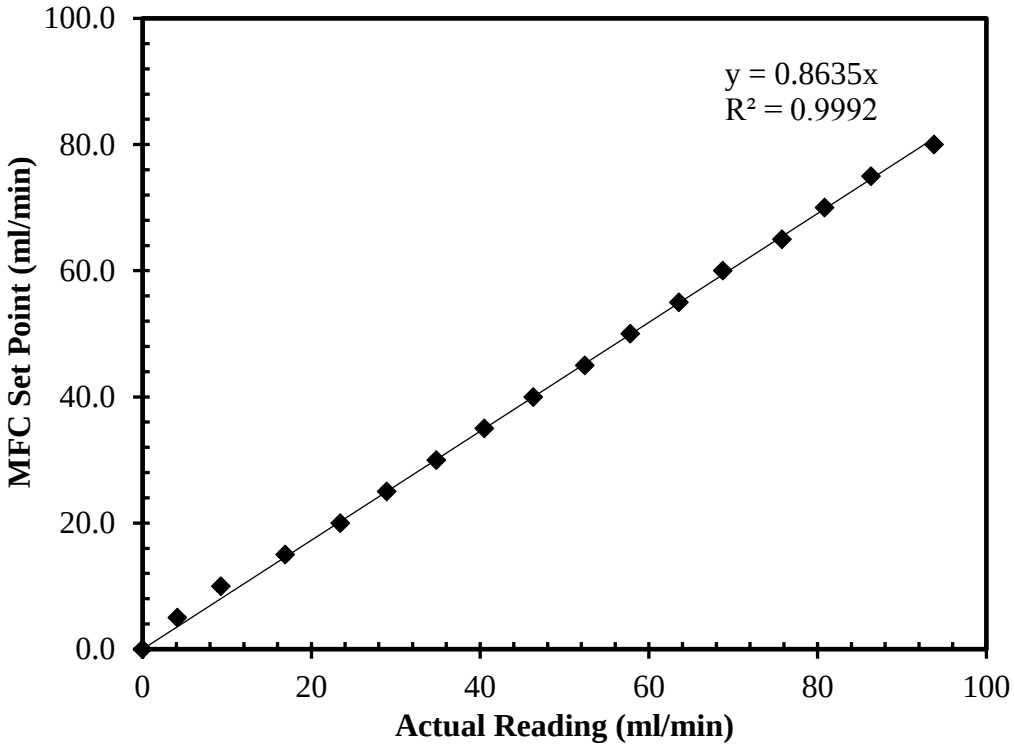

Figure A.2: Calibration curve for the mass flow controller of hydrogen at 5 Bar

APPENDIX B

XRD DATA OF METAL AND METAL OXIDE

In this section, PDF cards of Cu and CuO are given from Table B.1 to B.4.

Table B.1: XRD data of Cu

Formula: Cu **PDF Card No:** 01-070-3039 **Radiation:** CuKα_1 **Wavelength:** 1.54060 Å			
2θ (°)	**d spacing (Å)**	**Intensity (%)**	**h k l**
43.34	2.086	100	1 1 1
50.48	1.806	42.7	2 0 0
74.17	1.277	17.1	2 2 0

Table B.2: XRD data of CuO

Formula: CuO **PDF Card No:** 01-070-6829 **Radiation:** CuKα_1 **Wavelength:** 1.54060 Å			
2θ (°)	**d spacing (Å)**	**Intensity (%)**	**h k l**
32.56	2.748	7.3	1 1 0
35.56	2.523	94.6	0 0 2
38.82	2.318	100.0	1 1 1
46.27	1.960	1.9	-1 1 2
48.71	1.868	26.7	-2 0 2
51.51	1.773	1.2	1 1 2
53.55	1.710	9.4	0 2 0
56.79	1.620	0.8	0 2 1
58.52	1.576	12.7	2 0 2
61.58	1.505	16.7	-1 1 3
65.91	1.416	12.5	0 2 2
66.29	1.409	12.6	-3 1 1
68.12	1.375	9.1	1 1 3
68.21	1.374	12.3	2 2 0

Table B.2 (cont'd): XRD data of CuO

2θ (°)	d spacing (Å)	Intensity (%)	h k l
68.95	1.361	0.4	-2 2 1
71.69	1.315	0.3	-3 1 2
72.61	1.301	5.3	3 1 1
73.12	1.293	0.3	2 2 1
75.17	1.263	4.8	0 0 4
75.28	1.261	5.3	-2 2 2
79.89	1.200	0.2	0 2 3
80.17	1.196	1.4	-2 0 4
80.35	1.194	0.8	-1 1 4
82.34	1.170	3.2	-3 1 3
83.32	1.159	3.1	2 2 2
83.78	1.154	2.9	4 0 0
86.56	1.124	1.0	-4 0 2
86.79	1.121	0.6	-2 2 3
88.29	1.106	0.1	1 3 0
89.90	1.090	4.1	1 3 1

Table B.3: XRD data of CuO

Formula : CuO
PDF Card No : 01-080-0076
Radiation : CuKα_1
Wavelength : 1.54060 Å

2θ (°)	d spacing (Å)	Intensity	h k l
32.48	2.754	5.5	1 1 0
35.39	2.535	25.8	0 0 2
35.54	2.524	100.0	-1 1 1
38.64	2.328	44.2	1 1 1
38.97	2.309	16.4	2 0 0
46.25	1.961	1.4	-1 1 2
48.85	1.863	19.4	-2 0 2
51.23	1.782	0.9	1 1 2
53.36	1.716	6.9	0 2 0
56.59	1.625	0.6	0 2 1
58.16	1.585	9.6	2 0 2
61.52	1.506	8.1	-1 1 3
66.34	1.408	6	-3 1 1
66.51	1.405	3.4	3 1 0
67.73	1.382	8.5	1 1 3
68.02	1.377	8.9	2 2 0

Table B.3 (cont'd): XRD data of CuO

2θ (°)	d spacing (Å)	Intensity	h k l
68.85	1.363	0.3	-2 2 1
71.84	1.313	0.2	-3 1 2
72.34	1.305	6.3	3 1 1
72.81	1.298	0.3	2 2 1
74.86	1.267	3.3	0 0 4
75.23	1.262	3.6	-2 2 2
79.56	1.204	0.1	0 2 3
80.26	1.195	1.1	-2 0 4
82.54	1.168	3.7	-3 1 3
82.86	1.164	3.2	2 2 2
83.34	1.159	0.2	3 1 2
83.69	1.155	2.1	4 0 0
87.74	1.112	0.1	1 1 4
89.57	1.093	1.4	-1 3 1
91.44	1.076	3	1 3 1
95.27	1.043	0.6	2 0 4
96.59	1.032	0.1	-1 3 2
98.17	1.019	1.3	0 2 4
99.44	1.010	1.3	3 1 3
100.37	1.003	0.1	1 3 2
101.85	0.992	0.5	4 0 2
103.26	0.983	1.7	-1 1 5
103.53	0.981	2	-2 2 4
105.91	0.965	0.1	-4 2 1
107.05	0.958	1	4 2 0
109.23	0.945	1.8	-1 3 3
110.33	0.938	1.5	-4 2 2
111.59	0.931	0.8	-4 0 4
113.11	0.923	0.9	1 1 5
113.89	0.919	1.7	-3 3 1
115.30	0.912	0.7	1 3 3
117.14	0.903	1.3	-5 1 1
119.68	0.891	1.3	2 2 4
120.19	0.889	1.3	3 3 1
120.75	0.886	1	-5 1 2
122.42	0.879	0.1	3 1 4
123.89	0.873	0.1	0 2 5
127.48	0.859	1.1	4 2 2
127.78	0.858	0.5	0 4 0
128.10	0.857	0.7	-2 2 5
128.26	0.856	0.9	5 1 1
131.49	0.845	1	-5 1 3

Table B.3 (cont'd): XRD data of CuO

2θ (°)	d spacing (Å)	Intensity	h k l
132.57	0.841	0.6	-3 3 3
133.57	0.838	0.6	3 3 2
136.14	0.83	0.1	-1 1 6
140.45	0.819	0.7	-4 2 4
142.87	0.813	1	0 4 2
146.63	0.804	1	2 4 0
148.07	0.801	0.1	-2 4 1

Table B.4: XRD data of CuO

Formula: CuO **PDF Card No:** 01-089-5898 **Radiation:** CuKα_1 **Wavelength:** 1.54060 Å			
2θ (°)	**d spacing (Å)**	**Intensity**	**h k l**
32.53	2.750	7.3	1 1 0
35.45	2.530	36.0	0 0 2
35.56	2.523	91.4	-1 1 1
38.75	2.322	100.0	1 1 1
38.91	2.313	61.6	2 0 0
46.27	1.961	1.9	-1 1 2
48.70	1.868	26.2	-2 0 2
51.39	1.777	1.2	1 1 2
53.55	1.710	9.3	0 2 0
56.78	1.620	0.7	0 2 1
58.30	1.581	12.7	2 0 2
61.55	1.505	16.6	-1 1 3
65.87	1.417	12.5	0 2 2
66.21	1.410	12.6	-3 1 1
66.47	1.406	6.6	3 1 0
67.94	1.378	7.4	1 1 3
68.14	1.375	14.3	2 2 0
68.93	1.361	0.4	-2 2 1
71.66	1.316	0.3	-3 1 2
72.39	1.304	5.3	3 1 1
73.00	1.295	0.3	2 2 1
75.02	1.265	4.3	0 0 4
75.28	1.261	6.0	-2 2 2
79.80	1.201	0.2	0 2 3
80.16	1.196	1.4	-2 0 4

Table B.4 (cont'd) : XRD data of CuO

2θ (°)	**d spacing (Å)**	**Intensity**	**h k l**
80.29	1.195	0.4	-1 1 4
82.33	1.170	3.1	-3 1 3
83.13	1.161	3.1	2 2 2
83.55	1.156	2.9	4 0 0
86.48	1.124	1.0	-4 0 2
86.79	1.121	0.6	-2 2 3
88.04	1.109	0.1	1 1 4
89.89	1.090	4.0	-1 3 1

APPENDIX C

CALIBRATION FACTOR CALCULATIONS OF GASES

Calibration tests were done in order to determine the retention times and calibration factors of each component in the standard gas mixture which is composed of 1 volume % H_2, 1 volume % CO_2 , 1 volume % CO, 1 volume % CH_4, 1 volume % C_2H_4 and 95 volume % Ar.

GC calibration factor of each component could be calculated from Eqn. C.1 where β_{CO_2} was taken as 1 and n_i is the number of moles of species i.

$$\frac{n_i}{n_{CO_2}} = \frac{A_i \beta_i}{A_{CO_2} \beta_{CO_2}} \qquad [C.1]$$

Calculated beta factors of each component in the standard gas mixture is given in Table C.1. The areas are the average areas obtained after injecting the standard gas into GC for five times.

Table C.1: Calibration factors of the components

Compound	Mole Fraction	Retention Time(min)	Average Area	β Factor
H_2	0.0092	2.38	2993114	0.0126
CO	0.0097	5.79	195230	0.0346
CH_4	0.0099	10.46	98557	0.3700
CO_2	0.0100	13.86	36701	1.0000
C_2H_4	0.0084	18.05	50052	0.6200

APPENDIX D

CALCULATION OF THE MOLE FRACTIONS, HYDROGEN YIELD, HYDROGEN SELECTIVITY AND METHANOL CONVERSION OF THE PRODUCTS OF SRM

Analysis of the products obtained from the SRM reactions was done by using the areas in GC. Product distribution, methanol conversion, hydrogen selectivity and yield calculations were made by using the formulas below:

In order to calculate the molar flow rate of species i in the product stream, Eqn. D.1 was used.

$$F_i = Q_{Ar\ free\ gas} * C_{gas\ total} * y_i \quad [D.1]$$

where F_i is the molar flow rate of species i in the product stream, mol/s

$Q_{Ar\ free\ gas}$ is the volumetric flow rate of the gas without argon, ml/s

$C_{gas\ total}$ is the concentration of the gaseous product at 1 atm and 20°C, mol/ml

y_i is the mole fraction of species i in the product stream

$$Q_{Ar\ free\ gas} = Q_{\ gas\ total} - \ Q_{Ar} \quad [D.2]$$

where $Q_{\ gas\ total}$ is the total flow rate of gaseous products, ml/s

Q_{Ar} is the volumetric flow rate of argon at 5 Bar, 0.5ml/s

$$C_{gas\ total} = \frac{P}{R*T} \quad [D.3]$$

where P is the atmospheric pressure, 1 atm

R is the ideal gas constant, 82 ml.atm/mol.K

T is the room temperature, 293 K

The mole fraction of species i in the product stream could be found from Eqn. D.4.

$$y_i = \frac{A_i \beta_i}{A_{CO}\beta_{CO} + A_{CO_2}\beta_{CO_2} + n_{H_2}} \quad [D.4]$$

where β_i is the beta factor of species i calculated using the areas in GC,

n_{H_2} is the number of moles of hydrogen, which could be calculated from Eqn. D.5

$$n_{H_2} = A_{H_2}\beta_{H_2} = 2(A_{CO}\beta_{CO}) + 3(A_{CO_2}\beta_{CO_2}) \quad [D.5]$$

Conversion of methanol could be calculated by using Eqn. D.6.

$$X_{CH_3OH} = \frac{F_{CO} + F_{CO_2}}{F_{CH_3OH_0}} \quad [D.6]$$

where $F_{CH_3OH_0}$ is the initial molar flow rate of methanol water mixture fed to the reactor, mol/s, and could be calculated via Eqn. D.7

$$F_{CH_3OH_0} = \frac{Q_{liq} * 0.5 * \rho_{CH_3OH}}{MW_{CH_3OH}} \quad [D.7]$$

where Q_{liq} is the volumetric flow rate of the methanol water mixture, ml/s. It is multiplied by 0.5 because the methanol water mixture is 50 volume% methanol and 50 volume% water.

ρ_{CH_3OH} is the density of methanol at 293 K, 0.791 g/ml and

MW_{CH_3OH} is the molecular weight of methanol, 32.04 g/mol

The selectivity of hydrogen could be calculated via Eqn. D.8 :

$$S_{H_2} = \frac{2(A_{CO}\beta_{CO}) + 3(A_{CO_2}\beta_{CO_2})}{3(A_{CO}\beta_{CO} + A_{CO_2}\beta_{CO_2})} * 100 \quad [D.8]$$

Lastly, hydrogen yield could be calculated from equation D.9 :

$$Y_{H_2} = X_{CH_3OH} * S_{H_2} \quad [D.9]$$